Mitigating Heat-Induced Cellular Stress in Intestinal Epithelium: Insights from the IPEC-J2 Cell Line

Aoife McCormack

M.Sc. By Research **2026**

Mitigating Heat-Induced Cellular Stress in Intestinal Epithelium: Insights from the IPEC-J2 Cell Line

A research project dissertation submitted for the degree of Master of Science by

Aoife McCormack (B.Sc.)

Under the supervision of

Dr. Finbarr O'Sullivan; School of Biotechnology, Dublin City University

Dr. Karina Horgan; Alltech Ltd., Dunboyne, Co. Meath

Dublin City University

School of Biotechnology

September 2026

Declaration

I hereby certify that this material, which I now submit for assessment on the programme of study leading to the award of Master of Science is entirely my own work, and that I have exercised reasonable care to ensure that the work is original and have conformed to the regulations on the use and declaration of Generative AI, and does not to the best of my knowledge breach any law of copyright, and has not been taken from the work of others save and to the extent that such work has been cited and acknowledged within the text of my work. I hereby certify that no Generative Artificial Intelligence (Gen AI) tools have been used in the creation of the thesis.

Signed: Aoife McCormack

ID Number: 23261076

Date: 14th September 2026

Acknowledgements

Completing this thesis has been a journey, and I am so grateful to those who helped me along the way, both personally and professionally. First and foremost, I would like to express my sincere gratitude to my family and friends. I want to thank my Mam, Dad, and brother Cian, who have done nothing but love and support me throughout this journey. They have been my biggest support, cheering me on from the sidelines, and encouraged me every day. In addition, I owe a great deal of thanks to my friends, who kept me smiling and laughing, even when the workload felt overwhelming. Thank you all for listening to my rants and offering only support and kindness in return.

This work would not have been possible without the opportunity given to me by Alltech Inc. In particular, I would like to thank Dr. Karina Horgan, who this project would not have been possible without. I am so grateful to you for providing me with this opportunity, your constant support and guidance was sincerely appreciated. In addition, a special thanks goes to Dr. Cathal Connolly for his mentorship and support. Thank you for all the advice and for having the confidence in me to get this over the line. To everyone else in Alltech who were there to give a helping hand whenever you could, thank you for your unwavering support. You made the time in the lab memorable, with plenty of laughs and chats over countless cups of tea.

Finally, I am very grateful to Dublin City University for the opportunity to undertake this research. I wish to acknowledge Dr. Finbarr O'Sullivan and Dr. Joanne Keenan for their guidance throughout my academic journey.

Table of Contents

Acknowledgements ..... **iii**

Abbreviations ..... **viii**

Units ..... **x**

List of Figures ..... **xi**

List of Tables ..... **xx**

Abstract ..... **xviii**

1 Introduction **1**

1.1 Animal Production 2

1.2 Climate Change/Global Warming 2

1.3 Thermoregulation and Heat Stress in Swine 3

1.4 Small Intestinal Epithelium Structure and Function 6

1.4.1 Intestinal Health of Swine During Heat Stress **6**

1.5 Heat Shock Response 8

1.6 Heat Shock Proteins 10

1.6.1 Heat Shock Protein 70 (HSP70) **11**

1.7 Strategies to Mitigate Heat Stress 12

1.7.1 Selenium **13**

1.7.2 Vitamins **14**

1.8 Aim of Project 15

2 Materials & Methods **17**

2.1 Reagents & Materials 18

2.1.1 Purchased Reagents **18**

2.1.2 Materials **19**

2.1.3 Prepared Reagents **20**

2.2 Methods 20

2.2.1 Cell culture techniques **20**

2.2.2 Treatment Preparation **24**

2.2.3 Protein Work: **26**

2.2.4 Proteomic Analysis **30**

2.2.5 Statistical Analysis **33**

3 Results **34**

3.1 Development of an *in vitro* model for heat stress using IPEC-J2 cells 35

3.1.1 Evaluation of the relative metabolic activity of IPEC-J2 cells after exposure to 41°C, 42°C, and 44°C for 2 hrs and 24 hrs, respectively **35**

3.1.2 Investigation of Heat Shock Protein 70 (HSP70) in IPEC-J2 cells exposed to heat stress **39**

3.1.3 Investigation of the cellular morphology of IPEC-J2 cells exposed to heat stress at 42°C **42**

3.2 Investigation of treatment with different Selenium (Se) and vitamin compounds to mitigate the impacts of heat stress 45

3.2.1 Selenium concentration of digested samples **45**

3.2.2 Effect of 48-hour exposure to Se and vitamin compounds on IPEC-J2 cell metabolic activity at 37°C **46**

3.2.3 Investigation of 24-hour treatment with Se and vitamin compounds on IPEC-J2 cells to mitigate reduced cell metabolic activity under heat stress at 42°C **48**

3.2.4 Investigation of 48-hour treatment with Se and vitamin compounds on IPEC-J2 cells to mitigate reduced IPEC-J2 cell metabolic activity under heat stress at 42°C .. **52**

3.2.5 Effect of 48-hour exposure to vitamin C on IPEC-J2 cell metabolic activity at 37°C **55**

3.2.6 Investigation of 24-hour treatment with vitamin C on relative IPEC-J2 cell metabolic activity under heat stress at 42°C **57**

3.2.7 Investigation of 24-hour treatment with Se and vitamin compounds on Heat Shock Protein 70 (HSP70) abundance in IPEC-J2 cells prior to being exposed to 42°C for 24 hours **59**

3.3 Proteomic Analysis 63

3.3.1 Comparative proteomic analysis of heat-stressed and control IPEC-J2 cells ... **64**

3.3.2 Differential protein expression between heat-stressed IPEC-J2 cells treated with Organic Se-A compound compared to untreated heat-stressed control cells **82**

3.3.3 Differential protein expression between heat-stressed IPEC-J2 cells treated with Inorganic Se (E) compound compared to untreated heat-stressed control cells **85**

3.3.4 Differential protein expression between heat-stressed IPEC-J2 cells treated with vitamin E compound compared to untreated heat-stressed control cells 94

3.3.5 Differential protein expression between heat-stressed IPEC-J2 cells treated with vitamin C compound compared to untreated heat-stressed control cells 101

4 Discussion 111

4.1 Establishment and validation of an *in vitro* heat stress model using an IPEC-J2 cell line 112

4.1.1 Effect of heat stress on relative IPEC-J2 cell metabolic activity 113

4.1.2 Induction of HSP70 expression in response to heat stress in IPEC-J2 cells 114

4.1.3 Effects of heat stress on IPEC-J2 cell morphology 115

4.2 Effects of Se and vitamin supplementation under heat stress conditions ... 117

4.2.1 Effect of Se and vitamin supplementation on IPEC-J2 cell metabolic activity under heat stress conditions 118

4.2.2 Effect of Se and vitamin supplementation of HSP70 in IPEC-J2 cells under heat stress conditions 121

4.3 Proteomic Responses to Heat Stress 123

4.3.1 Effect of 24 hours of heat stress at 42°C on IPEC-J2 cell proteomic profile .. 123

4.3.2 Proteomic responses in IPEC-J2 cells treated with organic Se prior to being heat stressed at 42°C 129

4.4 Limitations 131

4.5 Conclusion 132

4.6 Future Work 133

5 Bibliography 134

6 Appendix 149

6.1 Relative metabolic activity of IPEC-J2 cells treated with Se and vitamin compounds prior to heat stress at 42°C 150

6.1.1 Effect of 24-hour supplementation with Se and vitamin compounds on relative IPEC-J2 cell metabolic activity 150

6.1.2 Effect of 48-hour supplementation with Se and vitamin compounds on relative IPEC-J2 cell metabolic activity 152

6.2 Western Blot Analysis Images 154

6.2.1 Investigation of HSP70 abundance in IPEC-J2 cells exposed to heat stress at 41°C, 42°C, and 44°C 154

6.2.2 Investigation of HSP70 abundance in IPEC-J2 cells treated with Se and vitamin compounds prior to heat stress exposure at 41°C, 42°C, and 44°C **155**

6.3 Proteomic Analysis 158

6.3.1 Differentially expressed proteins in IPEC-J2 cells treated with Organic Se-A compared to untreated heat-stressed cells 159

Abbreviations

AB	Alamar Blue®
AJ	Adherens Junctions
Bip	Binding immunoglobulin protein
CON	Control
DMEM	Dulbecco's Modified Eagle's Medium
ER	Endoplasmic Reticulum
EU	European Union
FBS	Foetal Bovine Serum
FDR	False Discovery Rate
GIT	Gastrointestinal Tract
GO	Gene Ontology
GPx	Glutathione Peroxidase
HS	Heat Stress
HSF	Heat Shock Factor
HSP	Heat Shock Protein
HSR	Heat Shock Response
IPEC-J2	Intestinal Porcine Epithelial Cells
LC-MS/MS	Liquid Chromatograph Tandem Mass Spectroscopy
LCT	Lower Critical Temperature
Mt	Million Tonnes
PPI	Protein-protein interaction
PVDF	Polyvinylidene Fluoride
ROS	Reactive Oxygen Species
SDS-PAGE	Sodium Dodecyl Sulphate Polyacrylamide Gel Electrophoresis
Se	Selenium
SeCys	Selenocysteine
SelP	Selenoprotein
SeMet	Selenomethionine
SS	Sodium selenite
STRING	Search Tool for the Retrieval of Interacting Genes
TJ	Tight Junctions
TNZ	Thermoneutral Zone
TrxR	Thioredoxin reductase

UCT	Upper Critical Temperature
UPR	Unfolded Protein Response
Zn	Zinc

Units

°C	degrees Celsius
g	grams
h	hours
L	litre
µg	microgram
µL	microlitre
mL	millilitre
M	molar
nm	nanometres
ppm	parts per million
rpm	revolutions per minute
V	volts

List of Figures

Figure 1.3-1: Thermal comfort concept in swine- image was created based on information from Vermeer and Hoofs (2024), where thermoneutral zone is the area of ambient temperature. When the environmental temperature rises, pigs reach their upper critical temperature (UCT) entering them into heat stress, but heat stress may begin in the warm section of the thermoneutral zone (Vermeer and Hoofs, 2024). 5

Figure 1.4-1: Schematic representation of a healthy and a heat-stressed intestinal tract- Image created using Biorender based on information from Fan, Tian and Li (2025). Image A depicts a healthy intestine consisting of columnar cells protected by a mucus layer containing immunoglobulins, which prevent the entry of harmful substances into the bloodstream. Image B illustrates an intestinal tract exposed to heat stress, distinguished by TJ disruption, compromised epithelial integrity, increased intestinal permeability, and mucosal atropy, facilitating the entry of unwanted substances into the bloodstream (Fan et al., 2025). 8

Figure 1.5-1: Visual representation highlighting heat-induced heat shock response- The HSR is activated in response to cells exposed to heat stress, the accumulation of misfolded proteins in the cytoplasm leads to the translocation and trimerization of HSF1 from the cytoplasm into the nucleus initiating the HSR pathway. Within the nucleus HSF1 binds to regulatory heat shock elements, which causes the gene expression of heat shock proteins, image created with Biorender based off Lian et al. 2020, (Lian et al., 2020). 9

Figure 3.1-1: Effect of 2 h heat stress on metabolic activity in IPEC-J2 cells as determined by Alamar blue assay- Cells were exposed to elevated temperatures (41°C, 42°C, and 44°C) for 2 h. Relative metabolic activity is expressed as a percentage relative to 37°C control cells. Bars represent the mean of three independent biological replicates (n=3), dots represent numerical value of each biological replicate, and error bars represent the standard deviation (SD). Statistical analysis was performed using One-way ANOVA with Tukey's post hoc test ($p > 0.05$). 36

Figure 3.1-2: Effect of 24 h heat stress on relative metabolic activity as determined by AB assay- IPEC-J2 cells were exposed to elevated temperatures (41°C, 42°C, and 44°C) for 24 h. Relative metabolic activity is expressed as a percentage relative to 37°C control cells. Bars represent the mean of three independent biological replicates (n=3), dots represent numerical value of each biological replicate, and error bars represent the standard deviation (SD). Statistical analysis was performed using One-way ANOVA with Tukey's post hoc test ($p > 0.05$). 37

Figure 3.1-3: Representative Western blot images of heat-stressed IPEC-J2 cells- Cells were heat-stressed for 2 h and 24 h, respectively, and samples were loaded at a protein concentration of 10 µg per lane , and membranes were incubated with target antibody (HSP70) and house-keeping antibody (Actin). Images represent 41°C (A), 42°C (B), and 44°C (C). 40

Figure 3.1-4: Densitometric analysis of HSP70 expression- IPEC-J2 cells exposed to 41°C (A), 42°C (B), and 44°C (C) for 2 h and 24 h, respectively. HSP70 expression was normalised to Actin, and values are expressed as relative protein expression to 37°C control. Bars represent the mean of three independent biological replicates (n=3), and error bars represent the standard deviation (SD). Data was analysed using One-way ANOVA with Tukey's multiple comparison with significance marked as *($p \leq 0.05$). 41

Figure 3.1-5: Effect of 2-hour heat stress on IPEC-J2 cell morphology- Representative phase-contrast images of IPEC-J2 cells maintained under optimal conditions (A, C) or exposed to heat stress at 42°C for 2 h (B, D). Images were captured at 10x (A, B) and 20x (C, D) magnification. Scale bars = 100µm. 43

Figure 3.1-6: Effect of 24-hour heat stress on IPEC-J2 cell morphology- Representative phase-contrast images of IPEC-J2 cells maintained under optimal conditions (A, C) or exposed to heat stress at 42°C for 24 h (B, D). Images were captured at 10x (A, B) and 20x (C, D) magnification. Scale bars = 100µm. 44

Figure 3.2-1: Effect of 48-hour treatment with Se and vitamin compounds on relative IPEC-J2 cell metabolic activity as determined by Alamar Blue assay- Cells were treated with Se compounds at a concentration of 0.2 µg/mL , vit E at 10.72 µg/mL, and it C at 250 µg/mL . IPEC-J2 cell metabolic activity was assessed using Alamar Blue assay and expressed as a percentage relative to the untreated control group. Bars represent mean IPEC-J2 cell metabolic activity , dots represent numerical value of each biological replicate, and error bars indicate standard deviation (n = 3). Data was analysed using One-way ANOVA with Tukey's multiple comparison with significance marked as *($p \leq 0.05$). 47

Figure 3.2-2: Effect of 24-hour treatment with Se and vitamin compounds on relative IPEC-J2 cell metabolic activity following 2-hour heat stress- Cells were treated with treatments organic Se compounds (Organic Se-A, Se-B, Se-C, Se-D, Se-F), Inorganic Se (E), and vitamin E for 24 h and subsequently exposed to 42°C for 2 h. Relative metabolic cell activity was measured using Alamar blue assay and expressed as a percentage relative to untreated cells maintained at 37°C. Bars represent mean ±SD of n=3 independent experiments. 49

Figure 3.2-3: Effect of 24-hour treatment with Se and vitamin compounds on relative IPEC-J2 cell metabolic activity following 24-hour heat stress- Cells were treated with treatments organic Se compounds (Organic Se-A, Se-B, Se-C, Se-D, Se-F), Inorganic Se (E), and vitamin E for 24 h and subsequently exposed to 42°C for 24 h. Cell metabolic activity was measured using Alamar blue assay and expressed as a percentage relative to untreated cells maintained at 37°C. Bars represent mean ±SD of n=3 independent experiments. Data was analysed was analysed using One-way ANOVA with Tukey's multiple comparison with significance marked as *($p \leq 0.05$) and **($p \leq 0.01$). 50

Figure 3.2-4: Effect of 48-hour treatment with Se and vitamin compounds on relative IPEC-J2 cell metabolic activity following 2-hour heat stress- Cells were treated with treatments organic Se compounds (Organic Se-A, Se-B, Se-C, Se-D, Se-F), Inorganic Se (E), and vitamin E for 48 h and subsequently exposed to 42°C for 2 h. IPEC-J2 cell metabolic activity was measured using Alamar blue assay and expressed as a percentage relative to untreated cells maintained at 37°C. Bars represent mean ±SD of n=3 independent experiments. 53

Figure 3.2-5: Effect of 48-hour treatment with Se and vitamin compounds on relative IPEC-J2 cell metabolic activity following 24-hour heat stress- Cells were treated with treatments organic Se compounds (Organic Se-A, Se-B, Se-C, Se-D, Se-F), Inorganic Se (E), and vitamin E for 48 h and subsequently exposed to 42°C for 24 h. IPEC-J2 cell metabolic activity was measured using Alamar blue assay and expressed as a percentage relative to untreated cells maintained at 37°C. Bars represent mean ±SD of n=3 independent experiments. 54

Figure 3.2-6: Effect of 48-hour treatment with vitamin C on relative IPEC-J2 cell metabolic activity as determined by Alamar Blue assay- Cells treated with increasing concentrations of vitamin C for 48 h, with IPEC-J2 cell metabolic activity expressed as a percentage relative to untreated control cells. Dots represent mean IPEC-J2 cell metabolic activity with error bars indicating standard deviation. Data was analysed using One-way ANOVA with Dunnett's test to compare each concentration with the control group, with significance marked as ***($p \leq 0.001$), n=3. 55

Figure 3.2-7: Effect of 24-hour treatment with vitamin C on IPEC-J2 cells' metabolic activity after being heat stressed at 42°C for 24 h- IPEC-J2 cells were treated with 50, 100, and 200 µg/mL vitamin C for 24 h prior to being heat-stressed at 42°C for a further 24 h. Data was analysed using One-way ANOVA with Dunnett's test, significance marked as *($p \leq 0.05$), n=3. 58

Figure 3.2-8: Representative Western blot membrane images- HSP70 protein expression in IPEC-J2 cells treated with Organic Se-A/ B/ C/ D/ F, Inorganic Se (E), vitamin E, and vitamin C compounds under control (37°C) and heat stress (42°C) conditions. Representative Western blots showing HSP70 expression in cells maintained at 37°C (A) and HSP70 expression in cells following exposure to 42°C (B). Cells were treated with compounds for 24 h prior to being heat stressed for a further 24 h. HSP0 expression was detected using specific primary and secondary antibodies, and membranes were probed with Actin as a loading control. 60

Figure 3.2-9: Densitometric analysis of HSP70 expression- IPEC-J2 cells treated with Se and vitamin compounds for 24 h then exposed to 37°C or 42°C for a further 24 h. HSP70 expression was normalised to actin, and values are expressed as relative protein expression to 37°C control. Data was analysed using One-way ANOVA with Tukey's multiple comparison with significance marked as *($p \leq 0.05$), n=5. 62

Figure 3.3-1: Volcano plot illustrating differential protein expression between heat-stressed and control IPEC-J2 cells. The x-axis shows $\log_2$ fold change, and the y-axis shows the $-\log_{10}$(p-value). Proteins significantly upregulated are highlighted in blue, significantly downregulated proteins are shown in orange, while grey dots are not significant. Horizontal and vertical dashed lines indicate the applied significance thresholds ($p \leq 0.05$, and $\log_2 FC \geq 0.585$). 64

Figure 3.3-2: STRING PPI network of proteins significantly upregulated in heat-stressed IPEC-J2 cells compared to control cells ($p \leq 0.05$)- Nodes represent proteins, and edges represent predicted or known functional interactions. The network was generated using high-confidence interaction score (0.7) and shows significant enrichment (PPI enrichment p-value < 1.0e-16). Functional clustering highlights enrichment of heat shock proteins and molecular chaperones, ER protein folding proteins, and smaller clusters related to calcium binding, nuclear localisation and vesicle trafficking. 66

Figure 3.3-3: KEGG and Gene Ontology (GO) enrichment analysis of differentially expressed proteins upregulated in IPEC-J2 cells under heat stress. Bubble plots show enrichment of (A) KEGG pathways, (B) cellular components, (C) biological processes, and (D) molecular functions. The x-axis represents -log (FDR), bubble size indicated gene count, and colour represents FDR. 68

Figure 3.3-4: Protein-protein interaction network, generated using STRING database, of proteins significantly downregulated in heat-stressed IPEC-J2 cells compared to cells maintained at optimal temperature. Nodes represent individual proteins and edges represent known or predicted interactions. The network was generated

using high-confidence interaction score (0.7) and shows significant enrichment (PPI enrichment p-value <1.0e-16). Proteins are grouped into clusters based on functional enrichment and interaction strength. Major clusters include proteins involved in translation and protein synthesis, proteasome-associated pathways, central carbon metabolism and glycolysis, aminoacyl-tRNA biosynthesis, cytoskeletal organisation, and the calpain complex. 74

Figure 3.3-5: KEGG and Gene Ontology (GO) enrichment analysis of differentially expressed proteins downregulated in IPEC-J2 cells under heat stress. Bubble plots show enrichment of (A) KEGG pathways, (B) cellular components, (C) biological processes, and (D) molecular functions. The x-axis represents -log (FDR), bubble size indicated gene count, and colour represents FDR. 76

Figure 3.3-6: Volcano plot illustrating protein expression between IPEC-J2 cells treated with Inorganic Se (E) for 24 h prior to being heat stressed at 42°C for 24 h and untreated IPEC-J2 cells heat stressed for 24 h. The x-axis represents $\log_2$(fold change), and the y-axis represents -$\log_{10}$(p-value). Significantly upregulated proteins are shown in blue, significantly downregulated proteins are highlighted in orange and grey dots represent non-significant proteins. Horizontal and vertical dashed lines indicate the applied significance thresholds (p-value ≤ 0.05, and $\log_2$FC ≥ 0.585). 85

Figure 3.3-7: Protein-protein interaction network of proteins upregulated in IPEC-J2 cells exposed to heat stress at 42°C for 24 hours, with Inorganic Se (E) supplementation- Nodes represent individual proteins, and edges indicate predicted or known protein-protein interactions. The network was generated using high-confidence interaction score (0.7) and shows significant enrichment (PPI enrichment p-value of 1.45e-06). Proteins are grouped into functional clusters based on interaction networks with colours indicating distinct clusters. Major clusters include proteins associated with ATP-dependent protein folding and chaperone complexes, glycolysis/gluconeogenesis, DNA replication and repair (MCM complex), and translation initiation. Lone nodes represent proteins with no known interactions within the dataset. 87

Figure 3.3-8: KEGG and Gene Ontology (GO) enrichment analysis of differentially expressed proteins upregulated in IPEC-J2 cells supplemented with Inorganic Se (E) under heat stress. Bubble plots show enrichment of (A) KEGG pathways, (B) cellular components, (C) biological processes, and (D) molecular functions. The x-axis represents -log (FDR), bubble size indicated gene count, and colour represents FDR. 89

Figure 3.3-9: Protein-protein interaction network of proteins downregulated in IPEC-J2 cells supplemented with Inorganic Se (E) and subsequently exposed to heat stress

(42°C), compared to untreated heat-stressed cells- Nodes represent individual proteins, while edges indicate known or predicted functional interactions between proteins. The network was generated using high-confidence interaction score (0.7) and shows significant enrichment (PPI enrichment p-value 1.35e-07). Proteins are organised into distinct clusters based on interaction patterns, with different colour representing separate functional groups. Prominent clusters include proteins associated with translation elongation (EEF1A1, EEF1D, EEF1G), cytoskeletal organisation (ACTB, ACTN4) and protein folding or stress-related processes (HSP90 family proteins). Additional clusters include proteins involved in ER function, metabolic processes, and cell signalling pathways. Disconnected nodes correspond to proteins with no identified interactions within the dataset. 91

Figure 3.3-10: KEGG and Gene Ontology (GO) enrichment analysis of differentially expressed proteins downregulated in IPEC-J2 cells supplemented with Inorganic Se (E) under heat stress. Bubble plots show enrichment of (A) KEGG pathways, (B) cellular components, (C) biological processes, and (D) molecular functions. The x-axis represents -log (FDR), bubble size indicated gene count, and colour represents FDR. 93

Figure 3.3-11: Protein-protein interaction network of proteins upregulated in IPEC-J2 cells supplemented with vit E and subsequently exposed to heat stress (42°C), compared to untreated heat-stressed cells- Nodes represent individual proteins, and edges indicated known or predicted functional associations between proteins. The network was generated using high-confidence interaction score (0.7) and PPI enrichment analysis yielded a p-value of 0.824, indicating that network connectivity was not greater than expected. Proteins are grouped into clusters based on interaction patterns, with colours representing distinct functional groupings. The primary cluster identified includes proteins associated with translation-related processes, including EEF2, PA2G4, and SERBP1. Disconnected nodes represent proteins with no known interactions within this dataset. 95

Figure 3.3-12: KEGG and Gene Ontology (GO) enrichment analysis of differentially expressed proteins upregulated in IPEC-J2 cells supplemented with vit E under heat stress. Bubble plots show enrichment of cellular components . The x-axis represents -log (FDR), bubble size indicated gene count, and colour represents FDR. 96

Figure 3.3-13: Protein-protein interaction network of proteins downregulated in IPEC-J2 cells supplemented with Vit E and subsequently exposed to heat stress (42°C), compared to untreated heat-stressed cells- Nodes represent individual proteins, and edges indicated known or predicted functional associations between proteins. The network was generated using high-confidence interaction score (0.7) and shows significant enrichment (PPI enrichment p-value 1.65e-14). Proteins are grouped into clusters based on

interaction patterns, with colours representing distinct functional groupings. Prominent clusters include proteins associated with glycolysis (PGK1, GAPDH), mitochondrial function and ATP synthesis (ATP5F1A, ATP6V1B2, MDH2), protein folding and ER processes (HSP90 family members, PDIA6, CALR), and cytoskeletal organisation (ACTB, ACTN4) Additional clusters include proteins involved in proteasome activity, immune-related pathways, and translation-related processes. Disconnected nodes represent proteins with limited or no known interactions within the dataset. 98

Figure 3.3-14: KEGG and Gene Ontology (GO) enrichment analysis of differentially expressed proteins downregulated in IPEC-J2 cells supplemented with Vit E under heat stress. Bubble plots show enrichment of (A) KEGG pathways, (B) cellular components, (C) biological processes, and (D) molecular functions. The x-axis represents -log (FDR), bubble size indicated gene count, and colour represents FDR. 100

Figure 3.3-15: Volcano plot illustrating protein expression between IPEC-J2 cells treated with vit C for 24 h prior to being heat stressed at 42°C for 24 h and untreated IPEC-J2 cells heat stressed for 24 h. The x-axis represents log2(fold change), and the y-axis represents -log10(p-value). Significantly upregulated proteins are shown in blue, significantly downregulated proteins are highlighted in orange and grey dots represent non-significant proteins. Horizontal and vertical dashed lines indicate the applied significance thresholds (p-value ≤ 0.05, and log2(FC) ≥ 0.585). 101

Figure 3.3-16: STRING protein-protein interaction network of proteins significantly upregulated in vitamin C treated cells at 42°C compared with untreated heat-stressed control cells- Nodes represent proteins and edges indicate known or predicted interactions. The network was generated using high-confidence interaction score (0.7) and shows significant enrichment (PPI enrichment p-value 1.64e-10). Functional clustering highlights enrichment of translation initiation, RNA splicing, DNA replication, proteasome activity, and glycolysis-related protein groups. 103

Figure 3.3-17: Pathway enrichment of proteins significantly upregulated in vitamin C treated IPEC-J2 cells at 42°C compared with untreated control cells at 42°C- Enriched KEGG pathways (A) and GO cellular components (B), biological processes (C), and molecular function (D) categories are shown. Bubble size represents the number of proteins associated with each term, and colour indicates false discovery rate (FDR). 105

Figure 3.3-18: STRING protein-protein interaction network of proteins significantly downregulated in vitamin C treated cells at 42°C compared with untreated heat-stressed control cells- Nodes represent proteins and edges indicate known or predicted interactions. The network was generated using high-confidence interaction score (0.7) and

shows significant enrichment (PPI enrichment p-value 5.01e-12). Proteins are organised into distinct clusters with prominent clusters including proteins involved in cytoskeletal organisation (ACTB, ACTN4), metabolic processes, protein folding and stress response (HSP90 family members), and RNA processing and translation. Disconnected nodes represent proteins with limited or no known interactions within the dataset. 107

Figure 3.3-19: Pathway enrichment of proteins significantly downregulated in vitamin C treated IPEC-J2 cells at 42°C compared with untreated control cells at 42°C- Enriched KEGG pathways (A) and GO cellular components (B), biological processes (C), and molecular function (D) categories are shown. Bubble size represents the number of proteins associated with each term, and colour indicates false discovery rate (FDR). 109

Figure 6.1-1: Relative IPEC-J2 cell metabolic activity following 24 h treatment with Se and vitamin compounds prior to heat stress at 42°C for 2 h- IPEC-J2 cells were treated for 24 h and maintained at 37°C (A), and heat stressed for 2 h (B) with relative metabolic activity measured using Alamar Blue assay, relative to the 37°C control group. Bars represent mean values ± SD, while dots represent individual biological replicate numerical values (n = 3). Data was analysed with One-way ANOVA with Tukey's post hoc, no significance observed. 151

Figure 6.1-2: Relative IPEC-J2 cell metabolic activity following 24 h treatment with Se and vitamin compounds prior to heat stress at 42°C for 24 h- IPEC-J2 cells were treated for 24 h and maintained at 37°C (A), and heat stressed for 24 h at 42°C (B) with relative metabolic activity measured using Alamar Blue assay, relative to the 37°C control group. Bars represent mean values ± SD, while dots represent individual biological replicate numerical values (n = 3). Data was analysed with One-way ANOVA with Tukey's post hoc, with significant marked *($p \leq 0.05$), **($p \leq 0.05$). 152

Figure 6.1-3: Relative IPEC-J2 cell metabolic activity following 48 h treatment with Se and vitamin compounds prior to heat stress at 42°C for 2 h- IPEC-J2 cells were treated for 48 h and maintained at 37°C (A), and heat stressed for 2 h at 42°C (B) with relative metabolic activity measured using Alamar Blue assay, relative to the 37°C control group. Bars represent mean values ± SD, while dots represent individual biological replicate numerical values (n = 3). Data was analysed with One-way ANOVA with Tukey's post hoc, no significance observed. 153

Figure 6.1-4: Relative IPEC-J2 cell metabolic activity following 48 h treatment with Se and vitamin compounds prior to heat stress at 42°C for 24 h- IPEC-J2 cells were treated for 48 h and maintained at 37°C (A), and heat stressed for 24 h at 42°C (B) with relative metabolic activity measured using Alamar Blue assay, relative to the 37°C control

group. Bars represent mean values ± SD, while dots represent individual biological replicate numerical values (n = 3). Data was analysed with One-way ANOVA with Tukey's post hoc, no significance observed. 154

Figure 6.2-1: Western blot images of heat-stressed IPEC-J2 cells- Cells were heat stressed for 2 h and 24 h, respectively, and samples were loaded at a protein concentration of 10 µg per lane , and membranes were incubated with target antibody (HSP70) and house-keeping antibody (Actin). Images represent 41°C (A), 42°C (B), and 44°C (C), n= 3. 155

Figure 6.2-2: Western blot images of IPEC-J2 cells treated with Se and vitamin compounds maintained at 37°C- Cells were treated with compounds for 24 h, and samples were loaded at a protein concentration of 10 µg per lane. Membranes were incubated with target antibody (HSP70) and house-keeping antibody (Actin), n= 5. 156

Figure 6.2-3: Western blot images of IPEC-J2 cells treated with Se and vitamin compounds prior to being exposed to 42°C for 24 hours- Cells were treated with compounds for 24 h,then exposed to 42°C for a further 24 hours. Samples were loaded at a protein concentration of 10 µg per lane and membranes were incubated with target antibody (HSP70) and house-keeping antibody (Actin), n= 5. 157

List of Tables

Table 1.6-1: A brief summary of HSP families, their cellular locations, and their main functions, adapted from (Hu et al., 2022). 11

Table 2.2-1: Qubit assay measurements 27

Table 3.2-1: Se concentrations (ppm) of digested organic and inorganic Se treatments as determined by ICP-OES, and the final concentration (µg/mL) added to IPEC-J2 cells 46

Table 3.3-1: Differentially expressed proteins identified in IPEC-J2 cells heat stressed at 42°C for 24 h- The table includes protein name, number of unique peptides, mean normalised abundance for each group (n = 3), fold change, direction of change, and protein-level ANOVA p-value. Proteins were filtered based on a peptide count ≥ 2, a maximum fold change ≥ 1.5, and a p-value ≤ 0.05. 71

Table 3.3-2: Differentially expressed proteins identified in IPEC-J2 cells heat stressed at 42°C for 24 h- The table includes protein name, number of unique peptides, mean normalised abundance for each group (n = 3), fold change, direction of change, and protein-level ANOVA p-value. Proteins were filtered based on a peptide count ≥ 2, a maximum fold change ≥ 1.5, and a p-value ≤ 0.05. 79

Table 3.3-3: Differentially expressed proteins identified in IPEC-J2 cells treated with Organic Se-A, compared to untreated heat-stress cells- The table includes protein name, number of unique peptides, mean normalised abundance for each group (n = 3), fold change, direction of change, and protein-level ANOVA p-value. Proteins were filtered based on a peptide count ≥ 2, a maximum fold change ≥ 1.5, and a p-value ≤ 0.05. 83

Table 6.3-1: Supplementary table containing significantly upregulated HSPs in heat-stressed IPEC-J2 cells compared to control cells maintained at 37°C 158

Table 6.3-2: Supplementary table containing all the differentially expressed proteins identified in IPEC-J2 cells heat stressed at 42°C for 24 h- The table includes protein name, number of unique peptides, mean normalised abundance for each group (n = 3), fold change, direction of change, and protein-level ANOVA p-value. Proteins were filtered based on a peptide count ≥ 2, a maximum fold change ≥ 1.5, and a p-value ≤ 0.05. 159

Abstract

Mitigating Heat-Induced Cellular Stress in Intestinal Epithelium: Insights from the IPEC-J2 Cell Line

Aoife McCormack

Heat stress (HS) represents a major challenge to livestock production due to rising global temperatures, negatively impacting the health of the animal, productivity, and welfare. The swine industry is particularly vulnerable, as pigs have limited ability to regulate their body temperature, making them susceptible to heat-induced intestinal dysfunction and impaired cellular function. In this study the porcine intestinal epithelial cell line, IPEC-J2, was used as an *in vitro* monoculture model to investigate the effects of HS and to evaluate the protective potential of five organic Selenium (Se) products, one inorganic Se source, and vitamin (E and C) supplementation. Initial studies were conducted to establish a suitable HS model. IPEC-J2 cells exposed to 41°C, 42°C, and 44°C for 2 hours and 24 hours were assessed for relative cell metabolic activity (n = 3), and expression of heat shock protein 70 (HSP70) (n = 3). Based on these results, exposure to 42°C for 24 hours was identified as the optimal condition to induce HS. Cells were subsequently treated with Se compounds at 0.2 µg/mL, vitamin E at 10.72 µg/mL, and vitamin C at varying concentrations (ranging between 25 and 300 µg/mL) for 24 and 48 hours prior to a further 24 hours heat exposure. The results demonstrated variability across Se products (n = 3). Notably, Inorganic Se (E) was associated with higher metabolic activity than untreated heat-stressed cells (n = 3) after 24-hour treatment and exhibited a similar HSP70 expression to untreated control cells at 37°C (n = 5). To further investigate the molecular mechanisms underlying these responses, proteomic analysis was performed (n = 3). HS induced alterations in proteins associated with oxidative stress, protein folding, and translational regulation. Se supplementation partially reversed these changes, supporting its role in maintaining redox balance and cellular homeostasis. IPEC-J2 monoculture model does not account for whole-animal physiological responses such as thermoregulation. Nevertheless, the findings demonstrate treatment-associated changes in cellular metabolic activity, stress responses, and protein expression patterns under HS conditions in this *in vitro* model.

1 Introduction

1.1 Animal Production

In recent years there has been an increase in global animal production, which has expanded in response to growing human dietary requirements. These increases are largely driven by rising global populations and disposable incomes worldwide (Bahar et al., 2020; Tullo et al., 2019).

Production across the major primary livestock categories has shown a steady increase over the past decade. In 2024, global meat output reached 374 million tonnes (Mt), representing a 28% increase compared with 2010. Poultry, pork, and beef were the three most widely produced meat types worldwide in 2024. Pig production increased by 17 Mt since 2010, reaching a total of 125 Mt in 2024, a 16% increase since 2010. The Americas and Asia led the global meat production in 2024. China represents 46% of global pig meat production, this is followed by the United States of America (10%), and Brazil, Spain, and the Russian Federation each at 4% (FAO, 2024).

The European Union (EU) saw a 1% increase in pig meat production in 2024 compared to 2023. Spain produced 24% of the market share in the EU, making it the largest pig meat producer in the EU in 2024, Germany made up 20%, France 10%, while Ireland made up 2% (Department of Agriculture, 2025).

1.2 Climate Change/Global Warming

Climate change has always been a concern for humans, but in the 21st century climate change is being viewed as one of the most critical concerns not only for humans but for all forms of life. The rise in global temperature is causing crucial complications with noticeable signs, notably , extreme weather events , an increase in the melting of polar ice, and the rising of sea levels . Over time, the impacts of climate change are intensifying, posing serious threats to the planet and leading to pressing consequences (Singh et al., 2017). The Synthesis Report of the IPCC Sixth Assessment Report stated that global surface temperature was 1.09°C higher in 2011-2020 compared to 1850-1900. It also predicts that there will be a further increase in global temperature, estimated to surpass 1.5°C by 2030, if the levels of greenhouse gases continue to rise (Calvin et al., 2023). With the rise in global temperature, heat waves are increasing in both frequency and duration. This is leading to health impacts on livestock and economic costs caused by heat being increased. In 2003 it was estimated that financial costs would be approximately $900

million/year in dairy products and more than $300 million/year in swine, solely in the USA (St-Pierre et al., 2003), but more recent estimates place the economic losses at US$1.5 billion for the dairy industry and US$1 billion for the swine industry in the USA alone (Key & Sneeringer, 2014; Mayorga et al., 2019).

Rising global temperatures and increases in relative humidity present significant challenges to livestock production systems (Osei-Amponsah et al., 2019). These environmental conditions compromise the thermoregulatory capacity of homeothermic animals, such as ruminants, pigs, and poultry, which normally maintain a stable body temperature within a defined thermoneutral zone (TNZ) (Joy et al., 2020). When environmental temperatures exceed the upper limit of the TNZ, animals are unable to dissipate excess heat efficiently through mechanisms such as sweating and panting, leading to an increase in body temperature, development of hyperthermia, and ultimately heat stress (HS) (Gonzalez-Rivas et al., 2020; Renaudeau et al., 2012).

1.3 Thermoregulation and Heat Stress in Swine

Pigs are one of the most affected animals by heat stress due to a limited number of functional sweat glands, and a thick layer of subcutaneous fat. Rather, when the temperature increases, vasodilation will occur in blood vessels in the skin, facilitating the transfer of warm blood from core organs to the outer organs. This enhances heat dissipation by increasing the thermal gradient between the animal and its external environment (Blatteis, 1998; Curtis, 1983). The movement of blood from core organs to peripheral organs can cause risk of reducing the blood flow to essential organs, such as less blood flow to the intestinal system, which can negatively impact the health and well-being of the pig, as necessary nutrient absorption is impaired (Collin et al., 2001; Koch et al., 2019).

As pigs are homeothermic animals, they maintain a constant body temperature, within a narrow range. This requires a finely regulated balance between heat production and heat dissipation, which is known as thermoregulation (Herpin et al., 2002). Thermoregulation is a process that is mediated through neural pathways. The process allows animals to maintain a stable internal environment by responding to their external environment through appropriate efferent responses, such as vasoconstriction or panting (Collier & Gebremedhin, 2015).

In animals, an increase in environmental temperature is detected by thermoreceptors which triggers the hypothalamus to activate physiological mechanisms to enhance heat dissipation, including sweating, an increase in respiratory rate, and a redistribution of blood flow (Gleeson, 1998). In pigs, as they lack functional sweat glands and have a thick layer of subcutaneous fat, they lose heat in the form of sensible and latent heat loss. Sensible heat loss occurs through conduction, convection, and radiation, whereas latent heat loss involves the process of evaporation of water, mainly through respiration (DeShazer et al., 2009). Conduction heat transfer takes place through the direct contact of two surfaces where the higher temperature is exchanged to the lower temperature, for example pigs lying down and wallowing in water or mud (Olsen et al., 2001). Convective heat loss occurs as a result of the temperature difference between the animal's body and the ambient air. Forced convection occurs when an external pressure gradient causes air to move across the animal's body, this is typically generated using mechanical systems such as fans to create the external pressure. Radiative heat transfer takes place between two surfaces, each emitting energy at wavelengths determined by the temperature of the emitting surface (Collier & Gebremedhin, 2015). Latent heat dissipation occurs through evaporative heat loss through the respiratory system and the skin (DeShazer et al., 2009). Two of the main autonomic responses that are exhibited by animals are sweating and panting. Sweating is a process that promotes evaporative cooling through water loss from the skin surface, whereas in panting, core body heat is used to heat water vapour which is then expelled from the lungs as vaporised moisture (Collier & Gebremedhin, 2015). As pigs have a lack of functional sweat glands, latent heat loss is mainly through respiration i.e. panting (Renaudeau et al., 2007).

Figure 1.3-1 provides a schematic representation of the relationship between the environmental temperature and heat production in pigs. Within the TNZ, pigs dissipate heat through sensible and latent heat loss, but when the ambient temperature goes above the upper critical temperature (UCT) pigs rely more on latent heat loss, by increasing their respiration rate, because sensible heat loss becomes inefficient as the temperature gradient between the skin and the ambient air decreases (Gourdine et al., 2021).

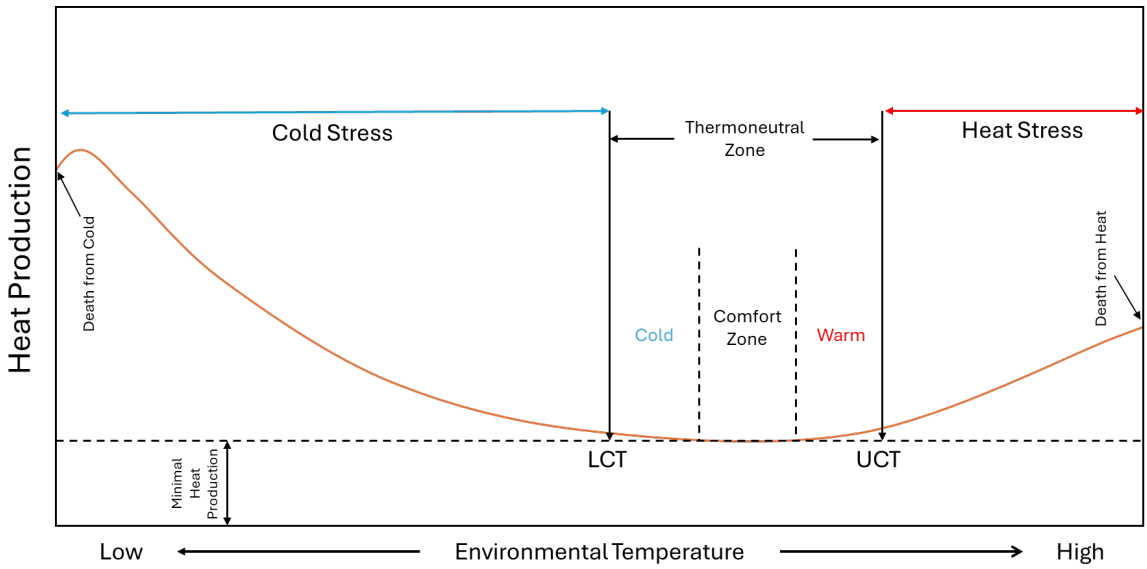


Figure 1.3-1: Thermal comfort concept in swine- image was created based on information from Vermeer and Hoofs (2024), where thermoneutral zone is the area of ambient temperature. When the environmental temperature rises, pigs reach their upper critical temperature (UCT) entering them into heat stress, but heat stress may begin in the warm section of the thermoneutral zone *(Vermeer & Hoofs, 2024)*.

A general concept of thermoregulation in animals was developed by Mount (Mount, 1979) which has been modified by Yousef (Yousef, 1985), which is shown in Figure 1.3-1. The TNZ lies between the lower critical temperature (LCT) and the upper critical temperature (UCT), within this zone pigs can maintain a constant core temperature. The TNZ varies depending on the animals' size, breed, feed intake, and environmental factors including the activity of the animal. Within the TNZ there is cold, comfort zone, and warm. In the cold zone, a reduction in heat loss can be achieved by behavioural changes such as huddling with other animals. In the comfort zone, animals do not need to adapt in any way to account for heat loss. In the warm zone, behavioural changes are used to regulate heat loss, in this case animals will rest in cool places such as shaded space, or on wet areas. If the temperature drops below the LCT, the animals' body temperature will also drop which can lead to cold stress. In response to this, the animal will aim to increase its body temperature through shivering thermogenesis. Whereas if the temperature rises above the UCT, animals will start showing signs of heat stress, for example their respiration rate will increase, they will increase their water intake, and their food intake will decrease (Vermeer & Hoofs, 2024).

1.4 Small Intestinal Epithelium Structure and Function

A healthy gastrointestinal tract (GIT) plays a critical role in nutrient digestion and absorption while acting as a barrier to prevent the translocation of pathogens and toxins from the intestinal lumen into the body (Liao & Nyachoti, 2017). The small intestinal epithelium consists of a single layer of specialised epithelial cells organised along a villus-crypt structure, which enables efficient nutrient absorption and continuous epithelial renewal. While enterocytes account for approximately 90% of the epithelial cell population, several other cell types contribute to intestinal function, including goblet cells which secrete mucus, Paneth cells which produce antimicrobial peptides, enteroendocrine cells that are involved in hormone secretion, microfold cells which participate in immune surveillance, and intestinal stem cells that are located at the base of the crypts which drive constant epithelial regeneration (Ali et al., 2020; Yu et al., 2024).

Overlaying the epithelium, the intestinal mucus layer serves as the first line of defence against intestinal injury, creating a physical barrier that protects the intestinal surface from bacteria and antigens while facilitating the movement of luminal contents (Herath et al., 2020). Beneath the epithelium, within the lamina propria, resides a substantial proportion of the body's immune cells, forming a highly specialised mucosal immune system. This establishes a well-defined and complex interaction between the gut microbiota, the epithelial barrier, and the underlying immune components, which together maintain intestinal homeostasis and protect against infection (Furness et al., 1999; Wiertsema et al., 2021).

1.4.1 Intestinal Health of Swine During Heat Stress

The intestinal epithelium of the small intestine serves as a defence mechanism, preventing the entry of harmful substances into the bloodstream, and is also important in the uptake of nutrients. A healthy intestinal barrier, Figure 1.4-1(A), primarily consists of a single layer of intestinal epithelial cells that are tightly interconnected via intercellular junctions called tight-junction proteins (TJs). A mucin layer covers the luminal surface of the cells comprised of a loose outer and an inner compact layer. Both of these components prevent the entry of any unwanted substances into the bloodstream (Ringseis & Eder, 2022).

Covering the luminal surface, the intestinal mucus layer forms the first line of extracellular defence, composed of secreted mucins, antimicrobial molecules, and immunoglobulins that provide both physical protection and targeted antimicrobial activity

(Johansson et al., 2013; McGuckin et al., 2011). This mucus layer consists of a loosely organised outer layer and a dense inner layer, primarily produced by specialised goblet cells distributed throughout the epithelium. The major gel-forming mucin, MUC2, is responsible for generating the continuous gel-like structure that lubricates the epithelial surface, maintains a stable microenvironment, and protects against luminal stressors such as pathogens and acidic conditions (Johansson et al., 2011; Oswald, 2006). In addition to goblet cells, other specialised cell types, including Paneth cells located at the base of crypts, contribute to host defence through the secretion of antimicrobial peptides. However, under stress conditions, the integrity of the intestinal barrier is compromised (Figure 1.4-1 B), with disruption of TJs and a reduction in mucus layer thickness, partly due to decreased MUC2 expression, leading to increased intestinal permeability and facilitating the translocation of harmful substances into the bloodstream (Fan et al., 2025; Yi et al., 2020).

The disruption of TJs which causes increased intestinal permeability can be referred to as “leaky gut”. Heat stress induced “leaky gut” broadly affects intestinal function by impairing barrier integrity and nutrient absorption. The resulting damage includes weakened mechanical defences, thinning of the chemical barrier, microbial imbalance, and altered immune responses (Fan et al., 2025).

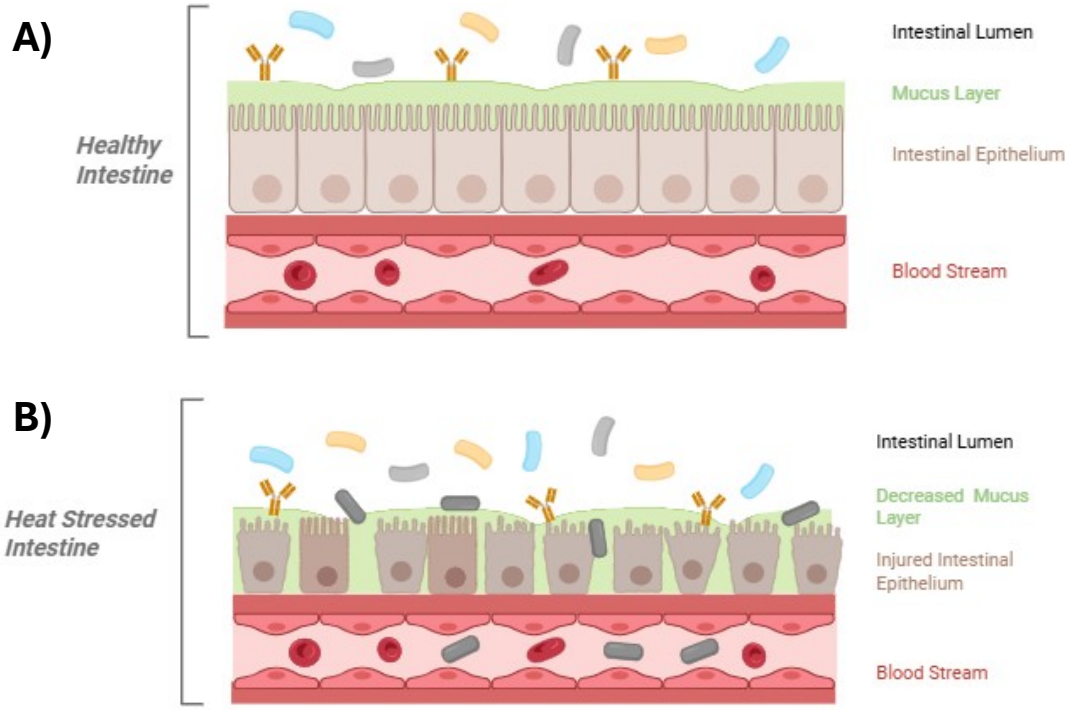


Figure 1.4-1: Schematic representation of a healthy and a heat-stressed intestinal tract- Image created using Biorender based on information from Fan, Tian and Li (2025). Image A depicts a healthy intestine consisting of columnar cells protected by a mucus layer containing immunoglobulins, which prevent the entry of harmful substances into the bloodstream. Image B illustrates an intestinal tract exposed to heat stress, distinguished by TJ disruption, compromised epithelial integrity, increased intestinal permeability, and mucosal atropy, facilitating the entry of unwanted substances into the bloodstream *(Fan et al., 2025)*.

1.5 Heat Shock Response

The heat shock response (HSR) is an essential component of the body's protective system against excessive heat. It also plays a broader role in coping with diverse stress conditions, including pathological and physiological challenges. The induction of the HSR is associated with protein misfolding; under normal conditions proteins maintain their native structure and function, however elevated temperatures can induce protein misfolding and aggregation which act as intracellular signals that will trigger the HSR (Parsell & Sauer, 1989; Sun et al., 2024).

One of the primary regulators of the eukaryotic cellular response to heat stress is the highly conserved heat shock factor (HSF) family of transcription factors. In vertebrates, this family comprises four members, HSF1, HSF2, HSF3, and HSF4, with HSF1 acting as the principal regulator of the HSR, while HSF2 and HSF4 exhibit broader or tissue specific

expression patterns, and HSF3 has been most extensively studied in avian species (Åkerfelt et al., 2010; Mahat et al., 2016). Under physiological conditions, heat shock factor 1 (HSF1) remains bound to heat shock protein (HSP) as an inactive monomer. However, during cellular stress, such as heat stress, the accumulation of misfolded and denatured proteins in the cytosol promotes the dissociation of the HSF1-HSP complex. Activation of HSF1 is associated with trimerization, nuclear localisation, binding to heat shock elements (HSEs) in the promoter regions of target genes, and post-translational modifications, ultimately initiating the transcriptional activation of HSPs (Figure 1.5-1) (Joly et al., 2010; Lian et al., 2020; Otaka et al., 2006). The conversion of HSF1 from its inactive form to active form is thought to be a multistep process. These include trimerization of HSF1 from its monomeric state, conformational changes that reveal transcriptionally active domains, and stress-induced hyperphosphorylation of HSF1 (Mercier et al., 1999).

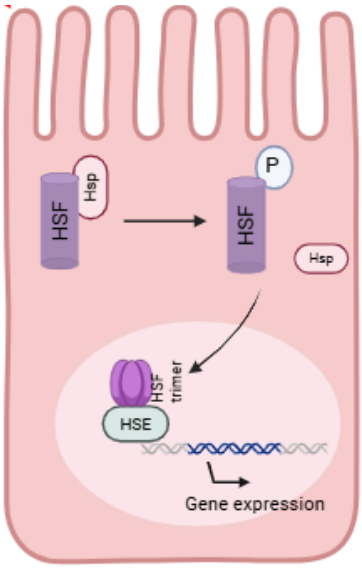


Figure 1.5-1: Visual representation highlighting heat-induced heat shock response- The HSR is activated in response to cells exposed to heat stress, the accumulation of misfolded proteins in the cytoplasm leads to the translocation and trimerization of HSF1 from the cytoplasm into the nucleus initiating the HSR pathway. Within the nucleus HSF1 binds to regulatory heat shock elements, which causes the gene expression of heat shock proteins, image created with Biorender based off Lian *et al*. 2020, *(Lian et al., 2020)*.

1.6 Heat Shock Proteins

A group of proteins, called heat shock proteins (HSPs), are induced in response to various environmental or metabolic stressors including hypoxia, viral agents, and heat. These proteins are also referred to as stress proteins as they can be induced by a variety of environmental and physiological stressors, not solely heat stress. However, they are most commonly known as HSPs (Mikhailova et al., 2025; Singh et al., 2024).

The activation of HSPs in response to heat stress is triggered by the heat shock response. HSPs belong to a large family of highly conserved stress proteins, produced in both prokaryotic and eukaryotic cells, and are named after their molecular weight. These proteins exhibit a wide range of molecular weights and biological functions; however, they generally serve as molecular chaperones in response to heat, hypoxia, and/or oxidative stress (Craig, 1988; Snoeckx et al., 2001). HSPs were first identified following the observation that heat exposure induced chromosomal puffing in the salivary glands of *Drosophila*. Diverse stressors, such as heat, viral agents, ischemia, and anoxia, trigger the expression of heat shock protein genes that are characterized by a high degree of DNA sequence conservation across species (Whitley et al., 1999). HSPs can be defined as molecular chaperones, meaning they interact with, stabilise, or help other proteins return to their native, active conformation, without being present in the final structure themselves (Hartl & Hayer-Hartl, 2009).

HSPs can be classified into six major families based on their approximate molecular weights, shown in Table 1.6-1, namely small HSPs, HSP40, HSP60, HSP70, HSP90, and HSP110 (Hu et al., 2022; H. Liu et al., 2014).

Table 1.6-1: A brief summary of HSP families, their cellular locations, and their main functions, adapted from *(Hu et al., 2022)*.

HSP Family	Major Members	Cellular Location	Main Functions
HSP110	HSP110	Cytoplasm/Nucleus	Chaperone activity/Thermal tolerance
HSP90	HSP90 GRP94/GP96	Cytoplasm ER	Involved in cell proliferation/binds to other proteins/maintains HSF1 monomeric state under normal conditions
HSP70	HSP70 HSC70 BiPmHSP70	Cytoplasm/nucleus Cytoplasm/peroxisome ER Mitochondrion	Assists in protein folding, prevents aggregation, facilitates protein translocation
HSP60	HSP60 TRiC	Mitochondrion Cytoplasm	Protein foldase
HSP40	DNAJA, DNAJB, DNAJC	Cytoplasm	Co-chaperone for HSP70/ regulates ATPase activity and substrate binding
Small HSPs	HSPB1-HSPB10 HSP27	Cytoplasm, Nucleus, Mitochondria Cytoplasm/nucleus	Chaperone activity Chaperone activity/actin dynamics

1.6.1 Heat Shock Protein 70 (HSP70)

Among the HSP families, HSP70 is one of the most conserved and inducible molecular chaperone protein. The protein has approximately 60% phylogenetic similarity between microbes and mammals (Bardwell & Craig, 1984). HSP70 is widely expressed across different tissues and is one of the most abundant and well-characterised HSP. In the small intestinal epithelium, HSP70 is one of the most prominent HSP, contributing to the maintenance of epithelial integrity and cellular protection during stress. They are essential in the protection of the mucosal barrier under both normal and stressed conditions and are widely used in assessing the molecular stress response of different organisms under heat and other stress conditions (Daugaard et al., 2007; Petrof et al., 2004). In prokaryotes the

protein expressed is DnaK, whereas HSP70 is the eukaryote counterpart. HSP70 can be found in multiple different cellular locations, including the cytosol, nucleus, endoplasmic reticulum (ER), and mitochondria. Their main role is to keep the balance of protein synthesis, folding, degradation, and translocation (Hu et al., 2022).

Under normal physiological conditions, HSP70 is involved in the folding of newly synthesized polypeptides, the assembly of multiprotein complexes, and the translocation of proteins across cellular membranes. In addition, HSP70 possesses anti-apoptotic properties, acting on multiple apoptotic pathways both upstream and downstream of the mitochondria. These effects include inhibition of early stress-induced signalling events, reduction of reactive oxygen species (ROS), and stabilizing pro-survival proteins such as kinases. This means that cell survival and resistance to stress is promoted with the presence of HSP70 (Arnal & Lallès, 2016; Joly et al., 2010). In times of cellular stress, such as heat, HSP70 helps protein folding, ubiquitination, renaturation, and protection (Kim et al., 2018).

Studies in intestinal epithelial cells have shown that heat stress leads to an upregulation of HSP70 (Musch et al., 1996; J. Tang et al., 2019). The upregulation of HSP70 may contribute to the protection of epithelial cells against oxidant and thermal injury (Cao et al., 2016; Musch et al., 1996; Pearce et al., 2013). Supporting this, a study by Musch *et al*. using rat intestinal epithelial IEC-18 cells, demonstrated a significant increase in HSP70 expression in response to heat stress, highlighting its role in cellular protection under stress conditions (Musch et al., 1996).

1.7 Strategies to Mitigate Heat Stress

In order to maintain homeothermy in pigs, mitigation strategies must focus on either reducing metabolic heat production or enhancing heat dissipation from the body. More recently, studies have been conducted towards the development of nutritional (Santos et al., 2018), environmental, and genetic strategies to alleviate the adverse effects of heat stress on pig production (Katiyar et al., 2025).

A number of environmental modifications can be used to alleviate the effects of a hot climate in animal production. Some examples include providing natural or artificial shade to reduce the solar radiation around the animal, reducing the air temperature using air conditioning or fans, and sprinkler systems can provide cooling by the addition of water directly to the skins surface. It is also important to have a constant and sufficient supply of

water to the animal, and to adjust feeding times to prevent eating during the hottest parts of the day (Renaudeau et al., 2012; Sejian et al., 2018).

As well as these environmental strategies, nutritional interventions have been used to mitigate the effects of heat stress in pigs. The addition of numerous antioxidants, including certain vitamins (E and C) and micro-minerals Selenium (Se) and Zinc (Zn), have been shown to prevent cell damage and enhance intestinal integrity in animals subjected to heat stress (F. Liu et al., 2016; Ortega et al., 2022). This study aimed to investigate the nutritional strategies of Se and vitamin compounds to mitigate the effects of heat stress on the intestinal tract of swine.

1.7.1 Selenium

Selenium (Se) is an essential trace element across all mammalian species. It exists in nature in both organic and inorganic forms. Organic forms of Se are selenomethionine (SeMet), and selenocysteine (SeCys), while the main inorganic forms include selenite (SeO_3^{2-}), selenate (SeO_4^{2-}), selenide (Se^{2-}), and elemental Se (Se^0) (Sharma et al., 2017; Zheng et al., 2022). The biological effects of Se are mediated by its incorporation into selenoproteins (SelP) in the form of SeCys, which is widely recognised as the 21st amino acid (Hoffmann, 2007). Driven by SelPs, Se exerts a wide range of physiological effects, including antioxidant and redox regulation, thyroid metabolism, reproduction, and muscle function (Kyoung et al., 2025). Heat-induced damage to the gastrointestinal barriers is associated with disruptions in membrane integrity, receptor activity, and transmembrane transport protein function. Se contributes to cellular protection by inhibiting apoptosis and attenuating heat stress-induced inflammatory responses (Zheng et al., 2022).

Se functions in antioxidant defence, immune function, and redox regulation through its incorporation into SelPs. These include glutathione peroxidase (GPX) enzymes, which catalyse the reduction of any harmful reactive oxygen species (ROS), and thioredoxin reductase (TrxR), which maintains intracellular redox balance by regulating the thioredoxin system and supporting the removal of oxidative stress induced radicals that may be produced during a high stress situation (Gan et al., 2014; Maggini et al., 2007). Tang *et al*. demonstrated that in heat-stressed IPEC-J2 cells, TJ proteins including claudin 1, occludin, and ZO-1 were downregulated, but cells supplemented with SeMet and sodium selenite (SS) increased the levels of these TJ proteins, concluding that the supplementation of SeMet and SS slow down the damage of TJ proteins. They also showed

that SeMet supplementation promotes HSP70 mRNA and protein levels in heat-stressed IPEC-J2 cells (J. Tang et al., 2019).

This study used concentrations of Se in accordance with the latest version of Nutrient Requirements of Swine. It is recommended that a concentration of 0.2ppm of Se is an appropriate level for growing pigs (National Research Council, 2012). In countries adhering to European Commission regulations, Se levels are limited to 0.5 mg/kg in complete feed, this is including contributions from both raw materials and supplements, of which no more than 0.2 mg/kg of Se may originate from organic sources (European Commission, 2019). Therefore, in this study cells were treated with 0.2 µg/mL Se.

1.7.2 Vitamins

Vitamins are essential trace organic micronutrients required for the proper functioning of metabolic pathways, immune responses, and gene regulation. Vitamins are classified into two groups: fat soluble and water soluble. The fat-soluble vitamins include vitamins A, D, E, and K, while the water-soluble group contains vitamins B and C (Upadhaya & Kim, 2020). Dietary supplementation of vitamins has been shown to reduce the impact of various stressors in animals, with studies demonstrating that vitamins, such as vitamin C and vitamin E, can help mitigate environmental stressors, including heat stress in pigs (Smołucha et al., 2024).

1.7.2.1 Vitamin E

Vitamin E is an essential micronutrient with diverse biological roles in animals. It exists in eight naturally occurring forms, classified into tocopherols and tocotrienols, with D-α-tocopherol being the most biologically active form (Shastak & Pelletier, 2025). In pigs, vitamin E primarily functions as an antioxidant by protecting cellular membranes from oxidative damage by neutralising free radicals (Boler et al., 2009; Pinelli-Saavedra, 2003). As vitamin E cannot be synthesized endogenously in animals, it must be supplemented into their diet (Widyasanti et al., 2025). The National Research Council and MSD Veterinary Manual recommend that 11-16 IU/kg as adequate levels of vitamin E for growing pigs (MSD Veterinary Manual, 2025; National Research Council, 2012). Under conditions of heat stress, the requirement for vitamin E may increase. Research suggests that supplementation with elevated levels of vitamin E may help alleviate heat stress-induced respiratory alkalosis. Liu et al. (2018) reported that while vitamin E supplementation did

not significantly reduce oxidative stress under heat stress conditions, it did mitigate respiratory alkalosis (F. Liu et al., 2018). Furthermore, combined supplementation of vitamin E and Se have been shown to improve intestinal integrity and function in heat-stressed pigs by enhancing intestinal epithelial function, reducing oxidative stress, and promoting overall intestinal health (F. Liu et al., 2016). These findings highlight the potential role of vitamin E as a protective agent against heat stress-induced cellular damage.

1.7.2.2 Vitamin C

Vitamin C (ascorbic acid) plays a crucial role in immune defence as it supports both innate and adaptive immune system cellular functions. It also exhibits antioxidant activity by readily donating electrons, thereby protecting biomolecules from oxidative damage generated during normal cellular metabolism and exposure to environmental toxins (Mainardi et al., 2024). While most animal species are capable of synthesising vitamin C endogenously, this capacity may be insufficient under conditions of physiological stress, when demand increases and synthesis becomes limited, although it typically returns to baseline once the stress is removed (Smołucha et al., 2024; Yin et al., 2018). In pigs, dietary vitamin C is not considered essential under normal conditions due to endogenous synthesis (MSD Veterinary Manual, 2025), however stressors may increase the demand for this vitamin. In the context of heat stress, supplementation with vitamin C can alleviate the negative effects of heat stress in pigs. For example, a study using pig thoracic vertebral chondrocytes (PTVCs) demonstrated that heat stress (41°C) reduced PTVC proliferation compared to control conditions (37°C), while supplementation with vitamin C (50-400 μM) in heat-stressed cells increased the proliferation, compared to untreated heat-stressed cells (Yang et al., 2024). Given the lack of dietary requirements for vitamin C supplementation in swine, this study investigated the effects of a range of vitamin C concentrations in IPEC-J2 cells to determine an appropriate level for reducing heat stress-induced cellular damage.

1.8 Aim of Project

The central questions that this study addressed were whether heat stress reduces IPEC-J2 cell metabolic activity and increases HSP70 expression, and whether supplementation with Se and vitamin compounds influences these cellular responses under heat stress conditions.

The primary objective was to establish and characterise an *in vitro* heat stress model using IPEC-J2 cells, and evaluate the effects of Se, and vitamin supplementation on cellular metabolic activity under heat stress conditions. The intestinal porcine enterocyte cell line (IPEC-J2) is derived from the jejunum of a neonatal unsuckled piglet. It is a non-transformed cell line thus serving as an effective model to investigate intestinal epithelial functions, and epithelial interactions with enteric bacteria and viruses (Vergauwen, 2015).

The objectives of this thesis were:

- Establish and characterise an *in vitro* heat stress model by investigating the metabolic activity of IPEC-J2 cells exposed to heat stress at 41°C, 42°C, and 44°C for 2 hours (h) and 24 hours (h), respectively, relative to cells maintained at optimal temperature of 37°C, using the Alamar Blue® (AB) assay.
- To determine whether heat stress alters HSP70 expression in IPEC-J2 cells using Western blot analysis.
- To identify a suitable heat stress condition for subsequent experiments based on metabolic activity changes and HSP70 expression.
- To evaluate the effects of supplementation with Organic Se-A/ B/ C/ D/ F, Inorganic Se (E), and vitamins (E and C) on cellular metabolic activity following heat exposure.
- To assess treatment-associated changes in HSP70 expression as a marker of the cellular heat stress response.
- To investigate heat stress and treatment-associated changes in protein expression using label-free quantitative proteomic analysis.

.

2 Materials & Methods

2.1 Reagents & Materials

2.1.1 Purchased Reagents

Reagent	Supplier	Catalogue Number
(±)-α-Tocopherol (vitamin E), ≥ 96%	Sigma Aldrich, St. Louis, MO, USA	T3251
Ascorbic Acid (vitamin C), ≥ 99.0%	Sigma Aldrich, St. Louis, MO, USA	A5960
Bovine Serum Albumin, pH 7, ≥ 98%	Sigma Aldrich	A7906
Buffer RLT	Qiagen	1015750
Dulbecco's Modified Eagle Medium (DMEM)	Merck	D6546
Fetal Bovine Serum (FBS), New Zealand	Thermo Fisher Scientific	10091148
Gibco L-glutamine (200 mM)	Fisher Scientific	11500626
Goat anti-mouse IgG Superclonal secondary antibody, HRP	Invitrogen, Carlsbad, CA, USA	A28177
Hank's Balanced Salt Solution (HBSS)	Gibco	14025-050
Hydroxy-selenomethionine (Organic Se- D)	Confidential	Confidential
Invitrogen Alamar Blue® Reagent	Fisher Scientific	10099022
IPEC-J2 Cell Line	DSMZ, Braunschweig, Germany	ACC-701
Laemmli Sample Buffer	BioRad	161-0737
Mercaptoethanol, ≥ 99%	Sigma Aldrich	M6250
Mouse monoclonal anti β-actin antibody (AC-15)	Invitrogen, Carlsbad, CA, USA	AM4302
Mouse monoclonal anti-HSP70 (3A3)	Thermo Fisher Scientific, Waltham, MA, USA	MA3-006
NuPAGE MES SDS Running Buffer (20X)	Invitrogen	NP0002

Organic Se (Organic Se-F)	Confidential	Confidential
Page-Ruler pre-stained Protein Ladder	Thermo Fisher Scientific	26619
Pancreatin from porcine pancreas, 8 x USP	Sigma Aldrich	P7545
Pepsin from porcine gastric mucosa, ≥ 250 units/mg solid	Sigma Aldrich	P7000
Protease Inhibitor Cocktail	Sigma Aldrich	P8340
Qubit Assay	Thermo Fisher Scientific	Q33211
Qubit Protein Assay	Thermo Fisher Scientific	Q33211
Selenium-enriched yeast (Organic Se-**A)**	Confidential	Confidential
Selenium-enriched yeast (Organic Se-B)	Confidential	Confidential
Selenium-enriched yeast (Organic Se-C)	Confidential	Confidential
Sodium Selenite (Inorganic Se (E)), 99%	Sigma Aldrich, St. Louis, MO, USA	214485
Super Signal TM West Femto trial kit	Invitrogen	34094
Transfer Buffer	Thermo Fisher Scientific	84731
Trypan Blue Staining	Sigma	T8154
Trypsin EDTA	Merck	T4049
TWEEN 20	Sigma	P1379

2.1.2 Materials

Name	**Supplier**
Cell Culture Flask T-25, vent cap (Cat No. 353109)	Corning
Cell Culture Flask, T-175, vent cap (Cat No. 83.3912.002)	Sarstedt
Cell Culture Flask, T-75, vent cap (Cat No. 83.3911.002)	Sarstedt
Cell scraper	Sarstedt
Corning 6-well Cell Culture Plate, flat bottom with lid, tissue culture treated, non-pyrogenic (Cat No. 3516)	Corning

Corning 12-well Cell Culture Plate, flat bottom with lid, tissue culture treated, non-pyrogenic (Cat No. 3513)	Corning
Corning 96-well Assay Plate, black plate, clear bottom with lid, tissue culture treated (Cat No. 3603)	Corning
Corning Sterile Serological Pipette (including 5 ml, 10 ml, and 50 ml)	Fisher Scientific
Invitrogen Countess Cell Counting Chamber Slides	Fisher Scientific
Pre-cast Bis-Tris gels, mPAGE 4-20%, 12 well, 1 mm (MP42G12)	Merck
PVDF Transfer Membrane, 0.45 µm (Cat No. 88518)	Thermo Fisher Scientific
Sterile Pipette Tips	Sarstedt
Sterile Screw Cap Tubes (including 15ml and 50ml)	Sarstedt
Whatman Gel Blotting Paper	Cytiva
Zeba Spin Desalting Columns	Fisher Scientific

2.1.3 Prepared Reagents

Reagent	**Recipe**
1X MES SDS Running Buffer	50 mL 20X stock, 950 mL H_2O
Blocking Solution	2.5 g milk marvel, 0.5 g Bovine serum albumin, PBST 0.05% Tween 20
PBST (0.05% Tween 20)	1L H_2O, 10 PBS tablets, 500 µL Tween 20
QuBit Standards	190 µL working solution, 10 µL standard (1-3)
QuBit Working Solution	1000 µL buffer, 5 µL protein reagent
SDS Running Buffer	950 µL Laemmli buffer, 50 µL mercaptoethanol
Super Signal West Femto	5 mL H_2O, 100 µL reagent A, 100 µL reagent B

2.2 Methods

2.2.1 Cell culture techniques

2.2.1.1 Cell Lines

The porcine jejunal epithelial cells, IPEC-J2 cells (DSMZ ACC-701, DSMZ, Braunschweig, Germany), were cultured in Dulbecco's modified Eagle medium (DMEM,

Sigma Aldrich) supplemented with 10% foetal bovine serum (FBS, Gibco) and 1% L-glutamine (Gibco). No antibiotics were included in the culture medium. Cells were grown at 37°C in a 5% CO_2 humidified incubator (Forma Steri-Cycle CO_2 Incubator, Model No:371, Thermo Fisher Scientific). Experiments were conducted using cells between passages 15 and 30. Cells were passaged at approximately 70-80% confluency every 3-4 days following enzymatic detachment using Trypsin EDTA (Gibco). All cell culture procedure were conducted aseptically in a Class II Biological Safety Cabinet (BioAir SafeFlow 1.2-BS, Euroclone). IPEC-J2 cells were isolated from the jejunum of a neonatal unsuckled piglet, it is a non-transformed, non-tumorigenic cell line (Geens & Niewold, 2011; Vergauwen, 2015).

2.2.1.2 Recovery of Cryopreserved Cells

IPEC-J2 cell lines were kept frozen in liquid nitrogen. Dulbecco's modified Eagle medium (DMEM, Sigma) supplemented with 10% foetal bovine serum (FBS) and 1% L-glutamine was pre-warmed at 37°C. Cells were removed from liquid nitrogen and placed at 37°C until partially thawed. 10 mL of pre-warmed DMEM was placed in tube, then using a Pasteur pipette the media was transferred from the tube to the vial of cells, carefully pipetting up and down. This was repeated until all the cells were taken up. The solution was centrifuged for 5 minutes at 1500 rpm in centrifuge (Eppendorf, 5804). The pellet was resuspended in 3 mL of media, and this was placed in a newly labelled T-25 flask. The flask was filled with a further 3 mL of pre-warmed media, so final volume was 6 mL. The flask was placed in 37°C incubator with 5% CO_2. Once cells were 70% confluent, they were passaged into larger T-75 flasks (Section 1.2.1.3).

2.2.1.3 Routine Maintenance of Cell Lines

Adherent cells were passaged at approximately 70-80% confluency. Trypsin EDTA (Gibco) was used to detach cells from flasks by adding pre-warmed Trypsin to flask (approximately 3 mL in a T-25, 5 mL in T-75, and 8 mL in T-175) then incubating the flask at 37°C for approximately 5 minutes, or until the cells were detached. Trypsin was inactivated by the addition of the same amount of DMEM (Sigma) supplemented with 10% FBS (Gibco) and 1% L-glutamine (Gibco). Solution was transferred to a tube, and cells were pelleted by centrifugation for 5 minutes at 1500 rpm (Eppendorf, 5804). The pellet was then resuspended in 5-10 mL of fresh pre-warmed media and cells were counted using a

haemocytometer, with desired number of cells being added to a new flask containing fresh media (T-25 flask contained 5ml, T-75 contained 15ml and T-175 contained 30 mL of media).

2.2.1.4 Relative Metabolic Activity of IPEC-J2 cells Exposed to Heat Stress (Alamar Blue®)

The relative metabolic activity of IPEC-J2 cells was determined using Alamar Blue® (Thermo Fisher) reagent. IPEC-J2 cells were seeded at a density of $1x10^4$ cells per mL in a 96-well plate (growth area of 0.32 cm^2 per well) with 100 µL in each well, yielding a seeding density of $1x10^3$ cells per well. Columns 1 and 12 were left blank, containing just media, while columns 2-11 contained cells, resulting in 10 technical replicates. The plates were incubated overnight at 37°C in a 5% CO_2 humidified incubator (Forma Steri-Cycle CO_2 Incubator, Model No:371, Thermo Fisher Scientific) to allow attachment of cells to the bottom of the wells. The following day plates were divided into control (CON) group (exposure to 37°C for 2 h and 24 h, respectively) and the heat stress (HS) group (exposure to higher temperature, 41°C, 42°C, or 44°C, for 2 h and 24 h, respectively). Heat stress conditions were selected in accordance with established IPEC-J2 heat stress models reported in literature (Cui et al., 2022; J. Tang et al., 2019; Zhou et al., 2020). HS groups were transferred to higher temperature incubator, while CON groups remained in 37°C incubator. After incubation time, Alamar Blue® reagent was added to each well at the manufacturers recommended 10% v/v reagent-to-medium ration, therefore 10 µL was added to each well and the plates were placed back in 37°C incubator for 3-4 h. The optical density values were determined using microplate reader by fluorescence with excitation at 545 nm and emission at 590 nm. This procedure was repeated so a total of 3 biological replicates were carried out. Fluorescence values from blank wells containing culture medium and Alamar Blue® reagent were subtracted from all experimental readings of wells containing cells. Results were normalised to 37°C Con plates using the formula: Relative Metabolic Activity (%) = (Heat stress fluorescence / Control fluorescence) x 100. Statistical analysis was carried out using GraphPad Prism, with statistical comparisons conducted using One-way ANOVA and post hoc Tukey's tests, with significance threshold of $p \leq 0.05$ applied.

2.2.1.5 Toxicity Assay (vitamin C)

IPEC-J2 cells were seeded in a 96-well plate (growth area of 0.32 cm^2 per well) at a density of $1x10^4$ cells per mL, with 100 µL in each well, yielding a seeding density of $1x10^3$ cells per well, leaving column 1 blank with just media. The plates were placed at 37°C in a 5% CO_2 incubator (Forma Steri-Cycle CO_2 Incubator, Model No:371, Thermo Fisher Scientific) overnight. The next day vitamin C solution was prepared at a concentration double the final desired concentration. Serial dilution was carried out to prepare solutions so final concentrations of vitamin C in the wells were 600, 500, 400, 300, 200, 100, 50, 25, 10, and 5 µg/mL. Using a multi-channel pipette, each of the pre-prepared solutions was added to the corresponding well of the plate with the highest concentration in column 12 and lowest in column 3. Media was added to column 2 which acted as the control. Once the vitamin C was added the plate was placed back in 37°C incubator for 48 h. After incubation, 20 µL of Alamar Blue® reagent was added to each well of the plate and the optical density values were determined using microplate reader by fluorescence with excitation at 545 nm and emission at 590 nm after 3-4 h incubation. Statistical analysis was carried out using GraphPad Prism, with statistical comparisons conducted using One-way ANOVA and post hoc Tukey's tests, with significance threshold of $p \leq 0.05$ applied.

2.2.1.6 Relative Metabolic Activity of IPEC-J2 Cells Following Selenium or vitamin treatment and Heat Stress (Alamar Blue®)

IPEC-J2 cells were seeded in a 96-well plate (growth area of 0.32 cm^2 per well) at a density of $1x10^4$ cells per mL with 100 µL in each well, yielding a seeding density of $1x10^3$ cells per well. The plates were placed at 37°C (Forma Steri-Cycle CO_2 Incubator, Model No:371, Thermo Fisher Scientific) overnight to allow for attachment. The following day plates were grouped into 24-hr treatment, and 48-hr treatment, then the Selenium treatments at 0.2 µg/mL(Bampidis et al., 2024; National Research Council, 2012), vitamin E at 10.72 µg/mL (MSD Veterinary Manual, 2025; National Research Council, 2012), and vitamin C at 25 µg/mL (post toxicity assay) were added to each plate in the respective wells. The plates were placed back in 37°C for their respective treatment time. After treatment plates were grouped into control group (CON, exposure to 37°C for 2 h and 24 h respectively) and heat stress group (HS, exposure to higher temperature for 2 h and 24 h respectively). Following the respective times of HS the plates were removed and 10 µL of Alamar Blue® was added to each well of the plate which was then placed at 37°C for a

further 3-4 h. The optical density values were determined using microplate reader by fluorescence with excitation at 545 nm and emission at 590 nm. Statistical analysis was carried out using GraphPad Prism, with statistical comparisons conducted using One-way ANOVA and post hoc Tukey's tests, with significance threshold of $p \leq 0.05$ applied.

2.2.1.7 Morphological changes in IPEC-J2 cells exposed to heat stress

Cells were grown in DMEM High Glucose media supplemented with 10% FBS and 1% L-glutamine. Cells were seeded in 6-well plates (growth area of 9.5 cm^2 per well) at a density of 5 x 10^5 cells per mL, with 2 mL in each well, yielding a density of 1 x 10^6 per well and placed in 37°C incubator (Forma Steri-Cycle CO_2 Incubator, Model No:371, Thermo Fisher Scientific) overnight to allow for attachment. A total of three technical replicates were performed. The following day CON group flasks were kept at 37°C while HS group were placed in 42°C incubator for 2 h and 24 h, respectively. After incubation times flasks were removed from incubator and images were captured using a phase-contrast microscope in Dublin City University with help from Dr. Finbarr O'Sullivan. Images were captured from three randomly selected fields of view per condition. Imaging was not performed under blinded conditions.

2.2.2 Treatment Preparation

2.2.2.1 Preparation of buffers/reagents for in vitro digestion

- 0.1M sodium phosphate buffer, pH 6.0, was prepared by dissolving 7 g of Na_2HPO_4 (Sigma Aldrich) in 250 mL of water and 6 g of NaH_2PO_4 (Sigma Aldrich) was dissolved in 250 mL of water. Then 61.5 mL of Na_2HPO_4 and 438.5 mL of NaH_2PO_4 were placed in 1L flask and filled to the 1L mark with water.
- 0.2M sodium phosphate buffer, pH 6.8, was prepared by dissolving 14 g of Na_2HPO_4 (Sigma Aldrich) in 250 mL of water and 12 g of NaH_2PO_4 (Sigma Aldrich) in 250 mL of water. Then 112.5 mL of Na_2HPO_4 and 127.5 mL of NaH_2PO_4 were placed in 500 mL glass bottle and filled to 500 mL mark with water.
- 1M HCl was prepared by adding 100 mL of water to 100 mL glass bottle. Then 8.6 mL of this water was removed and in fume hood 8.6 mL of HCl was added to the water.

- 0.2M HCl was prepared by placing 80 mL of water in 100 mL glass bottle. To this 20 mL of previously prepared 1M HCl was added to the bottle.
- 1M NaOH was prepared by dissolving 4 g of NaOH (Sigma Aldrich) in 100 mL of water.
- 0.6M NaOH was prepared by dissolving 2.4 g of NaOH in 100 mL of water.

2.2.2.2 In vitro digestion procedure

An enzymatic digestion was applied to Se compounds (A-F), vitamin E, and vitamin C using a modified three-step in vitro digestion model originally described by Boisen and Fernandez (Boisen & Fernandez, 1997), with experimental volumes adapted from Meunier et al. (Meunier et al., 2008). In short, pepsin solution was prepared by weighing out 0.1 g of pepsin from porcine gastric mucosa (≥ 250 units/mg solid, Sigma Aldrich) which was then dissolved in 1 mL of water. Then 37.5 µL of this was placed in 50 mL of water. 0.5 grams of each sample was weighed out and placed in a tube. To each tube 5 mL of 0.1M sodium phosphate buffer, pH 6.0, was added followed by 2 mL of 0.2M HCl. The pH of each solution was adjusted to pH 2.0 using 1M HCl, with pH being monitored continuously using a calibrated pH meter while HCl was added dropwise. When pH 2.0 was reached, 1 mL of pepsin solution was added to each tube. The tubes were placed in an incubator at 39°C for 2 h with constant shaking. To prepare the pancreatin solution 0.1 g of Pancreatin from porcine pancreas (8 x USP, Sigma Aldrich) was weighed out and dissolved in 10 mL of water. After 2 h in the shaker, 2 mL of sodium phosphate buffer, pH 6.8, was added to each tube, then 1 mL of 0.6M NaOH solution was added. The pH of each solution was adjusted to pH 6.8 by adding NaOH dropwise while continuously monitoring the pH using a calibrated pH meter. When the required pH was reached 1 mL of Pancreatin solution was added to each tube and the tubes were placed in shaking incubator at 39°C for 4 h with constant shaking. After the 4 h incubation, the samples were placed in Survall Legend T centrifuge (Thermo Fisher Scientific) for 15 minutes at 7000 rpm. Then the solution was transferred to a Vivaspin 20 centrifugal concentrator (10 kDa MWCO, Sartorius) and placed in MPW 350-R centrifuge (MPW) for 90 minutes at 9000 rpm. To balance the centrifuge the weight of each tube was taken, and the same weight (using water) was placed in a new tube. After the centrifuge, the sample was filter sterilized using Millex-GP Filter Unit (pore size 0.22 µm, Merck) and aliquoted into vials and placed in the -70°C freezer for maximum 18 months prior to analysis. Samples underwent a maximum of two freeze-thaw cycles prior to use. The final recovered filtrate volume after

centrifugation and ultrafiltration averaged at 13 mL. A 4 mL aliquot was set aside for determination of Se concentration (ppm) by inductively coupled plasma optical emission spectrometry (ICP-OES) using an Agilent 5100 SVDV instrument. Analysis was carried out by Rupali Ahashan and Dr. Cathal Connolly at Alltech Biotechnology Centre, Dunboyne, Co. Meath. Selenium concentrations were determined using a calibration range of 0.25 - 20 ppm Se. The method had a limit of detection (LOD) of 0.05 ppm Se and a limit of quantification (LOQ) of 0.15 ppm Se. Vitamin compounds were calculated based on the known mass of each compound added, and the final recovered filtrate volume of the solution, assuming complete dissolution during digestion procedure. Dissolution efficiency was not experimentally verified and therefore represents a limitation of this study.

2.2.3 Protein Work:

2.2.3.1 Extraction of total protein for 2 hr or 24 hr heat stress for Western blot analysis

IPEC-J2 cells were harvested using Trypsin EDTA (see Section 2.2.1.3) then IPEC-J2 cells were seeded in 6-well plates (growth area of 9.5 cm^2 per well) at a density of 5 x 10^5 cells per mL, with 2 mL in each well, yielding a density of 1 x 10^6 per well. The plates were placed at 37°C in a 5% CO_2 incubator (Forma Steri-Cycle CO_2 Incubator, Model No:371, Thermo Fisher Scientific) overnight. The following day plates were divided into control (CON) group (exposure to 37°C for 2 h and 24 h, respectively) and the heat stress (HS) group (exposure to 42°C for 2 h and 24 h, respectively). The HS group plates were placed in 42°C incubator for 2 h and 24 h and CON group remained at 37°C. After timepoint, plates were removed from incubator, solution was removed from each well and 100 µL of buffer RLT (Qiagen), supplemented with Protease Inhibitor cocktail (Sigma Aldrich), was added to each well. The bottom of each well was scraped using a cell scraper and the solution was placed in a labelled vial. Each vial was snap frozen in liquid nitrogen and placed in -70°C freezer.

2.2.3.2 Extraction of total protein from mammalian cells (treated cells) for Western blot analysis

IPEC-J2 cells were harvested using Trypsin EDTA (see Section 2.2.1.3). Cells were then seeded in 12-well plates (growth area of 3.8 cm^2 per well) at a density of 1 x 10^5 cells per mL for 24-hr treatment, and 1 x 10^4 cells per mL for 48-hr treatment, with 1 mL in each well. The plates were placed at 37°C in a 5% CO_2 incubator overnight to allow attachment.

The following day the Se (A-F) and vitamin (E and C) compounds were added to the respective wells at the correct concentration. The plates were placed at 37°C for 24-hr treatment and 48-hr treatment. After respective treatment times plates were divided into control (CON) group (exposure to 37°C for 24 h, respectively) and the heat stress (HS) group (exposure to 42°C for 24 h, respectively). The HS group plates were placed in 42°C incubator for 24 h and CON group remained at 37°C. After HS timepoint, plates were removed from the incubator and 300 µL of Buffer RLT (Qiagen), supplemented with Protease Inhibitor cocktail (Sigma Aldrich), was added to each well. Each well was scraped using a cell scraper and the solution was placed in a labelled vial and snap frozen in liquid nitrogen before being placed in -70°C freezer.

2.2.3.3 Determination of protein concentration using Qubit assay

Prior to protein quantification and electrophoresis, lysates were desalted using Zeba Spin Desalting Columns (Thermo Fisher Scientific) to remove buffer components that may interfere with downstream protein analysis. To ensure equal loadings of protein onto SDS-PAGE (Section 2.2.3.4), protein concentration was established using Qubit assay. In short, the Qubit working solution was prepared by diluting the protein reagent 1:200 in protein buffer. 190 µL of this prepared working solution was added to three 0.5 mL PCR tubes. 10 µL of each of the standards 1-3 was added to corresponding tube. The Qubit 4 Fluorometer (Thermo Fisher Scientific) was calibrated by reading each of the prepared standards 1-3. Next the samples were prepared by adding sample to working solution in PCR tubes, so the volume makes up to 200 µL (Table1). Each tube was vortexed and left at room temperature for 15 minutes, then the samples were read on the Qubit.

Table 2.2-1: Qubit assay measurements

Volume	**Standards**	**Sample**
Prepared Working Solution	190 µL	180-199 µL
Standard 1-3 (from kit)	10 µL	n/a
User samples	n/a	1-20 µL
Total volume	200 µL	200 µL

2.2.3.4 SDS-PAGE analysis

To separate proteins based on size, pre-cast 4-20% Bis-Tris gels (Millipore) were used for sodium dodecyl sulphate polyacrylamide gel electrophoresis (SDS-PAGE). Laemmli sample buffer was prepared by adding 50 µL of β-mercaptoethanol (≥ 99%, Sigma Aldrich) to 950 µL of Laemmli sample buffer (BioRad). Protein samples were made to 10 µg protein per well by adding protein sample and Laemmli buffer before denaturing by placing them at 95°C for 5 minutes. The gel was placed into tank, and the inner and outer chambers were filled with 1x MES SDS running buffer (Invitrogen) before removing the comb from the gel. Then, 5 µL of PageRuler pre-stained protein ladder (Thermo Fisher) was loaded into the first well of the plate. Then 20 µL of each sample was loaded into the wells of the gel. Gel electrophoresis was run at 60V for approximately 20 minutes, then the voltage was increased to 120V until the dye had reached the bottom of the gel.

2.2.3.5 Western Blot analysis

After the separation of proteins by SDS-PAGE, the gel was blotted onto polyvinylidene fluoride (PVDF) membrane (0.45 µm pore size, Thermo Fisher Scientific). The membrane was activated by placing it in methanol for 2 minutes and rinsed with water. The blotting paper was placed in transfer buffer for approximately 10 minutes. Transfer was performed using ThermoSci Pierce power blot cassette. A sandwich was made of blotting paper (1.5 mm, Cytiva), the membrane, the gel and another blotting paper, ensuring to roll each layer to remove any air bubbles. Transfer buffer (Thermo Fisher Scientific) was added to the top layer, and the lid was placed on. The transfer was performed at 25V and 1.3 amps for 46 minutes. Following protein transfer, the membrane was cut horizontally at the appropriate molecular weight marker to enable simultaneous detection of HSP70 and β-actin.

2.2.3.6 Western immunodetection

The membrane was incubated for 1 hr with gentle rocking in blocking solution, composed of 5% (w/v) milk marvel and 1% (w/v) bovine serum albumin (pH 7, ≥ 98%, Sigma Aldrich) prepared in PBST containing 0.05% (v/v) Tween 20. The upper portion of the cut membrane was incubated with mouse monoclonal anti-HSP70 antibody (3A3, Cat No. MA3-006, Thermo Fisher Scientific) diluted 1:1000, while the lower portion was incubated with mouse monoclonal anti-actin antibody (AC-15, Cat No. AM4302, Invitrogen) diluted 1:1000. Each membrane section was incubated with gentle rocking for

1-2 h. Each membrane was then rinsed using PBST (0.05% Tween 20) three times, rocking for 10 minutes each time. Then each membrane section was incubated with Goat anti-mouse IgG Superclonal secondary antibody, HRP (Cat No. A28177, Thermo Fisher Scientific) at 1:10000 dilution, for 30 minutes with gentle rocking. The blot was rinsed with PBST a further three times with PBST (0.05% Tween 20), for 10 minutes each time with gentle rocking. After, the membranes were placed on iBright CL 1500 Imaging System, then covered in Super Signal TM West Femto trial kit (34094, Thermo Fisher Scientific) developing solution, prepared following manufacturer's guidelines at a ratio of 1:1, Solution A: Solution B. Signal was detected and image of blot was developed using iBright Cl 1500 Imaging System. Exposure times were adjusted automatically using the instrument software to avoid signal saturation. Band intensities were quantified using the densitometric analysis function of the iBright software. HSP70 signal intensity was normalised to the corresponding actin signal intensity for each sample, and normalised values were expressed relative to the Control group.. Western blot analysis was performed using three independent biological replicates for each temperature group, and five independent biological replicates for each treatment group.

2.2.4 Proteomic Analysis

2.2.4.1 Retrieval of IPEC-J2 cells for proteomic analysis

IPEC-J2 cells were harvested using Trypsin-EDTA and counted with a haemocytometer. Cells were seeded into T-25 culture flasks at a density of 5×10^5 cells per flask and incubated overnight at 37°C in a humidified atmosphere containing 5% CO_2 (Forma Steri-Cycle CO_2 Incubator, Model No:371, Thermo Fisher Scientific) to allow for cell attachment. The following day, Selenium and vitamin treatments were prepared at appropriate concentrations and administered to the respective flasks. Cells were then incubated for 24 h under the same conditions. Post-treatment, flasks were assigned to either the control (CON) group, which remained at 37°C for 24 h, or the heat stress (HS) group, which were exposed to 42°C for 24 h. Following the exposure period, cells were detached using Trypsin-EDTA, neutralized with culture media, and transferred into 15 mL conical tubes. Cell suspensions were centrifuged at 1500 rpm for 5 minutes (Eppendorf, 5804). The supernatant was discarded, and the cell pellets were resuspended in 2 mL Hank's Balanced Salt Solution (HBSS), followed by a second centrifugation under the same conditions. Supernatant was removed and pellet was resuspended in 250 µL HBSS and transferred into 0.5 mL microcentrifuge tubes. Tubes were placed in microcentrifuge for 2 minutes at 1500 rpm. Supernatant was removed and a final centrifugation was conducted (2 minutes, 1500 rpm). The final supernatant was carefully removed, and cell pellets were snap-frozen in liquid nitrogen and stored at -80°C. A total of three independent biological replicates per temperature/ treatment group were subjected to proteomic analysis.

2.2.4.2 Proteomic analysis

Proteomic analysis was performed on three independent biological replicates per temperature and treatment group. Protein extraction, digestion, and peptide clean-up were performed by Dr. Marcus Maher in Dublin City University (DCU) using the PreOmics In-StageTip (iST) sample preparation kit (PreOmics GmbH, Martinsried, Germany). Cell pellets were lysed in 100 µL of PreOmics lysis buffer. The Pierce BCA Protein Assay Kit (Thermo Fisher Scientific, Cat No. 23225) was used to determine protein concentrations according to the manufacturer's instructions, and 100 µg of total protein was processed from each sample. Samples were heated at 95°C for 5 minutes with continuous agitation (1000rpm) to ensure efficient protein denaturation, reduction, and alkylation. Protein digestion was carried out using a LysC/Trypsin enzyme mixture (in kit). Following the

enzyme reconstitution according to the manufacturer's instructions, 50 µL of digestion solution was added to each sample, and the digestion was carried out at 37°C for 3 hours under continuous agitation (500 rpm). The reaction was stopped by the addition of stop solution. Resulting peptides were purified using integrated Stage Tip cartridges according to the manufacturer's protocol. After washing to remove salts, detergents, and other contaminants, peptides were eluted, vacuum-dried at 45°C, and reconstitution in LC-MS loading solvent at a concentration of 1 µg/µL prior to analysis.

Peptide samples were analysed in Dublin City University at the Life Sciences Research Facility using an Ultimate™ 3000 RSLCnano UHPLC system, (Thermo Fisher Scientific) coupled online to an Orbitrap Fusion™ Tribrid™ mass spectrometer (Thermo Fisher Scientific).

Peptides were trapped on an Acclaim™ PepMap™ 100 C18 trap column (300 µm x 5mm) and separated on an Acclaim™ PepMap™ 100 analytical column (75 µm x 50 cm). The loading solvent consisted of water containing 0.1% trifluoracetic acid (TFA), while the analytical mobile phases consisted of Solvent A (water containing 0.1% formic acid (FA)), and Solvent B (80% acetonitrile containing 0.08% FA). Peptides were loaded at 25 µL/min and separated at a flow rate of 300 nL/min using a 126 min gradient. The gradient was increased from 5% to 35% Solvent B over 90 min, followed by a ramp to 90% Solvent B for column washing and re-equilibration prior to the next injection.

Mass spectrometry data were acquired in positive ion mode using a data-dependent acquisition (DDA) method. Full MS scans were collected in the Orbitrap analyser at a resolution of 120000 (at m/z 200) across an m/z range of 380-15000, with an AGC target of 4×10^5 ions and a maximum injection time of 50 ms. The most abundant precursor ions with charge states of +2 to +6 were isolated using a 1.6 m/z quadrupole isolation window and fragmented by HCD at a normalised collision energy of 29%. MS/MS spectra were acquired in the ion trap using an AGC target of 2×10^4 ions and a maximum injection time of 35 ms. Dynamic exclusion was set to 60 s with a repeat count of one, and a cycle time of 3 s was maintained throughout the acquisition.

Protein identification was performed on MS/MS spectra and searched using Proteome Discoverer version 2.3 (Thermo Fisher Scientific) with the Sequest HIT search engine. Data was searched against the *Sus scrofa* protein database obtained from NCBI (downloaded 24th February 2026). Search parameters included trypsin digestion with up to two missed cleavages, a precursor mass tolerance of 10 ppm, and a fragment mass

tolerance of 0.6 Da. Carbamidomethylation of cysteine was specified as a fixed modification, whereas oxidation of methionine was treated as a variable modification. Peptide-spectrum matches were assessed using the Percolator algorithm with a target-decoy strategy, and results were filtered to achieve a 1% false discovery rate (FDR) at the peptide level.

Label-free quantitative proteomic analysis was performed using Progenesis QI for Proteomic (Nonlinear Dynamics, Waters Corporation). Raw LC-MS/MS data were imported and chromatographically aligned to correct fit retention time variation between runs. A representative run with high chromatographic quality was selected as the reference for alignment, and peptide ion features were automatically detected, matched, and quantified across all samples. Samples were assigned to their respective treatment groups, and feature abundances were normalised using the Progenesis global scaling normalisation algorithm to reduce technical variation between analyses.

MS/MS spectra corresponding to quantified peptide features were exported from Progenesis QI and searched using Proteome Discoverer v2.3, as described above. Validated peptide-spectrum matches were subsequently reimported into Progenesis QI for peptide annotation and protein identification. Protein inference was performed using a parsimonious of unique, non-conflicting peptides.

Prior to statistical analysis, peptide abundance data were normalised and arcsinh-transformed to improve variance homogeneity. One-way ANOVA was performed at the peptide level, and peptides with a p-value ≤ 0.05 were retained for downstream protein quantification. Proteins were considered differentially expressed if they met the following criteria; (i) protein-level ANOVA p-value ≤ 0.05, (ii) identification by at least two unique peptides, (iii) a fold change ≥ 1.5 or ≤ 0.67 between experimental groups, and (iv) an overall protein FDR $\leq 1\%$.

Mass spectrometry data acquisition, peptide identification, and the generation of differentially expressed protein lists were conducted by Dr. Michael Henry in Dublin City University. The resulting datasets were subsequently analysed by the author using the STRING database (https://string-db.org/) to investigate protein-protein interaction networks and perform functional enrichment analysis.

2.2.5 Statistical Analysis

The results of this study were analysed using one-way analysis of variance (ANOVA) with Tukey's post hoc multiple comparisons test. Statistical significance was assigned at $p \leq 0.05$, $p \leq 0.01$, and $p \leq 0.001$. Results are presented as mean values of independent biological replicates, where $n = 3$ or $n = 5$. Each heat-stressed and/or treated sample was analysed relative to its corresponding control.

3 Results

3.1 Development of an *in vitro* model for heat stress using IPEC-J2 cells

The establishment of a heat stress model *in vitro* is a foundational approach in research as it allows for a controlled study of how high temperatures affect a biological system. In this study IPEC-J2 cells were used as these cells mimic the intestinal tract of pigs. It is important to understand how higher temperatures affect pig intestinal epithelium as pigs are unable to dissipate heat resulting in a redistribution of blood flow away from the intestinal tract towards peripheral organs. This blood flow redistribution can damage the intestinal epithelium and establishing a heat stress model can give us an understanding of how the epithelium is affected at higher temperatures.

3.1.1 Evaluation of the relative metabolic activity of IPEC-J2 cells after exposure to 41°C, 42°C, and 44°C for 2 hrs and 24 hrs, respectively

To assess the effect of elevated temperatures on relative metabolic activity , IPEC-J2 cells incubated at their optimal temperature of 37°C were compared independently with cells exposed to higher temperature conditions. The higher temperatures examined were 41°C, 42°C, and 44°C, cells were exposed for 2-h heat stress and 24-h heat stress, respectively. Each temperature group was carried out alongside a control group kept at the optimum temperature of 37°C. The higher temperature group was compared to the control group, assuming the control group metabolic activity is 100%. In this study Alamar Blue® assay was used to measure the metabolic activity as an indicator of cell health in heat-stressed cells compared to cells maintained under physiological conditions.

3.1.1.1 Alamar Blue® assay after 2-h heat stress on relative IPEC-J2 cell metabolic activity at 41°C, 42°C, and 44°C

The relative metabolic activity of IPEC-J2 cells heat stressed for 2 h at elevated temperatures of 41°C, 42°C, and 44°C, was determined using the AB assay. The percentage of relative IPEC-J2 cell metabolic activity at higher temperatures was assessed relative to control cells maintained at optimal temperature of 37°C. Metabolic activity in IPEC-J2 cells exposed to 41°C for 2 h was approximately 104% when compared to control cells at 37°C. Following 2 h exposure to 42°C and 44°C, the percentage of metabolic activity relative to control cells decreased to approximately 78%, and 83%,

respectively (Figure 3.1-1). Three independent biological replicates were performed (n=3), with each temperature group analysed in 10 technical replicate columns on each 96-well plate. Statistical analysis was performed using One-way ANOVA with Tukey's post hoc test. No significance was observed between temperature groups ($p > 0.05$).

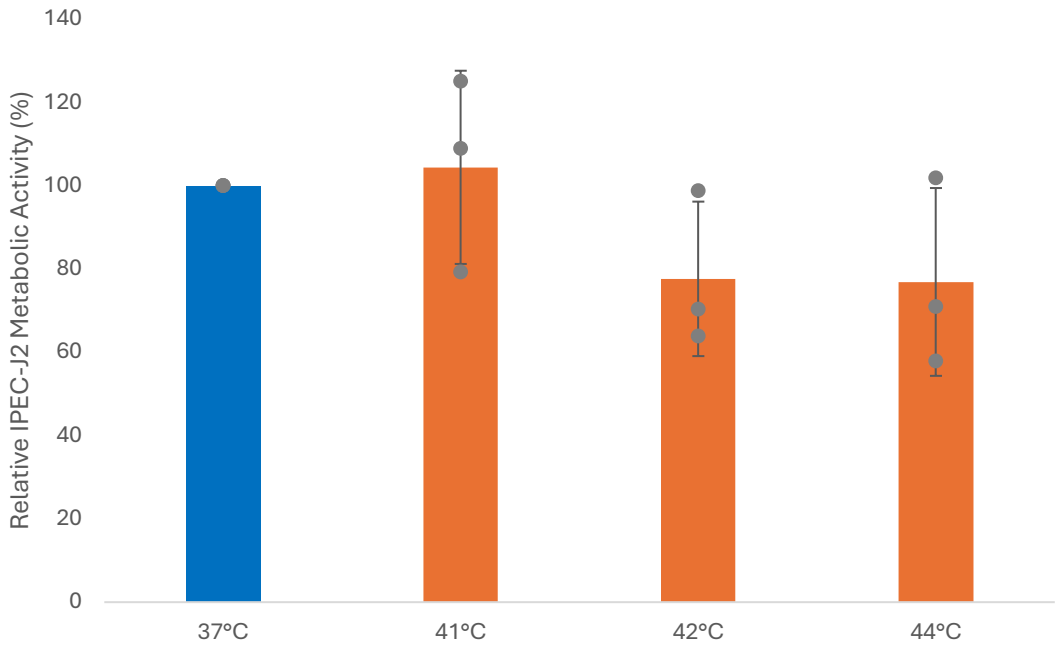


Figure 3.1-1: Effect of 2 h heat stress on metabolic activity in IPEC-J2 cells as determined by Alamar blue assay- Cells were exposed to elevated temperatures (41°C, 42°C, and 44°C) for 2 h. Relative metabolic activity is expressed as a percentage relative to 37°C control cells. Bars represent the mean of three independent biological replicates (n=3), dots represent numerical value of each biological replicate, and error bars represent the standard deviation (SD). Statistical analysis was performed using One-way ANOVA with Tukey's post hoc test ($p > 0.05$).

3.1.1.2 Alamar blue® assay after 24 h heat stress on relative IPEC-J2 cell metabolic activity at 41°C, 42°C, and 44°C

The aim was to determine the effect of prolonged heat stress on IPEC-J2 cell relative metabolic activity . Cells were heat stressed at 41°C, 42°C, and 44°C for 24 h, and metabolic activity was assessed using AB reagent, relative to cells maintained at optimal temperature of 37°C (Figure 3.1-2). Exposure to 41°C for 24 h resulted in approximately an 8% reduction of metabolic activity compared to control cells (37°C). After exposure to 42°C and 44°C for 24 h, the relative metabolic activity decreased to approximately 74% and 70%, respectively, when compared to 37°C control. A total of 3 independent biological replicates were performed (n=3), with 10 technical replicate columns per 96-well plate of each temperature group investigated. Statistical analysis was performed on the 3 independent biological replicates using One-way ANOVA with Tukey's post hoc test, but no significance was detected between any temperature group ($p > 0.05$).

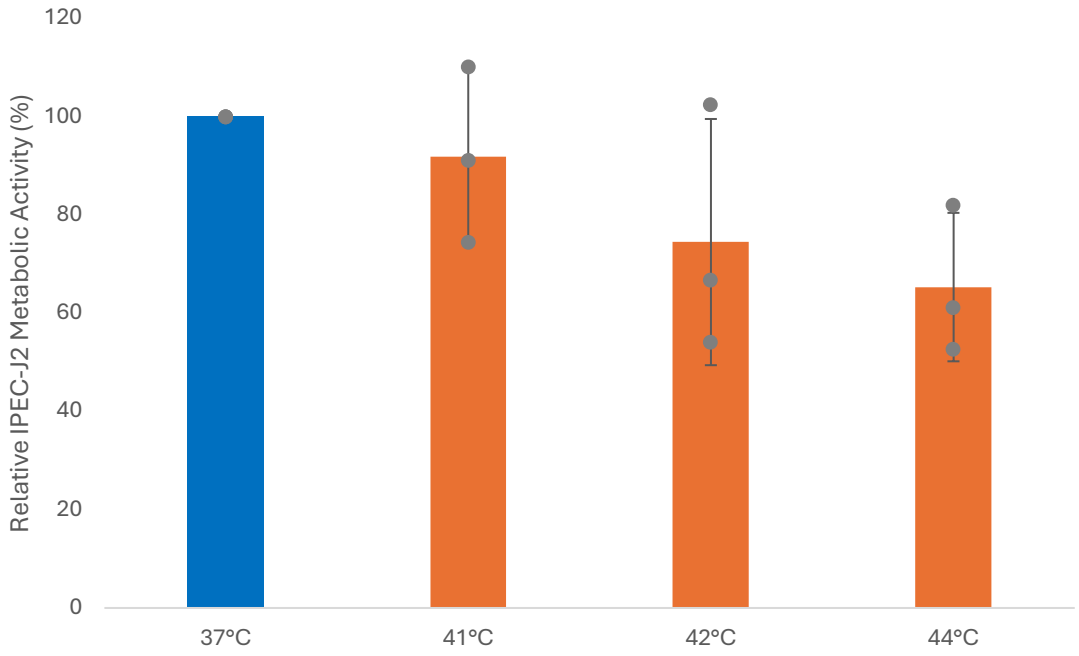


Figure 3.1-2: Effect of 24 h heat stress on relative metabolic activity as determined by AB assay- IPEC-J2 cells were exposed to elevated temperatures (41°C, 42°C, and 44°C) for 24 h. Relative metabolic activity is expressed as a percentage relative to 37°C control cells. Bars represent the mean of three independent biological replicates (n=3), dots represent numerical value of each biological replicate, and error bars represent the standard deviation (SD). Statistical analysis was performed using One-way ANOVA with Tukey's post hoc test ($p > 0.05$).

3.1.2 Investigation of Heat Shock Protein 70 (HSP70) in IPEC-J2 cells exposed to heat stress

HSP70 expression was selected as an indicator of the cellular heat stress response due to its role as a highly inducible and widely studied member of the heat shock protein family (Hu et al., 2022). It is also highly expressed in intestinal epithelial cells and plays a key cytoprotective role in maintaining gut homeostasis, making it a particularly appropriate marker for assessing the heat stress response in IPEC-J2 cells (Y. Wang et al., 2018; Zhong et al., 2010). Therefore, Western blot analysis was performed to determine whether heat stress at 41°C, 42°C, and 44°C for 2h and 24 h, respectively, induces HSP70 expression in IPEC-J2 cells, relative to control cells maintained at 37°C. This study used target protein HSP70, and house-keeping protein actin on each of the membranes.

3.1.2.1 Western blot images of IPEC-J2 cells exposed to 41°C, 42°C, and 44°C

Representative Western blot analysis of HSP70 and actin protein expression in IPEC-J2 cells exposed to heat stress is shown in Figure 3.1-3. Cells were grown under control conditions (37°C), and exposed to elevated temperatures of 41°C (Figure 3.1-3 A), 42°C (Figure 3.1-3 B), and 44°C (Figure 3.1-3 C) for 2 h and 24 h, respectively. HSP70 bands were detected across all conditions, with differences in band intensity observed between temperature groups. Variability was also observed between samples in both HSP70 and actin protein band intensity. Quantitative assessment of HSP70 expression was performed using densitometric analysis normalised to actin (Figure 3.1-4).

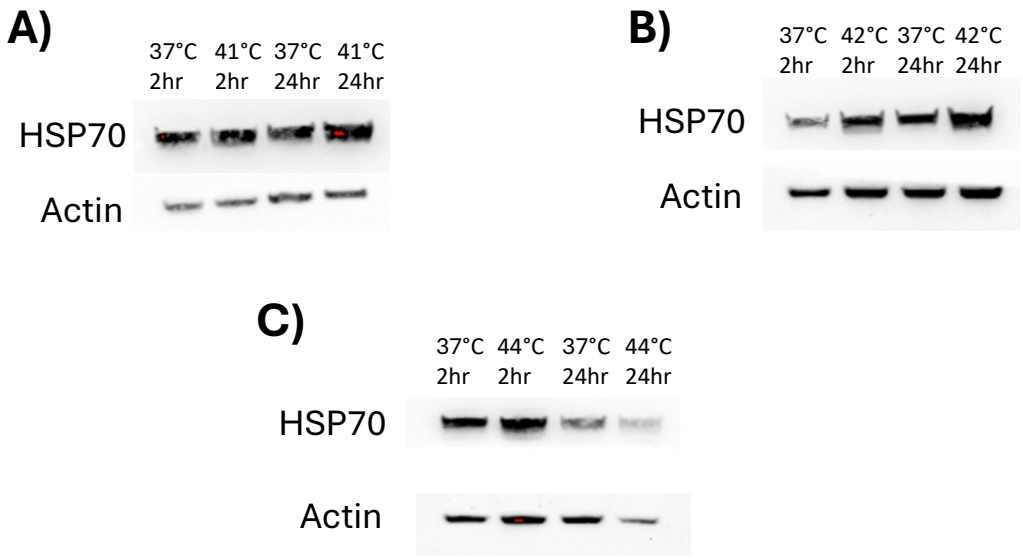


Figure 3.1-3: Representative Western blot images of heat-stressed IPEC-J2 cells- Cells were heat-stressed for 2 h and 24 h, respectively, and samples were loaded at a protein concentration of 10 µg per lane , and membranes were incubated with target antibody (HSP70) and house-keeping antibody (actin). Images represent 41°C (A), 42°C (B), and 44°C (C).

Densitometric analysis was performed to determine HSP70 protein expression normalised to actin in IPEC-J2 cells exposed to 41°C, 42°C, and 44°C for 2 h and 24 h, respectively (Figure 3.1-4).

Exposure to 41°C (Figure 3.1-4 A) resulted in increased HSP70 expression after both 2 h and 24 h exposure relative to control cells maintained at 37°C, with a significant increase observed following 24 h exposure ($p = 0.0183$). An increase in HSP70 abundance can also be observed in cells exposed to 42°C (Figure 3.1-4 B) and 44°C (Figure 3.1-4 C), at both timepoints; however, these differences were not statistically significant. Three independent biological replicates were performed for each temperature group investigated ($n = 3$). Statistical analysis was performed on the 3 independent biological replicates using One-way ANOVA with Tukey's post hoc test, with significance marked as *($p \leq 0.05$).

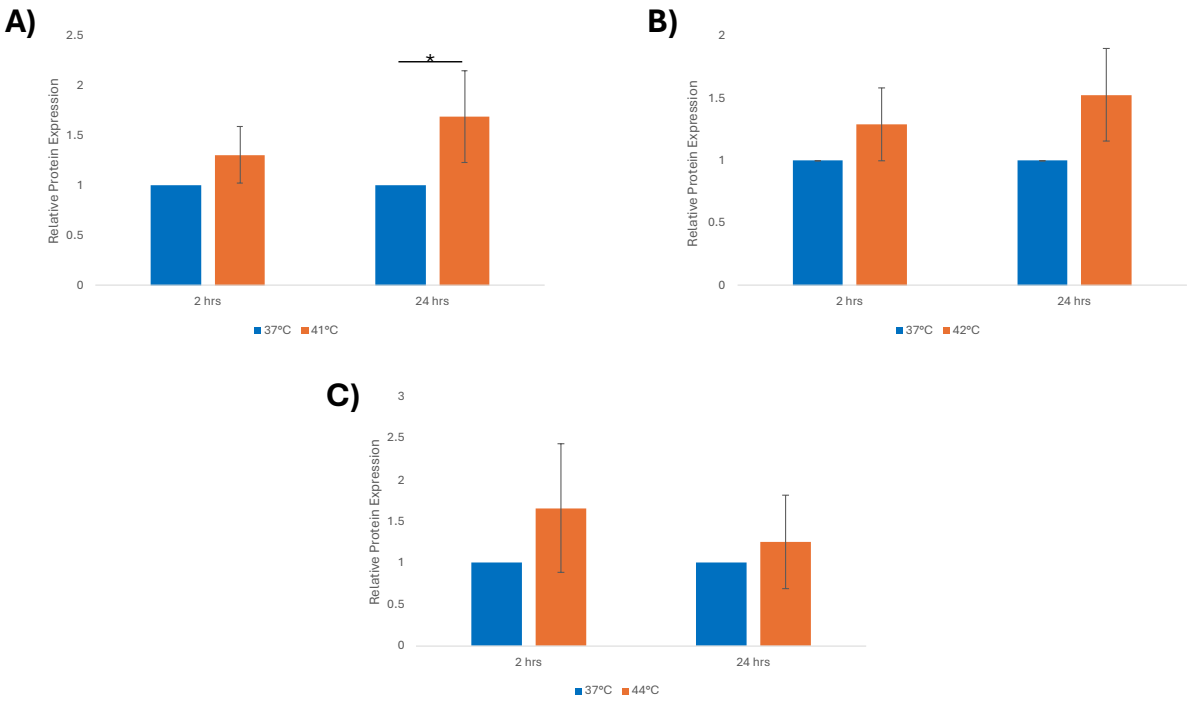


Figure 3.1-4: Densitometric analysis of HSP70 expression- IPEC-J2 cells exposed to 41°C (A), 42°C (B), and 44°C (C) for 2 h and 24 h, respectively. HSP70 expression was normalised to actin, and values are expressed as relative protein expression to 37°C control. Bars represent the mean of three independent biological replicates (n=3), and error bars represent the standard deviation (SD). Data was analysed using One-way ANOVA with Tukey's multiple comparison with significance marked as *($p \leq 0.05$).

3.1.3 Investigation of the cellular morphology of IPEC-J2 cells exposed to heat stress at 42°C

The aim of this was to determine if there are any visible changes in cell confluency and/or cell morphology. Images were taken of IPEC-J2 cells to compare normal cells grown at 37°C with cells exposed to the higher temperature of 42°C. Representative images are shown from three technical replicates, with three randomly selected fields of view captured per condition. Imaging was not performed under blinded conditions. These images were not intended for use as a quantitative assessment of morphological analysis; they are presented as observations only.

3.1.3.1 Effect of 2-hour heat stress on IPEC-J2 cell morphology

Representative phase-contrast images of IPEC-J2 cells at 10x and 20x magnification are shown in Figure 3.1-5 (A-D). Under optimal conditions of 37°C (Figure 3.1-5 A and C), cells displayed typical epithelial morphology, characterised by adherent, spread cells with irregular polygonal shapes. Following exposure to heat stress at 42°C for 2 h (Figure 3.1-5 B and D), no obvious morphological differences were observed. Cells remained adherent and retained a similar shape and overall structure at both magnifications.

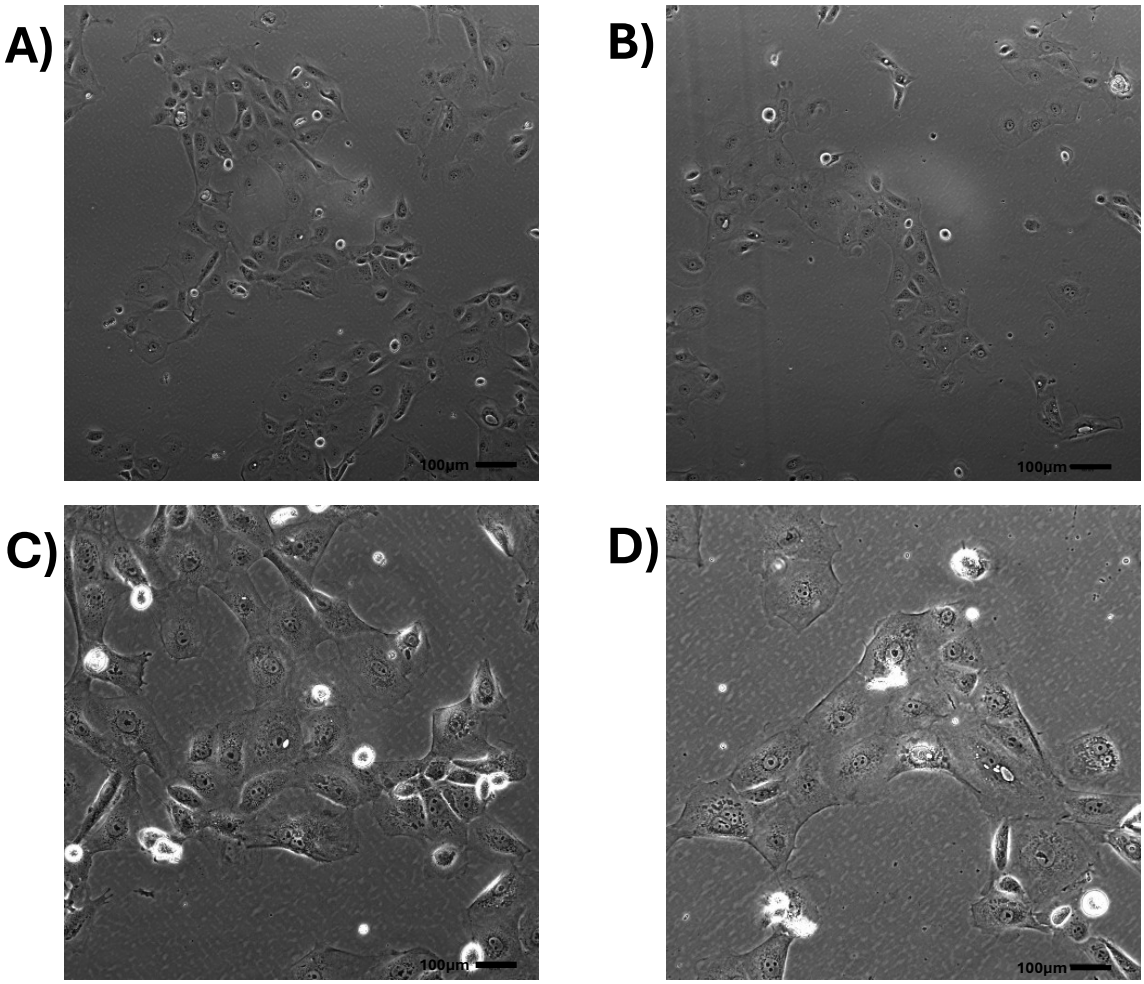


Figure 3.1-5: Effect of 2-hour heat stress on IPEC-J2 cell morphology- Representative phase-contrast images of IPEC-J2 cells maintained under optimal conditions (A, C) or exposed to heat stress at 42°C for 2 h (B, D). Images were captured at 10x (A, B) and 20x (C, D) magnification. Scale bars = 100µm.

3.1.3.2 Effect of 24-hour heat stress on IPEC-J2 cell morphology

Similarly to observations made at 2-hour heat stress, after 24 h exposure to 42°C there were no obvious morphological changes in IPEC-J2 cells. Figure 3.1-6 shows 10x magnification (A, B) and 20x magnification (C, D) of cells maintained at optimal temperature of 37°C (A, C) and cells exposed to 42°C for 24 h (B, D). In control images, cells appear to be adherent and in heat-stressed images cells retained similar morphology with no major changes in cell shape or adherence. An apparent increase in rounded cells and variation in cell density was observed following 24-hour heat exposure; however, these observations were not quantitatively assessed.

Overall, prolonged heat stress did not induce pronounced morphological changes in IPEC-J2 cells, although minor qualitative differences were observed at 24 h.

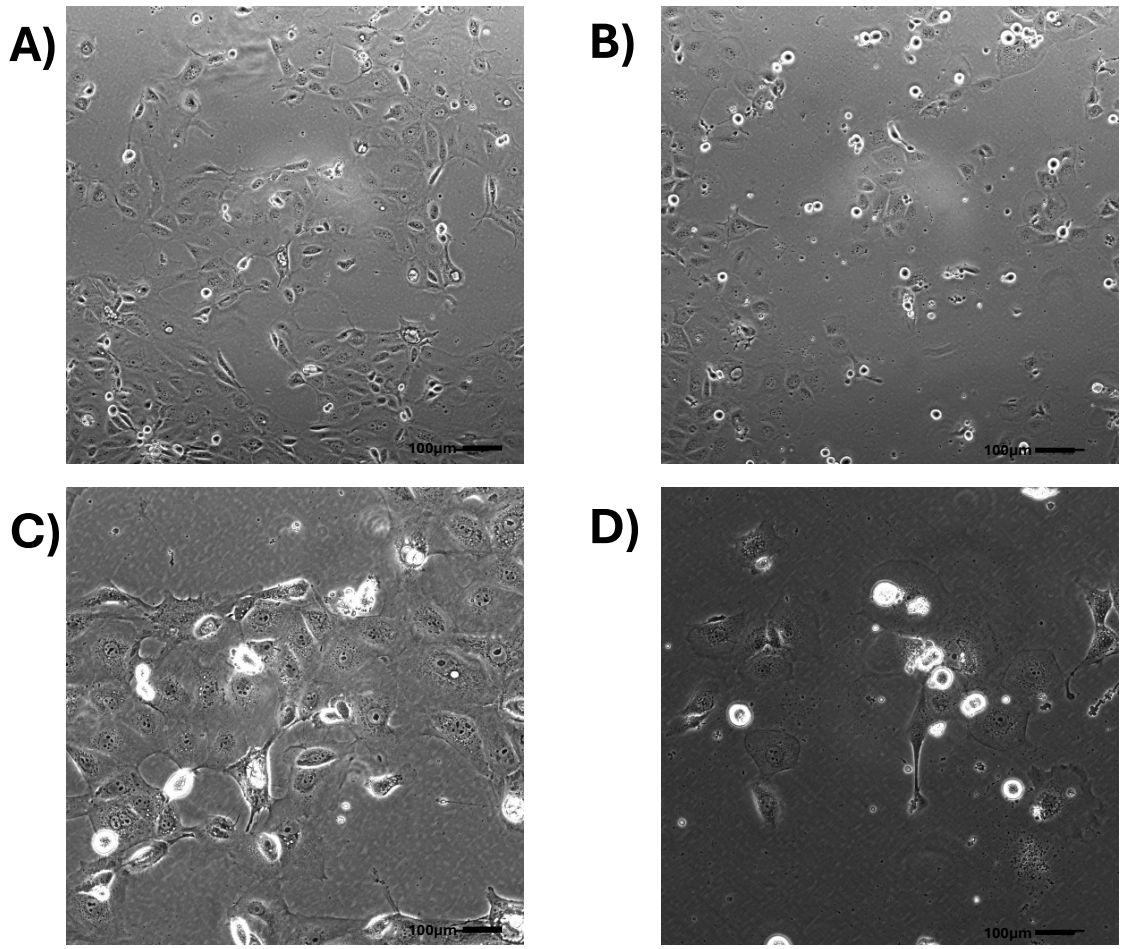


Figure 3.1-6: Effect of 24-hour heat stress on IPEC-J2 cell morphology- Representative phase-contrast images of IPEC-J2 cells maintained under optimal conditions (A, C) or exposed to heat stress at 42°C for 24 h (B, D). Images were captured at 10x (A, B) and 20x (C, D) magnification. Scale bars = 100µm.

3.2 Investigation of treatment with different Selenium (Se) and vitamin compounds to mitigate the impacts of heat stress

Selenium (Se) compounds were selected for investigation due to their reported ability to alleviate heat-induced cellular stress. Previous studies have shown that selenium can enhance cellular resilience in IPEC-J2 cells (J. Tang et al., 2019). The effects of treatment with organic Se compounds for 24 h and 48 h were therefore investigated to determine if Se compounds can alleviate the decrease in relative metabolic activity of heat-stressed IPEC-J2 cells.

IPEC-J2 cells were treated with five different organic Selenium compounds (Organic Se-A/B/C/D/F), one inorganic Selenium compound (Inorganic Se (E)), and two vitamins (E & C) to determine if they can alleviate the effects of heat stress. The organic Se compounds differed in composition and were sourced from different suppliers, allowing comparison of their relative effects under identical experimental conditions. Each of the compounds went through a standardised *in vitro* digestion (Boisen & Fernandez, 1997; Meunier et al., 2008), of which the total Se content (ppm) was determined using ICP-OES. In contrast, vitamin concentrations were calculated based on the known mass of compounds added and the final volume of the prepared solutions. From these results Se and vitamin compounds were added to the cells based on established dietary recommendations for swine nutrition. Organic Se supplementation is limited to a maximum of 0.2 mg/kg, while vitamin E is commonly included at 11-16 IU/kg (Crenshaw, 2025; Official Journal of the European Union, 2022). vitamin C was also investigated despite the absence of a dietary requirement; in this study it was added at varying concentrations between 25 and 300 µg/mL .

3.2.1 Selenium concentration of digested samples

Se concentrations of the organic and inorganic Se samples that underwent in vitro digestion were determined by ICP-OES. This was done to verify the Se content (ppm) of the digested preparations prior to cell treatment. The measured Se content for each sample is presented in Table 3.2-1.

Table 3.2-1: Se concentrations (ppm) of digested organic and inorganic Se treatments as determined by ICP-OES, and the final concentration (µg/mL) added to IPEC-J2 cells

Treatment	Se concentration (ppm)	Final concentration applied to cells (µg/mL)
Organic Se-A	58.8	0.2
Organic Se-B	41.5	0.2
Organic Se-C	29.2	0.2
Organic Se-D	477.5	0.2
Inorganic Se (E)	11342	0.2
Organic Se-F	57.98	0.2

3.2.2 Effect of 48-hour exposure to Se and vitamin compounds on IPEC-J2 cell metabolic activity at 37°C

To assess the effects of Se and vitamin compounds on IPEC-J2 cell metabolic activity under optimal conditions, cells were treated with each of the compounds at the specified concentration for 48 h. AB was used to determine the metabolic activity of heat-stressed cells, expressed relative to untreated control, results presented in Figure 3.2-1. Following treatment with each of the products for 48 h, there was a significant impact on the metabolic activity of cells treated with vitamin C when compared to untreated control group ($p < 0.00000001$). The relative metabolic activity reduced to approximately 12% in cells treated with vitamin C. The largest increase is observed in cells treated with Organic Se-A with relative cell metabolic activity increasing to approximately 103%. Three independent biological replicates were performed ($n = 3$). Within each biological replicate, each treatment was analysed using two columns of a 96-well plate, serving as technical replicates. Statistical analysis was carried out on the three biological replicates, using One-way ANOVA with Tukey's post hoc test, with significance marked as *($p \leq 0.05$).

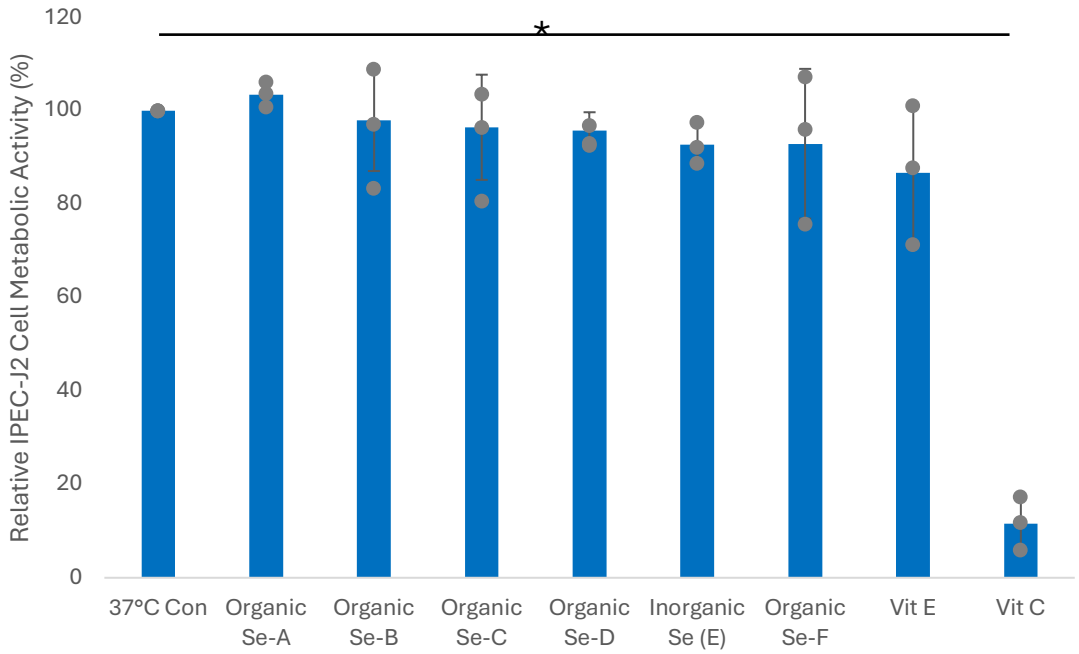


Figure 3.2-1: Effect of 48-hour treatment with Se and vitamin compounds on relative IPEC-J2 cell metabolic activity as determined by Alamar Blue assay- Cells were treated with Se compounds at a concentration of 0.2 µg/mL , vit E at 10.72 µg/mL, and it C at 250 µg/mL . IPEC-J2 cell metabolic activity was assessed using Alamar Blue assay and expressed as a percentage relative to the untreated control group. Bars represent mean IPEC-J2 cell metabolic activity , dots represent numerical value of each biological replicate, and error bars indicate standard deviation (n = 3). Data was analysed using One-way ANOVA with Tukey's multiple comparison with significance marked as *($p \leq 0.05$).

3.2.3 Investigation of 24-hour treatment with Se and vitamin compounds on IPEC-J2 cells to mitigate reduced cell metabolic activity under heat stress at 42°C

IPEC-J2 cells were treated with Se and vitamin compounds for 24 h prior to being heat-stressed at 42°C for 2 h and 24 h, respectively. AB reagent was used to determine the relative metabolic activity of heat-stressed IPEC-J2 cells, expressed as a percentage relative to untreated cells maintained at optimal temperature of 37°C. Experiments were performed using three biological replicates (n = 3), with parallel plates maintained at 37°C (Con) or subjected to heat stress at 42°C. Due to previously observed cytotoxic effects (Section 3.2.1), vitamin C at 250 µg/mL was excluded from this analysis. See Appendix (Figures 6.6-1 to 6.1-4) that display individual temperature and treatment graphs with dots representing individual biological replicate numerical data points.

3.2.3.1 Effect of 24-hour treatment with Se and vit compounds on IPEC-J2 cell metabolic activity following 2-hour heat stress

Cells treated with Se and vitamin compounds for 24 h were subsequently exposed to heat stress at 42°C for 2 h, and metabolic activity was assessed relative to cells maintained at optimal temperature of 37°C (Figure 3.2-2). Under control conditions, heat stress reduced relative metabolic activity from 100% to approximately 73%. Under optimal conditions, cells treated with Inorganic Se (E) showed the greatest reduction in relative metabolic activity , with a reduction of roughly 20%, while treatment with Organic Se-D increased metabolic activity to approximately 114%, relative to untreated control. The relative metabolic activity of cells treated with all other compounds ranged between roughly 90-100%. Under heat stress conditions, cells treated with Organic Se-A shows the greatest reduction with relative metabolic activity approximately 58%. Although Inorganic Se (E) treatment under normal physiological conditions showed the greatest reduction in relative metabolic activity, under heat stress conditions it show the largest increase in relative metabolic activity, reaching 114%. Cells treated with Organic Se-F and vitamin E show a similar increase in relative metabolic activity, reaching approximately 113% and 110%, respectively. Cells treated with Organic Se-B to D show a reduced metabolic activity relative to 37°C control, with relative metabolic activity ranging between approximately 70-90%. Three independent biological replicates were performed (n = 3). Within each biological replicate, each treatment was analysed using two columns of a 96-well plate,

serving as technical replicates. Statistical analysis was carried out on the three biological replicates, using One-way ANOVA with Tukey's post hoc test, no significance was observed ($p > 0.05$).

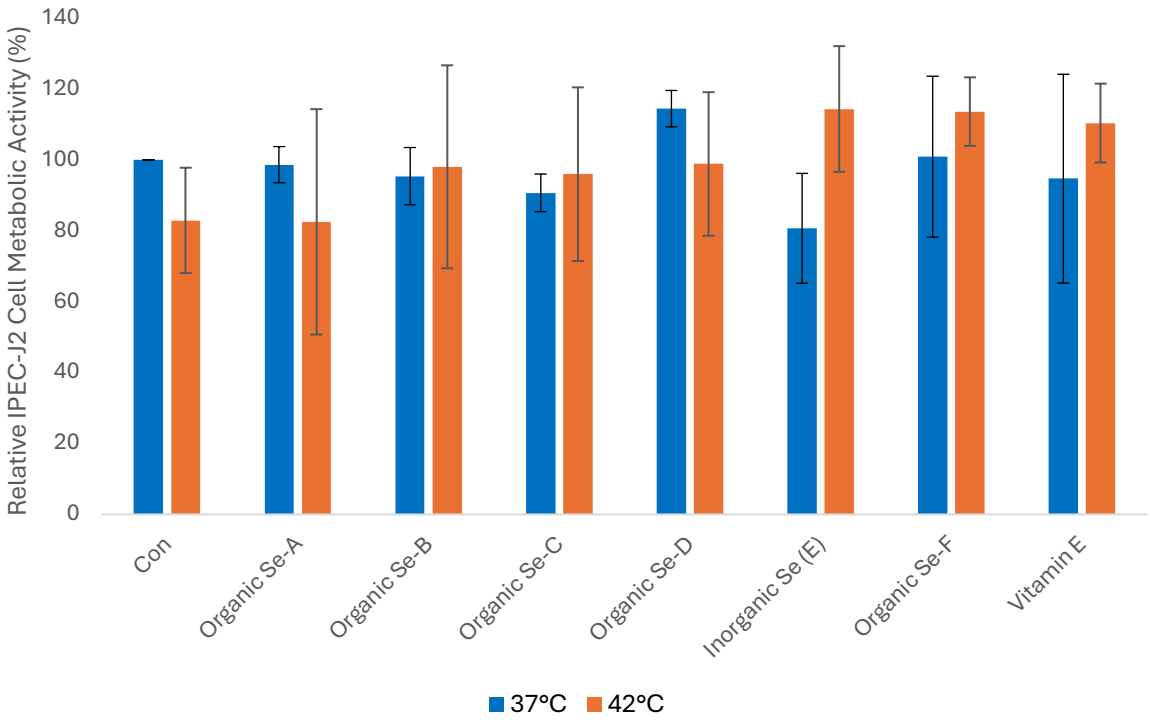


Figure 3.2-2: Effect of 24-hour treatment with Se and vitamin compounds on relative IPEC-J2 cell metabolic activity following 2-hour heat stress- Cells were treated with treatments organic Se compounds (Organic Se-A, Se-B, Se-C, Se-D, Se-F), Inorganic Se (E), and vitamin E for 24 h and subsequently exposed to 42°C for 2 h. Relative metabolic cell activity was measured using Alamar blue assay and expressed as a percentage relative to untreated cells maintained at 37°C. Bars represent mean ±SD of n=3 independent experiments.

3.2.3.2 Effect of 24-hour treatment with Se and Vit compounds on relative IPEC-J2 cell metabolic activity following 24-hour heat stress

Following 24-hour treatment with Se and vitamin compounds, cells were subjected to heat stress at 42°C for 24 h, and IPEC-J2 cell metabolic activity was assessed relative to cells maintained at 37°C using the AB assay (Figure 3.2-3). Heat exposure for 24 h resulted in a significant reduction of relative cell metabolic activity , decreasing from 100% at 37°C to approximately 50% at 42°C ($p = 0.0015$). A similar trend was observed across all the

treatments at 37°C, with cell metabolic activity ranging between roughly 87% and 103%, relative to untreated 37°C control. Under heat stress conditions, each of the treatments increased the IPEC-J2 cell metabolic activity when compared to 42°C control group. Treatment with Inorganic Se (E) showed the greatest increase in relative metabolic activity , reaching approximately 80%, while treatment with Organic Se-A, B, C, and D showed a similar trend with relative cell metabolic activity ranging between approximately 52-59%. Organic Se-F and vitamin E supplementation showed a slightly higher relative cell metabolic activity of roughly 64-65%. Three independent biological replicates were performed (n = 3). Within each biological replicate, each treatment was analysed using two columns of a 96-well plate, serving as technical replicates. Statistical analysis was carried out on the three biological replicates, using One-way ANOVA with Tukey's post hoc test, no significance was observed ($p > 0.05$).

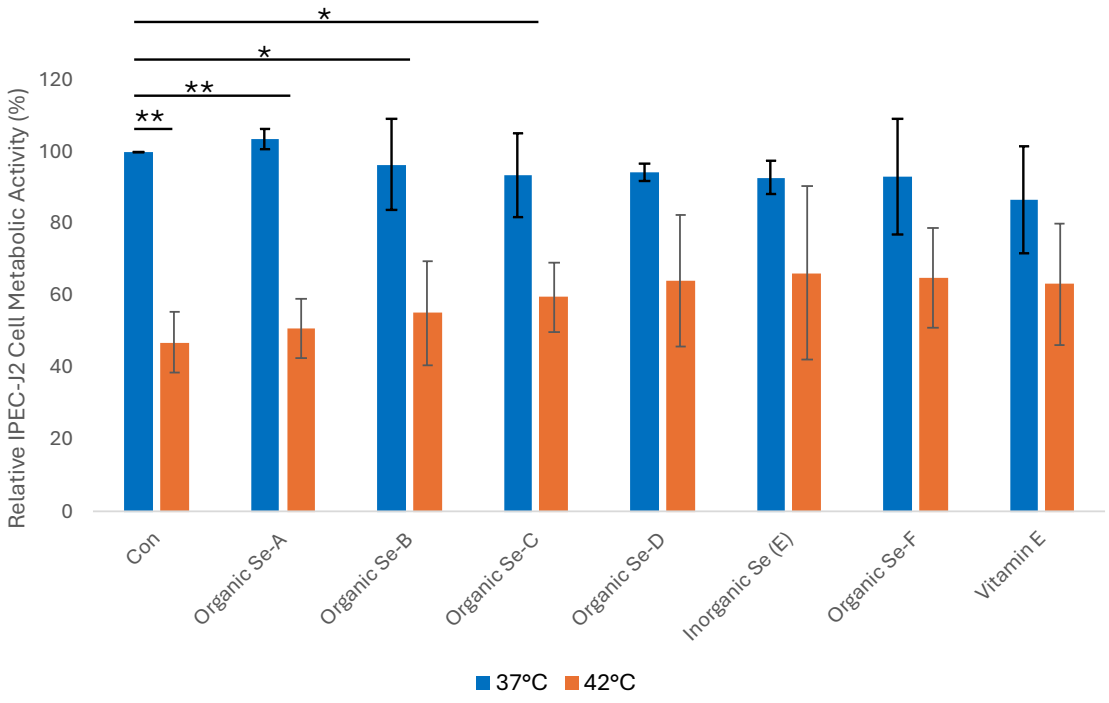


Figure 3.2-3: Effect of 24-hour treatment with Se and vitamin compounds on relative IPEC-J2 cell metabolic activity following 24-hour heat stress- Cells were treated with treatments organic Se compounds (Organic Se-A, Se-B, Se-C, Se-D, Se-F), Inorganic Se (E), and vitamin E for 24 h and subsequently exposed to 42°C for 24 h. Cell metabolic activity was measured using Alamar blue assay and expressed as a percentage relative to untreated cells maintained at 37°C. Bars represent mean ±SD of n=3 independent experiments. Data was analysed was analysed using

One-way ANOVA with Tukey's multiple comparison with significance marked as *($p \leq 0.05$) and **($p \leq 0.01$).

3.2.4 Investigation of 48-hour treatment with Se and vitamin compounds on IPEC-J2 cells to mitigate reduced IPEC-J2 cell metabolic activity under heat stress at 42°C

Similarly to Section 3.2.2, IPEC-J2 cells were treated with Se and vitamin compounds, this time for 48 h, prior to exposure to heat stress at 42°C for either 2 h or 24 h. IPEC-J2 cell metabolic activity was assessed using AB assay and expressed as a percentage relative to untreated control cells maintained at the optimal temperature of 37°C. A total of three biological replicates was performed, with parallel plates at 37°C (Con) and HS at 42°C.

3.2.4.1 Effect of 48-hour treatment with Se and vitamin compounds on relative IPEC-J2 cell metabolic activity following 2-hour heat stress

Following 48-hour treatment with Se and vitamin compounds, cells were subjected to heat stress at 42°C for 2 h, and IPEC-J2 cell metabolic activity was assessed relative to cells maintained at 37°C using AB assay (Figure 3.2-4). Following 2 h heat stress, untreated control IPEC-J2 cells decreased in metabolic activity to approximately 79% compared to control cells maintained at optimal temperature. Treatment with Organic Se-A, B, C, and D for 48 h increased the cell metabolic activity , compared to their respective treatment at 37°C, and to the controls, with relative IPEC-J2 cell metabolic activity ranging between roughly 104-111%. Inorganic Se (E), Organic Se-F, and vitamin E supplementation for 48 h increased cell metabolic activity compared to the heat-stressed control, with relative cell metabolic activity at approximately 88%, 91%, and 90%. Three independent biological replicates were performed (n = 3). Within each biological replicate, each treatment was analysed using two columns of a 96-well plate, serving as technical replicates. Statistical analysis was carried out on the three biological replicates, using One-way ANOVA with Tukey's post hoc test, no significance was observed ($p > 0.05$).

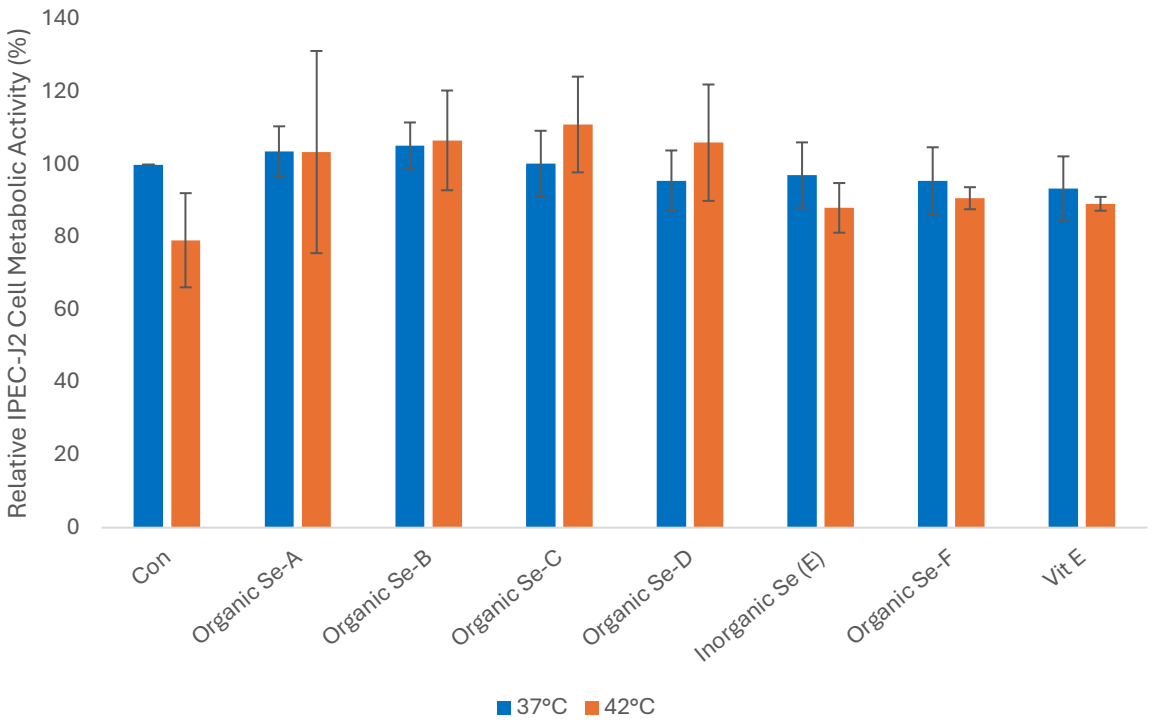


Figure 3.2-4: Effect of 48-hour treatment with Se and vitamin compounds on relative IPEC-J2 cell metabolic activity following 2-hour heat stress- Cells were treated with treatments organic Se compounds (Organic Se-A, Se-B, Se-C, Se-D, Se-F), Inorganic Se (E), and vitamin E for 48 h and subsequently exposed to 42°C for 2 h. IPEC-J2 cell metabolic activity was measured using Alamar blue assay and expressed as a percentage relative to untreated cells maintained at 37°C. Bars represent mean ±SD of n=3 independent experiments.

3.2.4.2 Effect of 48-hour treatment with Se and vitamin compounds on relative IPEC-J2 cell metabolic activity following 24-hour heat stress

Cells treated with Se and vitamin compounds for 48 h were subsequently exposed to heat stress at 42°C for 24 h, and IPEC-J2 cell metabolic activity was assessed relative to cells maintained at optimal temperature of 37°C (Figure 3.2-5). Under control conditions, heat-stressed cells decreased in metabolic activity to approximately 63%, compared to control cells maintained at 37°C. At optimal temperature cells treated with Organic Se-A, B, and C increased the cells' metabolic activity compared to control cells at optimal temperature, ranging from roughly 110% to 111%. Cells treated with Organic Se- D, F, Inorganic Se (E), and vitamin E at 37°C showed a very slight reduction in metabolic activity compared to 37°C. Similar trend was seen in heat-stressed cells treated with compounds for 48 h. Organic Se-A, B, C, and D showed an increase in IPEC-J2 cell metabolic activity compared to 42°C control, with cells' metabolic activity at approximately 80%, 86%, 90%,

and 88%, respectively. While Inorganic Se (E), Organic Se-F, and vitamin E showed a slight reduction in cell metabolic activity compared to the heat-stressed control, with cell metabolic activity ranging between approximately 67% and 71%. Three independent biological replicates were performed (n = 3). Within each biological replicate, each treatment was analysed using two columns of a 96-well plate, serving as technical replicates. Statistical analysis was carried out on the three biological replicates, using One-way ANOVA with Tukey's post hoc test, no significance was observed ($p > 0.05$).

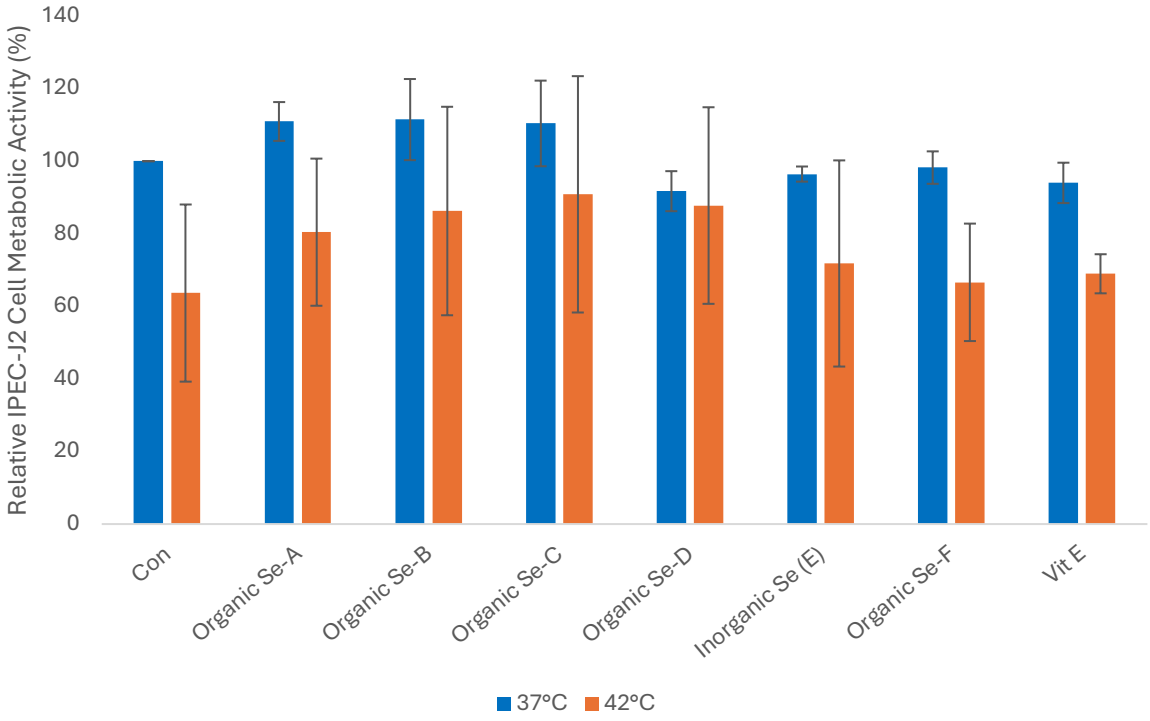


Figure 3.2-5: Effect of 48-hour treatment with Se and vitamin compounds on relative IPEC-J2 cell metabolic activity following 24-hour heat stress- Cells were treated with treatments organic Se compounds (Organic Se-A, Se-B, Se-C, Se-D, Se-F), Inorganic Se (E), and vitamin E for 48 h and subsequently exposed to 42°C for 24 h. IPEC-J2 cell metabolic activity was measured using Alamar blue assay and expressed as a percentage relative to untreated cells maintained at 37°C. Bars represent mean ±SD of n=3 independent experiments.

3.2.5 Effect of 48-hour exposure to vitamin C on IPEC-J2 cell metabolic activity at 37°C

Based on the results from Section 3.2.1, the initial concentration of vitamin C at 250 µg/mL resulted in a substantial reduction in relative IPEC-J2 cell metabolic activity to approximately 12% (Figure 3.2-1). To determine an appropriate working concentration of vitamin C, the cytotoxic effects were assessed across a range of concentrations. IPEC-J2 cells were exposed to increasing doses of vitamin C, ranging between 5 µg/mLand 600 µg/mL, for 48 h, and the cell metabolic activity was measured using AB reagent, relative to untreated control. Three independent biological replicates were performed (n = 3). Within each biological replicate, each vitamin C concentration was analysed using one column of a 96-well plate. Statistical analysis was carried out on the three biological replicates, using One-way ANOVA with Dunnett's test, with significance marked as ***($p \leq 0.001$).

As shown in Figure 3.2-6, the concentrations of 100 µg/mL and higher resulted in a significant decrease ($p \leq 0.001$) in cell metabolic activity , with activity ranging between approximately 8% and 22%, relative to untreated control cells. Treatment with 50 µg/mL of vitamin C also reduced IPEC-J2 cells metabolic activity to roughly 66%. In contrast, lower concentrations of 5, 10, and 25 µg/mL slightly increased the metabolic activity of cells, to approximately 115%, 112%, and 107%, respectively, relative to control cells.

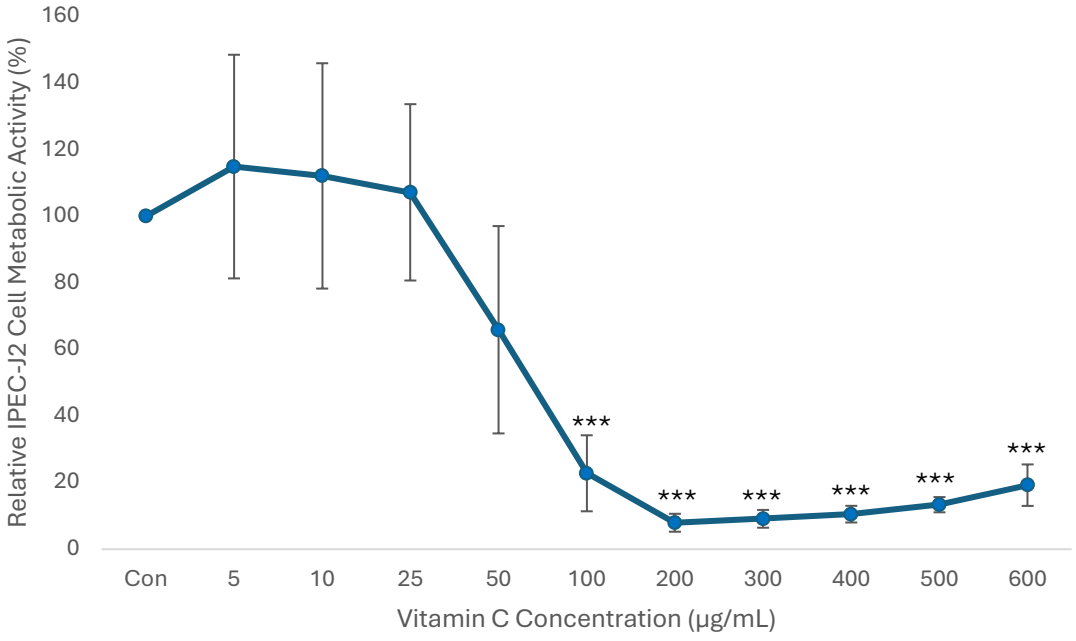
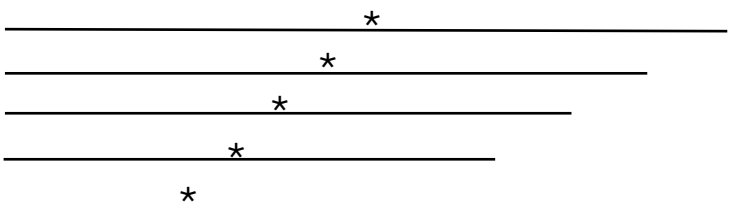


Figure 3.2-6: Effect of 48-hour treatment with vitamin C on relative IPEC-J2 cell metabolic activity as determined by Alamar Blue assay- Cells treated with increasing concentrations of vitamin C for 48 h, with IPEC-J2 cell metabolic activity expressed as a percentage relative to

untreated control cells. Dots represent mean IPEC-J2 cell metabolic activity with error bars indicating standard deviation. Data was analysed using One-way ANOVA with Dunnett's test to compare each concentration with the control group, with significance marked as ***($p \leq 0.001$), n=3.

3.2.6 Investigation of 24-hour treatment with vitamin C on relative IPEC-J2 cell metabolic activity under heat stress at 42°C

Using the results from the toxicity assay (Section 3.2.4), the concentrations of 200, 100, 50 and 25 µg/mL were selected for further analysis. To determine the effects of vitamin C concentration on relative IPEC-J2 cell metabolic activity in heat-stressed IPEC-J2 cells, they were treated for 24 h, and cells' metabolic activity was assessed after 24 h of heat stress at 42°C. AB reagent was used to assess metabolic activity , with the metabolic activity expressed as a percentage relative to untreated cells that were maintained at optimal temperature of 37°C (Figure 3.2-7). After 24 h of heat stress, the metabolic activity of untreated heat-stressed cells was decreased to approximately 81%, compared to 37°C control. A similar trend of metabolic activity in treated cells maintained at 37°C was seen compared with Section 3.2.4, with metabolic activity increasing in cells treated with 25µg/mL vitamin C to roughly 101%, and a decrease in metabolic activity in cells treated with 5, 100, and 200 µg/mL, decreasing to approximately 47%, 14%, and 7%, respectively, compared to 37°C control. In heat-stressed cells, 25 µg/mL vitamin C increased the cells' metabolic activity to approximately 84% compared to heat-stressed control at around 81%. The concentrations of 50, 100, and 200 µg/mL showed a decrease in cell metabolic activity compared to 42°C control with metabolic activity ranging between approximately 46%, 8%, and 5%, respectively. Three independent biological replicates were performed (n = 3). Within each biological replicate, each treatment was analysed using two columns of a 96-well plate, serving as technical replicates. Data was analysed using One-way ANOVA with Dunnett's test and significance marked as *($p \leq 0.05$).



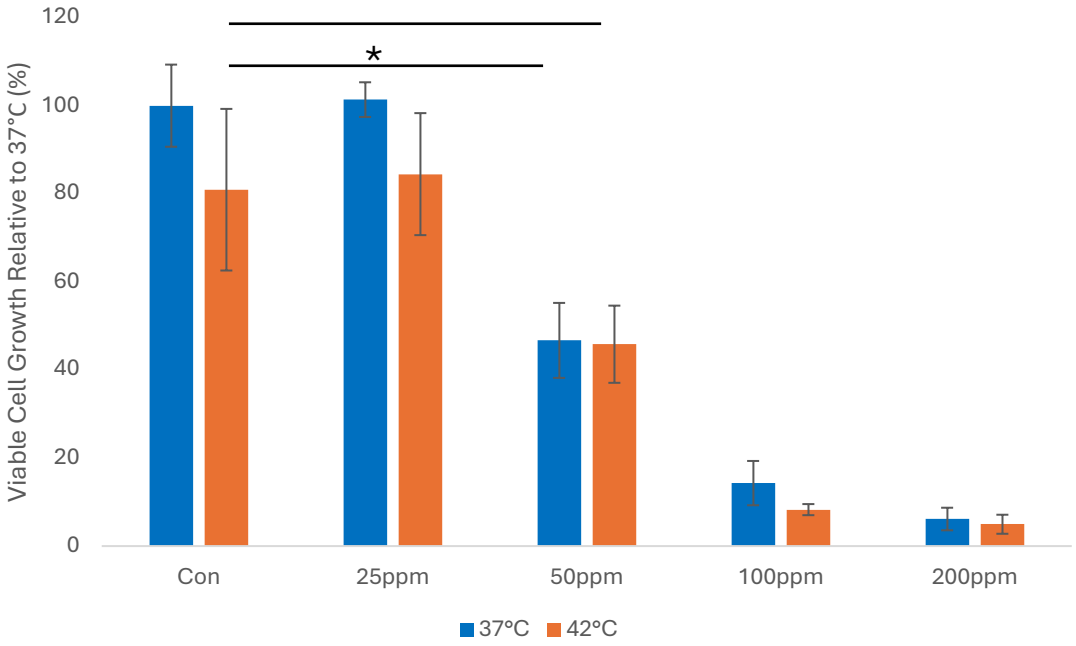


Figure 3.2-7: Effect of 24-hour treatment with vitamin C on IPEC-J2 cells' metabolic activity after being heat stressed at 42°C for 24 h- IPEC-J2 cells were treated with 50, 100, and 200 µg/mL vitamin C for 24 h prior to being heat-stressed at 42°C for a further 24 h. Data was analysed using One-way ANOVA with Dunnett's test, significance marked as *($p \leq 0.05$), n=3.

3.2.7 Investigation of 24-hour treatment with Se and vitamin compounds on Heat Shock Protein 70 (HSP70) abundance in IPEC-J2 cells prior to being exposed to 42°C for 24 hours

The aim of this was to determine if 24-hour treatment with organic Se, inorganic Se, and vitamin compounds in heat-stressed IPEC-J2 cells affects the abundance of molecular chaperone protein, HSP70. Western blot analysis was used as it can quantify total protein abundance in a sample. The house-keeping protein used in this study was actin, with each of the target protein (HSP70) bands normalised to this house-keeping protein, then protein abundance was determined relative to untreated control group. In short, IPEC-J2 cells were treated with each compound for 24 h, then, control cells remained at 37°C while HS cells were exposed to 42°C for 24 h. A total of five independent biological replicates were run with each blot containing 37°C control, 42°C control, and treated cells, with bands present at 70kDa (HSP70) and 45kDa (actin). Western blots were performed with treated samples maintained at 37°C and treated heat-stressed samples run on separate membranes. Membranes were first probed with HSP70 primary antibody followed by the corresponding secondary antibody. Then, membranes were probed with actin primary and secondary antibodies as a loading control.

Representative blots are shown for treated cells maintained at 37°C (Figure 3.2-8 A) and treated cells exposed to heat stress at 42°C for 24 h (Figure 3.2-8 B). Under control conditions (37°C), HSP70 expression was detected across all treatment groups, with relatively consistent band intensity observed between treatment groups. A larger band can be seen in 42°C Con group compared to samples maintained at 37°C. Actin was used as a loading control and showed consistent and intensity across all samples, indicating comparable protein loading between lanes. In contrast, exposure to heat stress at 42°C (Figure 3.2-8 B) resulted in an overall increase in HSP70 band intensity across all samples compared to the 37°C Con on the blot. Actin bands showed relatively consistent band intensity across all heat-stressed samples. It can be observed that with some treatments (Organic Se-A and vitamin C) appear to exhibit relatively stronger HSP70 band intensity under heat stress conditions. See supplementary figures (Figures 6.6-2 and 6.2-3) for all membrane images (n = 5).

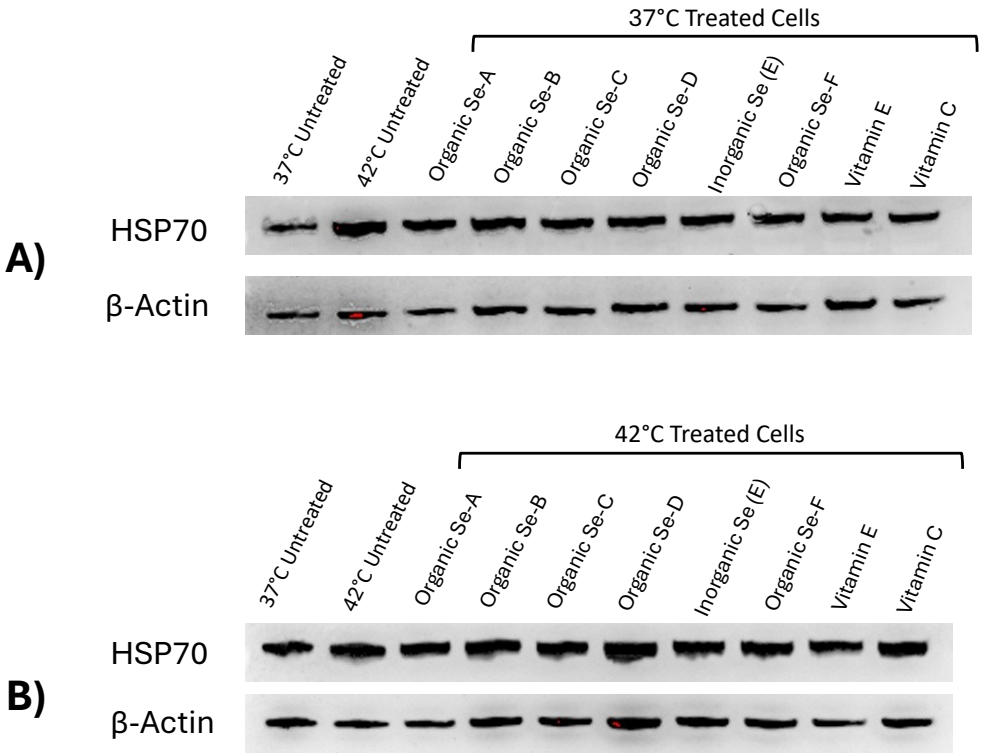


Figure 3.2-8: Representative Western blot membrane images- HSP70 protein expression in IPEC-J2 cells treated with Organic Se-A/ B/ C/ D/ F, Inorganic Se (E), vitamin E, and vitamin C compounds under control (37°C) and heat stress (42°C) conditions. Representative Western blots showing HSP70 expression in cells maintained at 37°C (A) and HSP70 expression in cells following exposure to 42°C (B). Cells were treated with compounds for 24 h prior to being heat stressed for a further 24 h. HSP0 expression was detected using specific primary and secondary antibodies, and membranes were probed with actin as a loading control.

Densitometric analysis was then performed to determine HSP70 protein expression normalised to actin in IPEC-J2 cells treated with Se and vitamin compounds for 24 h prior to exposure to heat stress at 42°C for 24 h (Figure 3.2-9). A total of five independent biological replicates were performed (n = 5). Data was analysed using One-way ANOVA with Tukey's post hoc test, with significance marked as *($p \leq 0.05$).

Under control conditions (37°C) each of the compounds, except for vitamin E, increased the abundance of HSP70 compared to untreated control, with relative HSP70 expression ranging between approximately 1.2 and 1.7. Supplementation with vitamin E under optimal conditions caused a decrease in HSP70 expression, with expression reduced to 0.75, compared to untreated 37°C control.

A significant increase ($p = 0.0151$) in HSP70 expression was observed in the untreated control cells following heat stress compared to cells maintained at 37°C, with expression increased to approximately 2.2. Each of the treatment groups under heat stress conditions resulted in an increase in HSP70 expression when compared to the 37°C control and to their respective treatment at 37°C. The highest increase in HSP70 expression is seen in heat-stressed cells treated with Organic-Se A, Inorganic Se (E), and vitamin C, with expression increased to approximately 1.9 relative to 37°C control. Supplementation with Organic Se-C and F showed the lowest HSP70 expression, at roughly 1.3, while Organic Se-B, D, and vitamin E show similar expression ranging between approximately 1.6 and 1.8. Overall, these findings demonstrate that heat stress induces HSP70 expression in IPEC-J2 cells, with variation in response observed depending on the treatment applied.

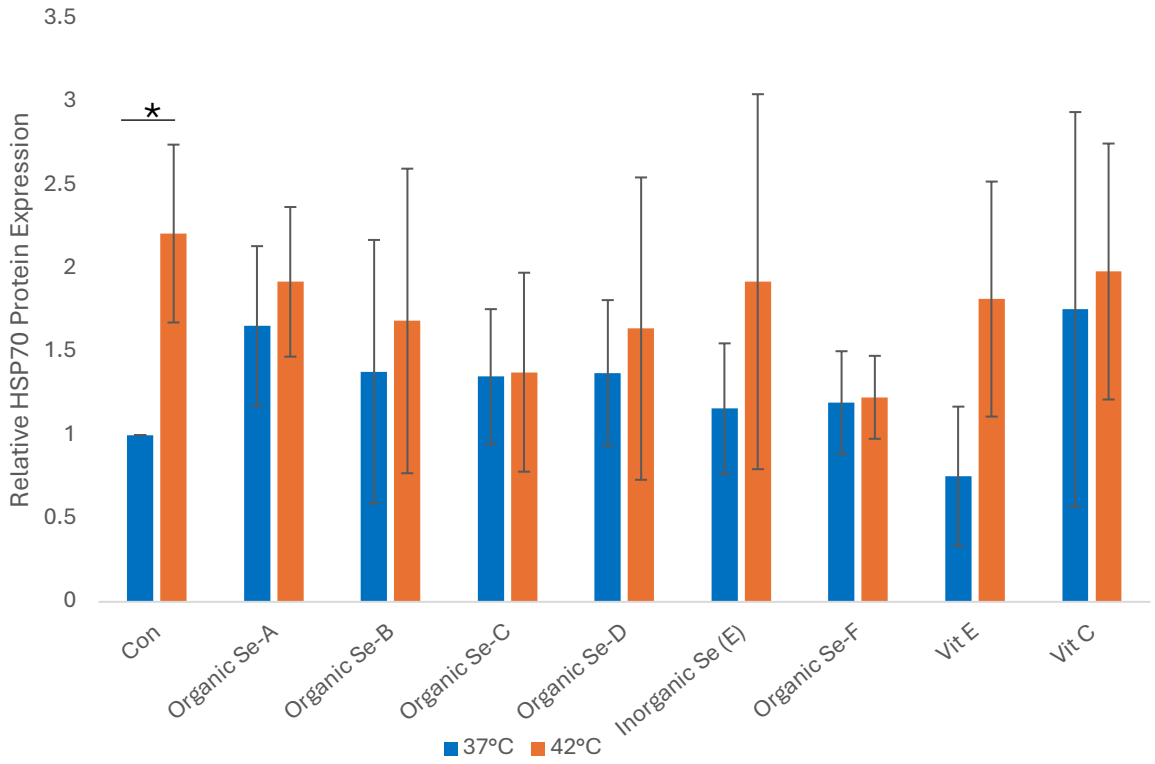


Figure 3.2-9: Densitometric analysis of HSP70 expression- IPEC-J2 cells treated with Se and vitamin compounds for 24 h then exposed to 37°C or 42°C for a further 24 h. HSP70 expression was normalised to actin, and values are expressed as relative protein expression to 37°C control. Data was analysed using One-way ANOVA with Tukey's multiple comparison with significance marked as *($p \leq 0.05$), n=5.

3.3 Proteomic Analysis

A heat stress model was established using IPEC-J2 cells exposed to 42°C for 24 h, which resulted in a decrease in IPEC-J2 cell metabolic activity using AB assay, and increased expression of HSP70 confirmed by Western blotting. This model was subsequently used to investigate the proteomic response of IPEC-J2 cells to heat stress, and to evaluate the impact of nutritional supplementation on this model.

Firstly, a comparative quantitative proteomic analysis was performed between cells exposed to heat stress for 24 h at 42°C, and control cells maintained at 37°C. Protein samples were extracted from cells, digested into peptides and analysed using tandem LC-MS/MS, where peptides were separated based on physicochemical properties and identified based on their mass-to-charge ratios. Heat-stressed cells supplemented with organic Se, inorganic Se, vit E, and vit C were then compared to untreated heat-stressed cells to assess the effects of supplementation under heat stress conditions. In this study, Organic Se-A was selected for further investigation in order to investigate the molecular mechanisms associated with Se-mediated responses to heat stress . Due to commercial confidentiality, the rationale for selection cannot be described in greater detail.

Proteins that were identified was achieved by matching peptide spectra to protein databases, and relative abundance was determined based on peptide intensities. Differentially expressed proteins were identified using statistical analysis ($p \leq 0.05$ and $\log_2(FC) \geq 0.0585$). Functional annotation and pathway enrichment analyses were performed using the Search Tool for the Retrieval of Interacting Genes (STRING) database (https://string-db.org/) to identify significantly affected biological processes, and protein-protein interaction (PPI) networks. Since adjusted p-values for differential abundance were not available from the exported dataset, these findings should be considered exploratory.

Significantly altered proteins ($p \leq 0.05$) were mapped onto interaction networks, and clustering analysis was applied to identify groups of proteins associated with shared biological functions. These analyses provide an overview of the coordinated cellular pathways that are impacted by heat stress, and the modulatory effects of nutritional supplementation in IPEC-J2 cells under heat stress.

3.3.1 Comparative proteomic analysis of heat-stressed and control IPEC-J2 cells

From the quantitative analysis a total of 960 proteins were detected between cells exposed to 42°C and control cells maintained at 37°C. The data was sorted so the proteins included in analysis had a peptide count ≥ 2, fold change (FC) ≥ 1.5, and a p-value ≤ 0.05. This reduced the number of proteins to 361, with 152 of these proteins being upregulated in the heat-stressed cells while 209 were downregulated. The proteins with a fold change value ≥ 1.5, and p-value ≤ 0.05 were plotted on a volcano plot (Figure 3.3-1).

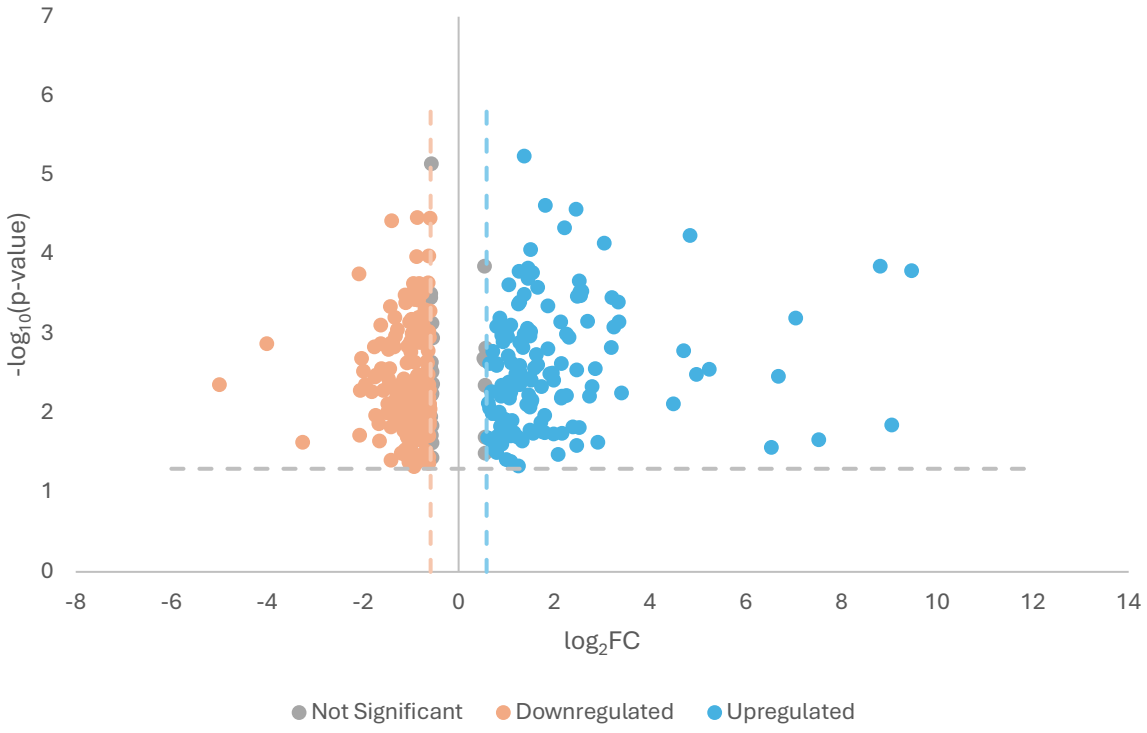


Figure 3.3-1: Volcano plot illustrating differential protein expression between heat-stressed and control IPEC-J2 cells. The x-axis shows $\log_2$ fold change, and the y-axis shows the $-\log_{10}$(p-value). Proteins significantly upregulated are highlighted in blue, significantly downregulated proteins are shown in orange, while grey dots are not significant. Horizontal and vertical dashed lines indicate the applied significance thresholds ($p \leq 0.05$, and $\log_2 FC \geq 0.585$).

3.3.1.1 STRING analysis on upregulated proteins in heat-stressed IPEC-J2 cells compared to control cells

The STRING database was used to determine protein-protein interactions (PPIs) and examine relationships between proteins that were significantly upregulated ($p \leq 0.05$) in heat-stressed IPEC-J2 cells compared to cells maintained at optimal temperature. The resulting interaction (Figure 3.3-2) shows a high degree of connectivity, indicating coordinated regulation of multiple cellular pathways in response to heat stress.

The most prominent cluster comprised molecular chaperones and heat shock proteins, including HSP90AA1, HSP90B1, HSPA8, HSPD1, and HSPH1, alongside co-chaperones such as STIP1, DNAJA2, DNAJB1, DNAJC9, and FKBP4. This cluster was enriched for functions related to protein folding and the HSP90 chaperone cycle.

Another major cluster included proteins involved in protein folding within the ER, such as CALR, PDIA3, PDIA4, PDIA6, ERP29, and ERO1A. Additional smaller clusters were associated with calcium-binding proteins and nuclear associated components, including Lamin proteins.

Overall, the STRING interaction network demonstrated enrichment of pathways related to molecular chaperone activity and ER protein processing in response to heat stress.

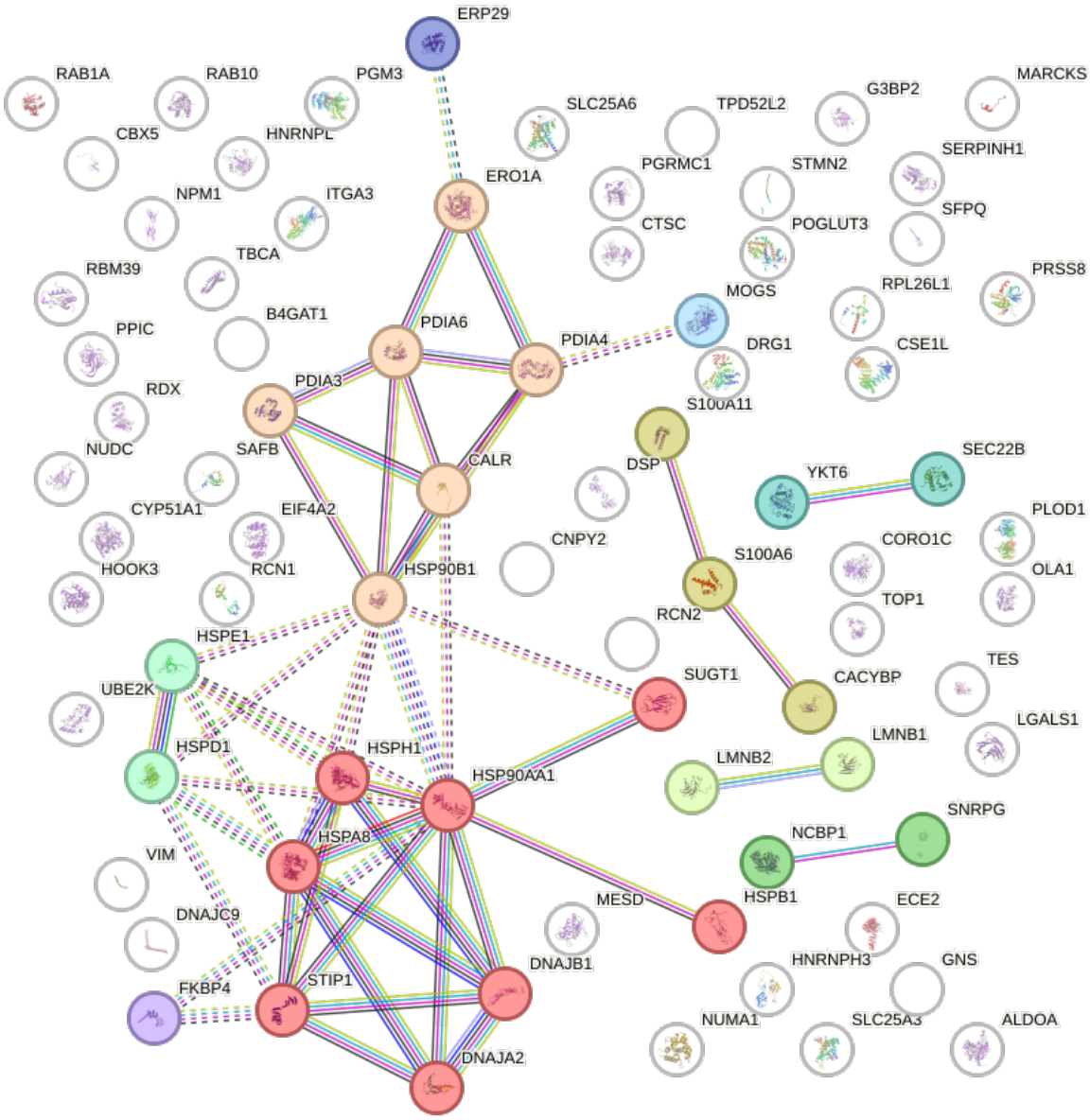


Figure 3.3-2: STRING PPI network of proteins significantly upregulated in heat-stressed IPEC-J2 cells compared to control cells ($p \leq 0.05$)- Nodes represent proteins, and edges represent predicted or known functional interactions. The network was generated using high-confidence interaction score (0.7) and shows significant enrichment (PPI enrichment p-value < 1.0e-16). Functional clustering highlights enrichment of heat shock proteins and molecular chaperones, ER protein folding proteins, and smaller clusters related to calcium binding, nuclear localisation and vesicle trafficking.

Pathway enrichment analysis was performed to identify cellular pathways and functions associated with the upregulated proteins in heat-stressed IPEC-J2 cells compared to cells maintained at optimal temperature. Enrichment was assessed using adjusted false discovery rate (FDR) values, with pathways visualised according to significance and gene count (Figures 3.3-3, A-D).

Kyoto Encyclopaedia of Genes and Genomes (KEGG) pathway analysis (Figure 3.3-3 A), highlighted protein processing in the ER as the most significantly enriched pathway (FDR ≈11), while antigen processing and presentation showed lower enrichment. Gene ontology (GO) analysis further supported these findings, with cellular component (Figure 3.3-3 B) terms enriched for intracellular structures, including cytoplasm, intracellular organelle, and ER lumen. GO biological process analysis (Figure 3.3-3 C) demonstrated strong enrichment of pathways related to protein folding, intracellular transport, and cellular localisation. Similarly GO molecular function analysis (Figure 3.3-3 D) identified significant enrichment of chaperone binding, unfolded protein binding, and protein folding chaperone activity.

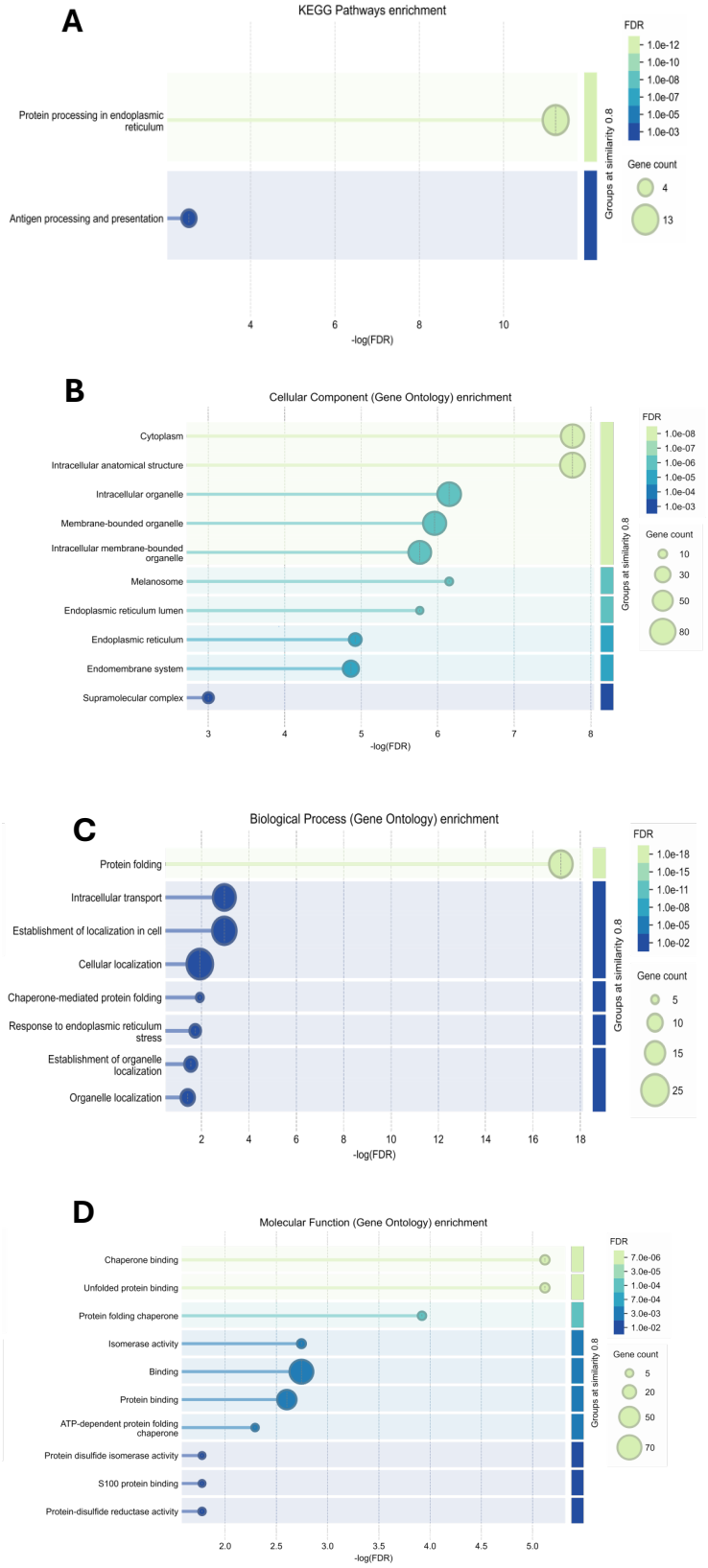


Figure 3.3-3: KEGG and Gene Ontology (GO) enrichment analysis of differentially expressed proteins upregulated in IPEC-J2 cells under heat stress. Bubble plots show enrichment of (A) KEGG pathways, (B) cellular components, (C) biological processes, and (D) molecular functions. The x-axis represents -log (FDR), bubble size indicated gene count, and colour represents FDR.

To further characterise the proteomic response to heat stress, a list of 10 differentially upregulated proteins was compiled based on the fold change ($p \leq 0.05$) (Table 3.3-1). The most markedly upregulated protein was B-cell receptor-associated protein 31 (BCAP31), which showed a 706.2-fold increase in abundance in heat-stressed cells compared to control cells maintained at 37°C. This was followed by 26S proteasome non-ATPase regulatory subunit 2 (PSMD2) with a 531.9-fold increase, and proliferating cell nuclear antigen (PCNA) with a max fold change of 449.5. Several molecular chaperone-associated proteins were also among the most upregulated, including DNAJ homolog subunit A member 2 (184.7-fold change), alongside calcium-binding proteins such as S100A11 and S100A6 with fold changes of 132.2 and 28.8, respectively. Other highly upregulated proteins included glutamine—fructose-6-phosphate aminotransferase (GFPT1), and 14-3-3 protein zeta/delta, with fold changes ranging between 102.9 and 93.0, as well as Ras-related protein Rab-1A (38.0-fold change), and eukaryotic translation initiation factor 2 subunit 3 (31.4-fold change).

These proteins are primarily associated with protein quality control mechanisms, including ER stress, molecular chaperone activity, proteasome-mediated protein degradation, and regulation of translation and cell cycle processes, demonstrating a coordinated cellular response to manage protein misfolding and maintain proteostasis under heat stress conditions.

Some of the proteins in Table 3.3-1 exhibited exceptionally high fold changes, no missing or zero values were identified, but low protein abundance in the 37°C Con samples contributed to the observed fold-change. Therefore, fold-change values should be interpreted carefully. The mean abundance was calculated from three independent biological replicates ($n = 3$).

Table 3.3-1: Differentially expressed proteins identified in IPEC-J2 cells heat stressed at 42°C for 24 h- The table includes protein name, number of unique peptides, mean normalised abundance for each group (n = 3), fold change, direction of change, and protein-level ANOVA p-value. Proteins were filtered based on a peptide count ≥ 2, a maximum fold change ≥ 1.5, and a p-value ≤ 0.05.

Protein Description	Unique Peptides	Mean Abundance (37°C Con)	Mean Abundance (42°C Con)	Fold Change	Direction	ANOVA p-value
B-cell receptor-associated protein 31	3	300.9	212486.4	706.2	Up	0.00016
26S proteasome non-ATPase regulatory subunit 2	2	88.4	46994.1	531.9	Up	0.01423
DNA sliding clamp PCNA	2	1166.2	524177.7	449.5	Up	0.00014
DNAJ homolog subfamily A member 2	2	292.6	54054.6	184.7	Up	0.02178
Protein S100-A11	2	25041.8	3311029.4	132.2	Up	0.00064
Glutamine--fructose-6-phosphate aminotransferase	2	4031.7	414730.4	102.9	Up	0.00344
14-3-3 protein zeta/delta	5	100957.7	9391292.8	93.0	Up	0.02695
Ras-related protein Rab-1A	2	5126.8	194724.9	38.0	Up	0.00282
Eukaryotic translation initiation factor 2 subunit 3	3	10167	319458.0	31.4	Up	0.00322

Protein S100-A6	2	5300934.3	15412792.8	28.8	Up	5.71e-05

3.3.1.2 STRING analysis on downregulated proteins in heat-stressed IPEC-J2 cells compared to control cells

PPI analysis of downregulated proteins in IPEC-J2 cells under heat stress, revealed a well-connected network comprising several distinct functions.

The largest and most highly connected cluster primarily consists of proteins that are involved in translation and protein synthesis, including multiple ribosomal proteins and translation initiation and elongation factors. The high degree of connectivity is indicating regulation of components associated with translational machinery.

Additional clusters included proteasome-related proteins (PSMs), enzymes involved in central carbon metabolism and glycolysis, and proteins associated with aminoacyl-tRNA biosynthesis. Cytoskeletal-related proteins formed smaller, distinct interaction groups. Several nodes appear as isolated nodes, suggesting limited connectivity within the network.

Overall, the PPI network highlights enrichment of pathways associated with translation, metabolism, and cytoskeletal organisation among proteins significantly downregulated under heat stress conditions.

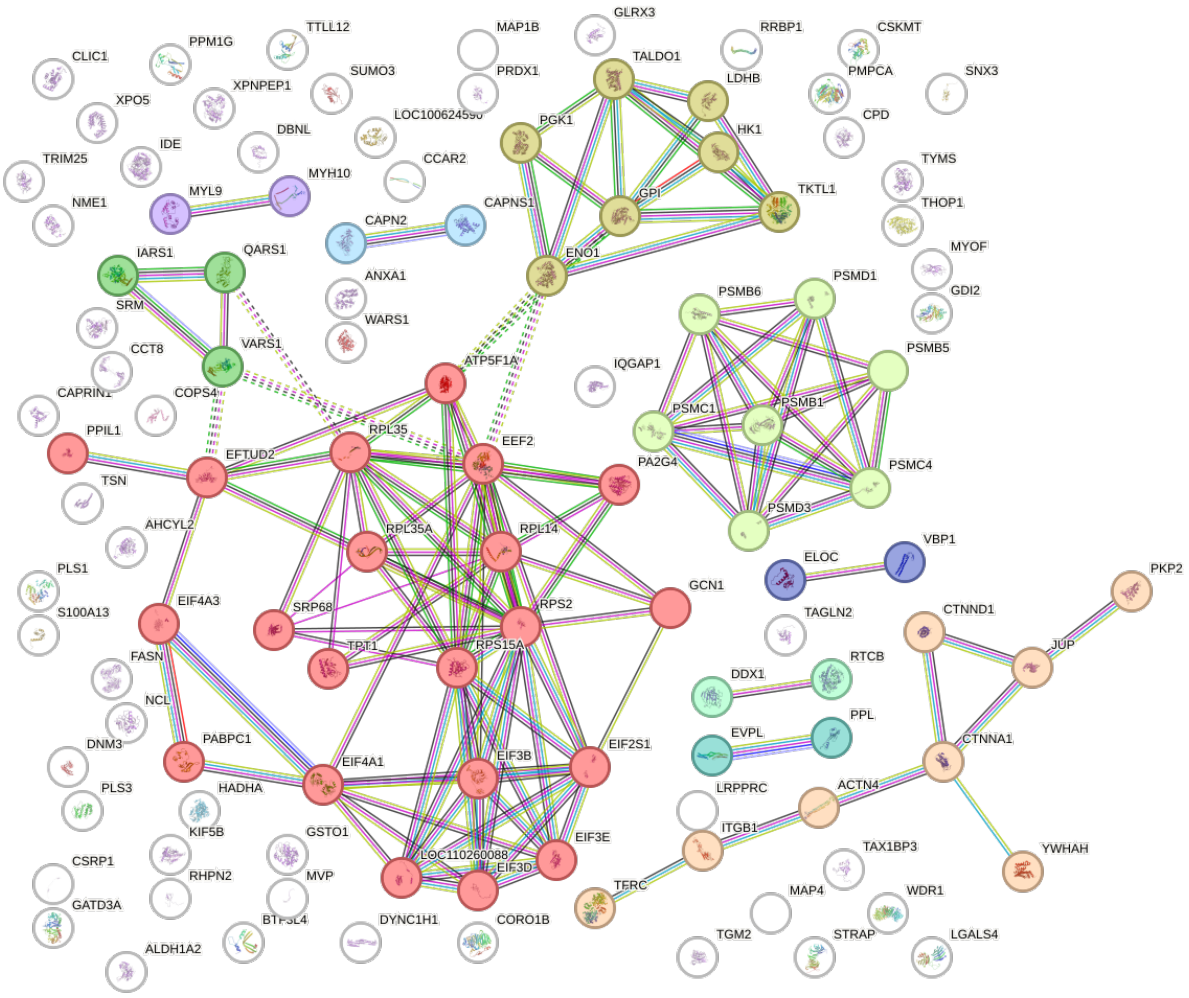


Figure 3.3-4: Protein-protein interaction network, generated using STRING database, of proteins significantly downregulated in heat-stressed IPEC-J2 cells compared to cells maintained at optimal temperature. Nodes represent individual proteins and edges represent known or predicted interactions. The network was generated using high-confidence interaction score (0.7) and shows significant enrichment (PPI enrichment p-value <1.0e-16). Proteins are grouped into clusters based on functional enrichment and interaction strength. Major clusters include proteins involved in translation and protein synthesis, proteasome-associated pathways, central carbon metabolism and glycolysis, aminoacyl-tRNA biosynthesis, cytoskeletal organisation, and the calpain complex.

Pathway enrichment analysis was performed to identify cellular pathways and functions associated with downregulated proteins in heat-stressed IPEC-J2 cells compared to control cells maintained at optimal temperature. Pathways were visualised according to significance and gene count, with enrichment assessed using adjusted false discovery rate (FDR). Pathways in Figure 3.3-5 are divided into four different groups; KEGG pathways (A), Cellular component enrichment (B), Biological process enrichment (C), and Molecular function enrichment (D).

Proteomic analysis of IPEC-J2 cells heat stressed at 42°C for 24 h revealed significant downregulation of pathways associated with protein synthesis, RNA processing, and cellular metabolism. KEGG pathway enrichment (Figure 3.3-5 A) identified suppression of the proteasome and RNA transport pathways, alongside metabolic pathways including carbon metabolism and glycolysis/gluconeogenesis. GO biological process analysis (Figure 3.3-5 C) demonstrated enrichment of downregulated terms related to translation, gene expression, and peptide biosynthetic processes, indicating reduced protein synthesis. Consistent with this, GO molecular function analysis (Figure 3.3-5 D) showed decreased enrichment of translation initiation factor activity, RNA binding, and ribonucleoprotein complex binding. Additionally, pathways associated with cytoskeletal protein binding and actin filament binding were reduced suggesting alterations in cellular structural organisation. GO cellular component analysis (Figure 3.3-5 B) further supported these findings, with downregulated proteins predominantly localised to cytoplasm, intracellular organelles, and ribonucleoprotein complexes.



Figure 3.3-5: KEGG and Gene Ontology (GO) enrichment analysis of differentially expressed proteins downregulated in IPEC-J2 cells under heat stress. Bubble plots show enrichment of

(A) KEGG pathways, (B) cellular components, (C) biological processes, and (D) molecular functions. The x-axis represents -log (FDR), bubble size indicated gene count, and colour represents FDR.

A list of 10 significantly downregulated proteins in response to heat stress was generated ($p \leq 0.05$) (Table 3.3-2). Tax1-binding protein 3 (TAXBP3) showed a significant decrease (2.8) in heat-stressed cells. Envoplakin and plakophilin, were downregulated with fold decreases of 2.8 and 2.8, respectively, both of which are associated with cellular structural organisation. Additional proteins showing reduced abundance included prefoldin subunit 3, serine/threonine-protein phosphatase 2A regulatory subunit A beta isoform, galectin-4, and insulin-degrading enzyme, with fold changes of 2.8 and 2.7, respectively. Proteins involved in mitochondrial and signalling processes, including cytochrome b-c1 complex subunit 1 (2.7-fold), protein phosphatase 1G (2.7-fold) and eIF-2-alpha kinase activator GCN1 (2.6-fold), were also downregulated.

These proteins are primarily associated with cytoskeletal organisation, cell adhesion, intracellular signalling, metabolic processes, and regulation of protein synthesis, suggesting a coordinated suppression of structural integrity, cellular signalling pathways, and energy metabolism under heat stress conditions.

Table 3.3-2: Differentially expressed proteins identified in IPEC-J2 cells heat stressed at 42°C for 24 h- The table includes protein name, number of unique peptides, mean normalised abundance for each group (n = 3), fold change, direction of change, and protein-level ANOVA p-value. Proteins were filtered based on a peptide count ≥ 2, a maximum fold change ≥ 1.5, and a p-value ≤ 0.05.

Protein Description	Unique Peptides	Mean Abundance (37°C Con)	Mean Abundance (42°C Con)	Fold Change	Direction	ANOVA p-value
Tax1-binding protein 3	2	3388158	1211960	2.8	Down	0.0044
Envoplakin	3	1623393	214623	2.8	Down	0.0013
Plakophilin-2	2	372203	134791	2.8	Down	0.0232
Prefoldin subunit 3	2	639343	232228	2.8	Down	0.000175
Serine/threonine-protein phosphatase 2A 65kDa regulatory subunit A beta isoform	2	917832	338182	2.7	Down	0.0190
Galectin-4	3	2010386	747351	2.7	Down	0.00519
Insulin-degrading enzyme	2	413981	154771	2.7	Down	0.00204
Cytochrome b-c 1 complex subunit 1, mitochondrial	4	1171011	442643	2.7	Down	0.00298
Protein phosphatase 1G	3	1528325	575304	2.7	Down	0.00441
eIF-2-alpha kinase activator GCN1	2	238531	126010	2.6	Down	0.00539

Pathway enrichment analysis of proteomic data revealed distinct patterns of upregulated and downregulated pathways in IPEC-J2 cells exposed to 42°C for 24 h, compared to cells that were maintained at optimal temperature of 37°C. Proteins upregulated under heat stress were primarily enriched in pathways related to protein folding, molecular chaperone activity, and ER function, including protein processing in the ER. Enrichment was also observed for pathways associated with intracellular transport and cellular localisation. In contrast, proteins downregulated in heat-stressed cells were enriched in pathways involved in central metabolism, protein synthesis, and gene expression, including glycolysis, translation, peptide biosynthesis, RNA transport, and proteasome-related pathways.

3.3.2 Differential protein expression between heat-stressed IPEC-J2 cells treated with Organic Se-A compound compared to untreated heat-stressed control cells

Quantitative proteomic analysis was performed to assess the effects of Organic Se-A treatment on IPEC-J2 cells under heat stress conditions by comparing treated cells exposed to 42°C with untreated heat-stressed control cells. A total of 188 proteins were identified in this comparison. Proteins were filtered based on a peptide count ≥ 2, a maximum fold change ≥ 1.5, and a p-value ≤ 0.05, which reduced the number of proteins to 6. Of these six proteins, three were significantly upregulated and three were significantly downregulated in 42°C cells treated with Organic Se-A ($p \leq 0.05$) (Table 3.3-3). The number of proteins detected in this comparison is substantially fewer than the other treatment comparisons. The reason for this is unclear and may reflect a combination of biological and technical factors. A complete list of the proteins identified in this comparison is provided in Appendix Table 6.3-2.

Of the three significantly upregulated proteins, heat shock 70 kDa protein 1B (HSP70) ($p = 0.00437$), thioredoxin reductase 1 (TrxR1) ($p = 0.00164$) both showed a 2.1-fold increase in abundance, while matrin-3 exhibited a 1.7-fold increase. The upregulation of HSP70 is consistent with its established role in the heat shock response, whereas TrxR1 is a Se-dependent SelP which is a key component of the cellular antioxidant defence system. Matrin-3 participates in nuclear structure and stress-response pathways, was also moderately upregulated suggesting involvement in cellular adaptation to stress conditions.

In contrast, the three significantly downregulated proteins included peptidyl-prolyl cis-trans isomerase FKBP4 ($p = 0.00326$), talin-1 isoform X1 ($p = 0.000313$), and beta-hexosaminidase subunit alpha precursor ($p = 0.000142$). Peptidyl-prolyl cis-trans isomerase FKBP4 showed the greatest reduction, with a fold decrease of 3.4, while both talin-1 and beta-hexosaminidase subunit alpha precursor showed a fold decrease of 1.5. FKBP4 functions as a co-chaperone involved in protein folding, while talin-1 is associated with cytoskeletal organisation and cell adhesion and beta-hexosaminidase participates in lysosomal metabolism.

Due to the limited number of significantly expressed proteins and the lack of strong functional overlap between them, STRING PPI and pathway enrichment analysis did not identify significantly enriched KEGG pathways or GO terms for either the upregulated or downregulated protein sets. These results indicate that treatment with Organic Se-A under

heat stress conditions results in the selective alterations to the abundance of a small number of proteins rather than a broad pathway level modulation of the heat-stress proteomic response.

Table 3.3-3: Differentially expressed proteins identified in IPEC-J2 cells treated with Organic Se-A, compared to untreated heat-stress cells- The table includes protein name, number of unique peptides, mean normalised abundance for each group (n = 3), fold change, direction of change, and protein-level ANOVA p-value. Proteins were filtered based on a peptide count ≥ 2, a maximum fold change ≥ 1.5, and a p-value ≤ 0.05.

Protein Description	Unique Peptides	Mean Abundance (42°C Con)	Mean Abundance (42°C Organic Se-A)	Fold Change	Direction	ANOVA p-value
Heat shock 70 kDa protein 1B	2	59275	125659	2.1	Up	0.00437
Thioredoxin reductase 1, cytoplasmic	4	759233	1573467	2.1	Up	0.00164
Matrin-3, isoform X1	2	213867	355631	1.7	Up	0.02612
Peptidyl-prolyl cis-trans isomerase FKBP4	2	1653407	484806	3.4	Down	0.00326
Talin-1 isoform X1	2	1031610	690755	1.5	Down	0.000313
Beta-hexosaminidase subunit alpha precursor	2	1270533	868836	1.5	Down	0.000142

3.3.3 Differential protein expression between heat-stressed IPEC-J2 cells treated with Inorganic Se (E) compound compared to untreated heat-stressed control cells

To determine whether treatment with Inorganic Se (E) for 24 h modified the proteomic response of IPEC-J2 cells to heat stress, quantitative proteomic analysis was performed comparing inorganic Se-treated heat-stressed cells to untreated heat-stressed control cells. A total of 787 proteins were detected across all samples. Proteins were filtered based on a peptide count ≥ 2, a maximum fold change ≥ 1.5, and a p-value ≤ 0.05. Application of these criteria reduced the number of proteins in further analysis to 180. Of these, 47 were upregulated, and 133 proteins downregulated in Se-treated cells exposed to 42°C, relative to untreated cells heat stressed at 42°C. The distribution of significantly upregulated and downregulated proteins in Inorganic Se (E)-treated heat-stressed cells is visualised in a volcano plot (Figure 3.3-6).

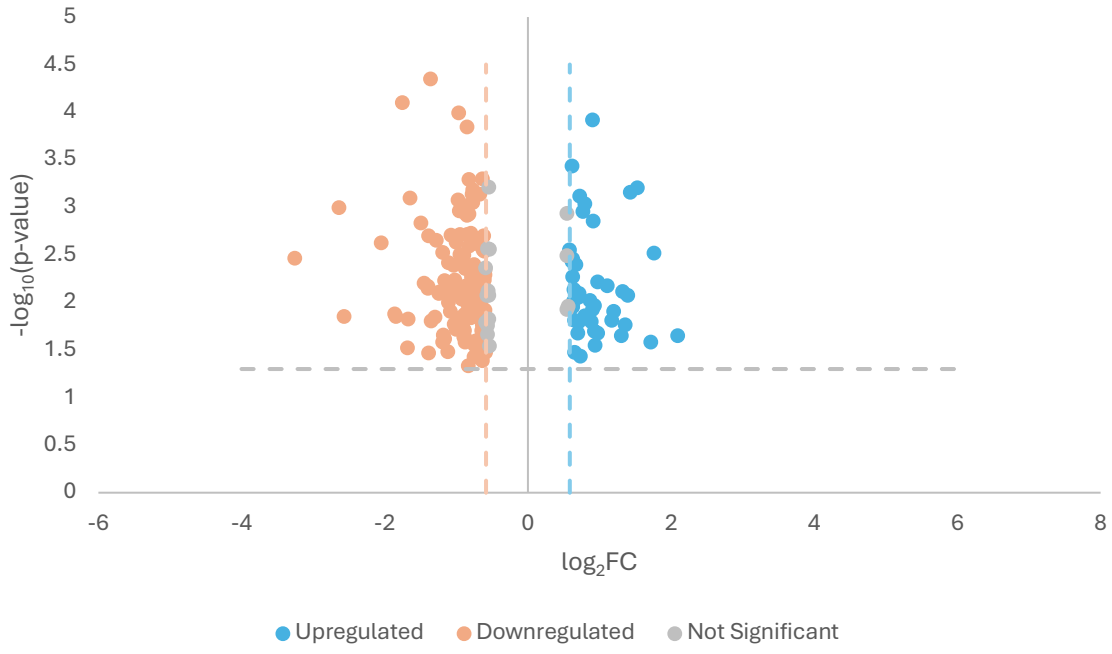


Figure 3.3-6: Volcano plot illustrating protein expression between IPEC-J2 cells treated with Inorganic Se (E) for 24 h prior to being heat stressed at 42°C for 24 h and untreated IPEC-J2 cells heat stressed for 24 h. The x-axis represents $\log_2$(fold change), and the y-axis represents -$\log_{10}$(p-value). Significantly upregulated proteins are shown in blue, significantly downregulated proteins are highlighted in orange and grey dots represent non-significant proteins. Horizontal and vertical dashed lines indicate the applied significance thresholds (p-value ≤ 0.05, and $\log_2$FC ≥ 0.585).

3.3.3.1 STRING analysis on upregulated protein in heat-stressed IPEC-J2 cells treated with Inorganic Se (E) for 24 hours compared to untreated heat-stressed control cells

STRING PPI analysis of proteins upregulated in IPEC-J2 cells treated with Inorganic Se (E) for 24 h prior to being heat stressed at 42°C for a further 24 h, were compared to untreated cells that were heat stressed for 24 h. The resulting interaction map (Figure 3.3-7) identified several functionally connected clusters associated with protein folding, metabolism, and cellular stress responses.

The most prominent cluster, consisted of proteins involved in ATP-dependent protein folding chaperone activity, and the chaperonin-containing T complex, including HSPA8, TCP1, CCT3, and CCT6B.A second cluster consisting of PGK1, ALDOA, and LDHB was associated with glycolysis/gluconeogenesis, suggesting modulation of cellular energy metabolism under heat stress conditions. Another prominent cluster contained proteins, involved in double-strand break repair via break-induced replication and the CMG complex, such as MCM2, MCM3, and MCM5.

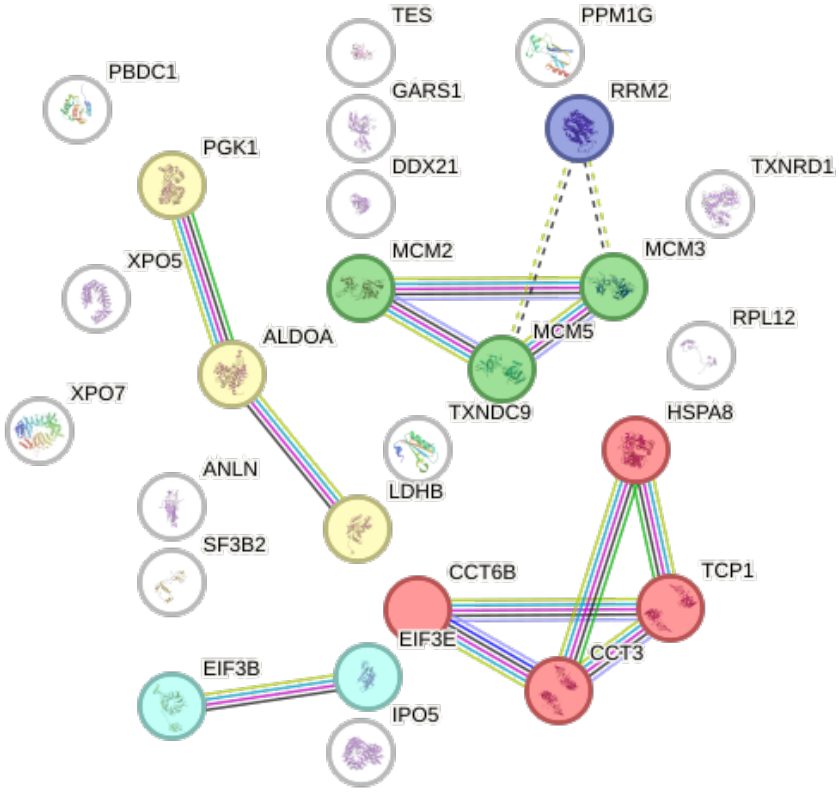


Figure 3.3-7: Protein-protein interaction network of proteins upregulated in IPEC-J2 cells exposed to heat stress at 42°C for 24 hours, with Inorganic Se (E) supplementation- Nodes represent individual proteins, and edges indicate predicted or known protein-protein interactions. The network was generated using high-confidence interaction score (0.7) and shows significant enrichment (PPI enrichment p-value of 1.45e-06). Proteins are grouped into functional clusters based on interaction networks with colours indicating distinct clusters. Major clusters include proteins associated with ATP-dependent protein folding and chaperone complexes, glycolysis/gluconeogenesis, DNA replication and repair (MCM complex), and translation initiation. Lone nodes represent proteins with no known interactions within the dataset.

Pathway enrichment analysis was performed to identify cellular pathways and functions associated with upregulated proteins in heat-stressed IPEC-J2 cells treated with Inorganic Se (E) compound compared to untreated cells heat stressed at 42°C. Pathways were visualised according to significance and gene count, with enrichment assessed using adjusted false discovery rate (FDR). Pathways were divided into KEGG pathways (A), GO Cellular component enrichment (B), GO Biological process enrichment (C), and GO Molecular function enrichment (D), Figure 3.3-8.

KEGG pathway enrichment indicated that cells treated with inorganic Se under heat stress conditions is associated with an increased abundance of proteins involved DNA replication, cell cycle activity, as well as central carbon metabolism and hypoxia related signalling. Compared to heat stress alone, treatment with inorganic Se induces cell cycle and metabolic pathways. GO enrichment of cellular component demonstrated proteins are enriched in components including cytosol/cytoplasm, intracellular anatomical structure, CMG and MCM complexes, chaperonin-containing T-complex, protein containing complex, and eukaryotic translation initiation complexes. This indicates an increased abundance of replication and translation-related complexes in inorganic Se treated cells. Analysis indicated enriched GO biological processes include DNA replication, DNA replication initiation, DNA unwinding, and protein folding, demonstrating an enhanced regulation of genome maintenance and replication-associated stress responses, alongside continued engagement of protein folding pathways. Molecular function enriched pathways reflect increased activity of energy-dependent pathways, and DNA replication machinery, with pathways including ATP-dependent protein folding chaperone activity, ATP binding and ATP hydrolysis activity, small molecule and nucleotide binding, and helicase activity.

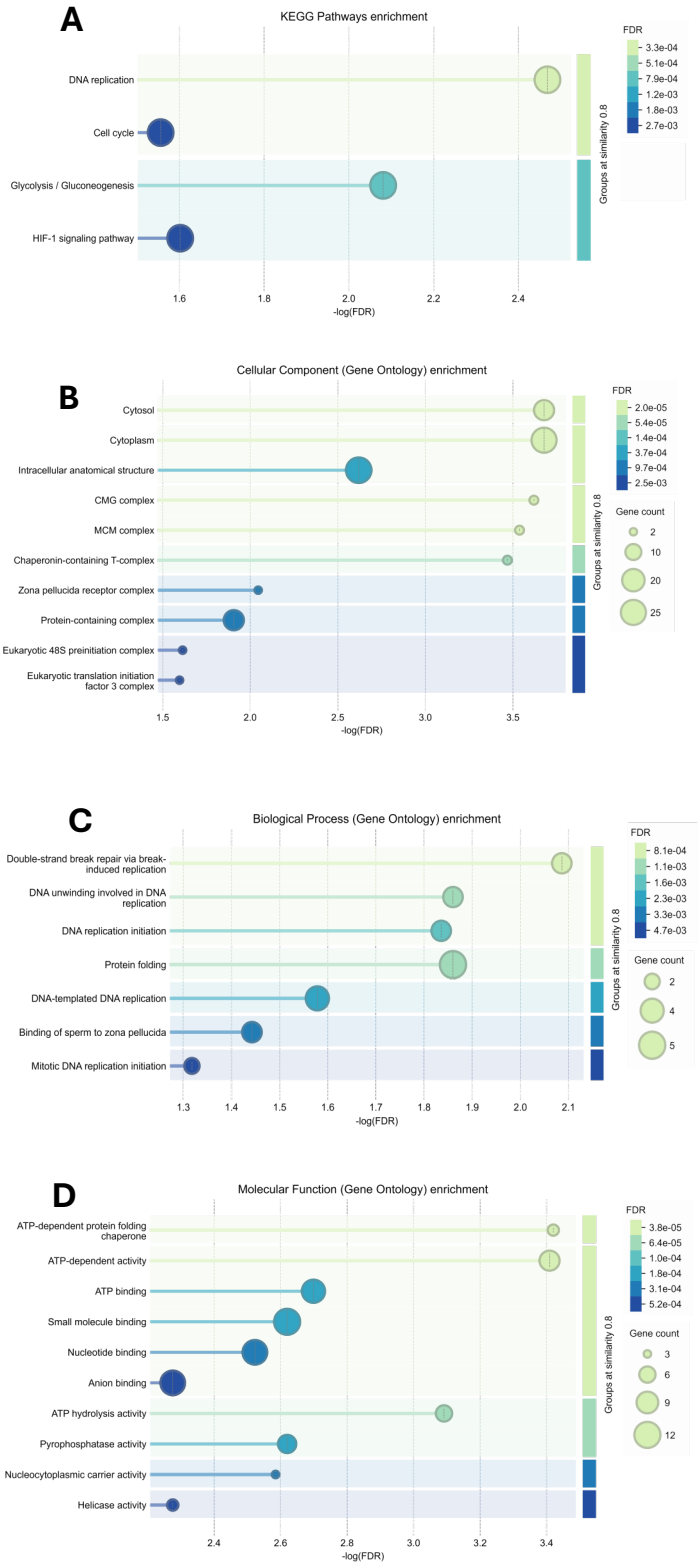


Figure 3.3-8: KEGG and Gene Ontology (GO) enrichment analysis of differentially expressed proteins upregulated in IPEC-J2 cells supplemented with Inorganic Se (E) under heat stress. Bubble plots show enrichment of (A) KEGG pathways, (B) cellular components, (C) biological processes, and (D) molecular functions. The x-axis represents -log (FDR), bubble size indicated gene count, and colour represents FDR.

3.3.3.2 STRING analysis on downregulated protein in heat-stressed IPEC-J2 cells treated with Inorganic Se (E) for 24 hours compared to untreated heat-stressed control cells

PPI analysis of proteins downregulated in IPEC-J2 cells supplemented with Inorganic Se (E) prior to exposure to heat stress (42°C) revealed moderately connected interaction network comprising several distinct functional clusters. The network demonstrated interactions between proteins involved in translation and protein synthesis, cytoskeletal organisation, and intracellular transport (Figure 3.3-9).

A prominent cluster included proteins associated with translation elongation and ribosome-associated processes, including EE1A1, EEF1D, and EEF1GIn addition, a cluster centred around cytoskeletal and structural proteins, such as ACTB, ACTN4, and ITGB1, suggesting alterations in cytoskeletal organisation and cell structural integrity.

Proteins involved in protein folding and stress responses, including HSP90 family members, were also present within interconnected clusters, alongside proteins associated with ER and protein processing functions. Several smaller clusters and isolated nodes were observed, representing proteins with limited or unknown interactions within the dataset.

Overall, the PPI network highlights the presence of multiple functionally related groups of downregulated proteins, indicating that Inorganic Se (E) supplementation prior to heat stress is associated with changes in pathways related to protein synthesis, cytoskeletal organisation, and intracellular transport.

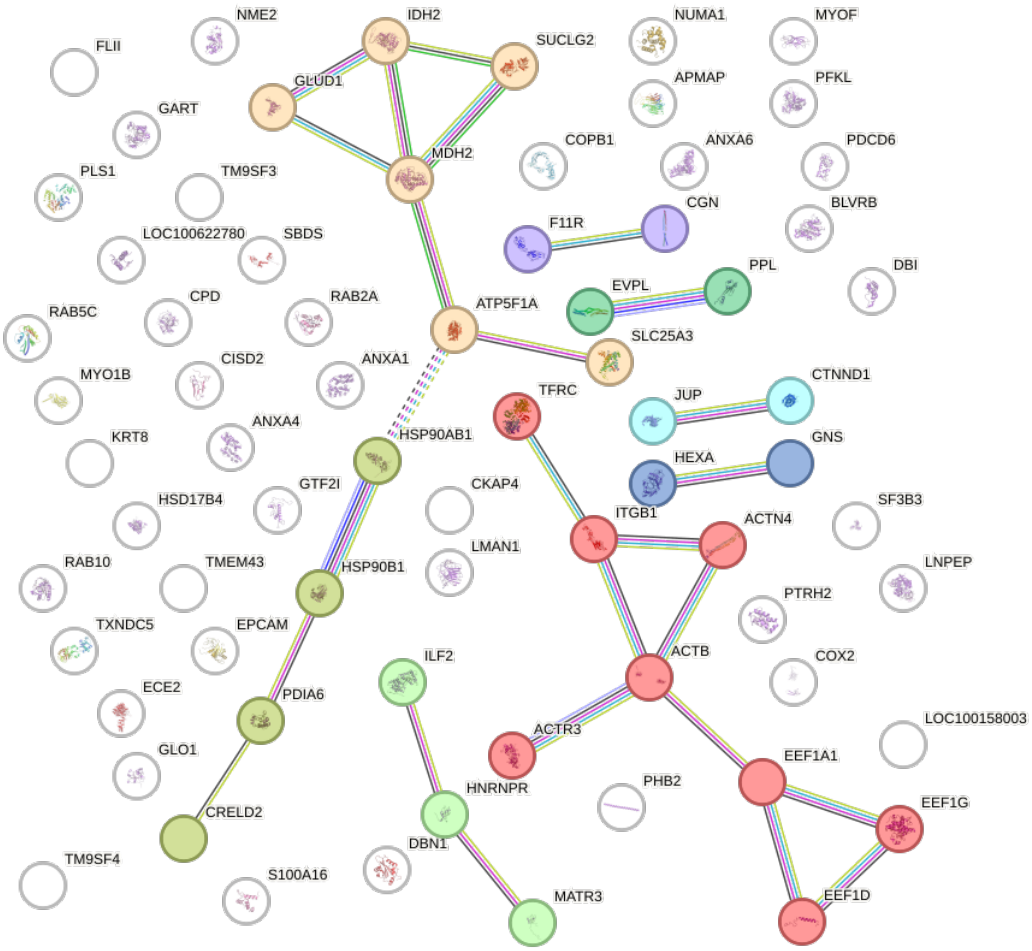


Figure 3.3-9: Protein-protein interaction network of proteins downregulated in IPEC-J2 cells supplemented with Inorganic Se (E) and subsequently exposed to heat stress (42°C), compared to untreated heat-stressed cells- Nodes represent individual proteins, while edges indicate known or predicted functional interactions between proteins. The network was generated using high-confidence interaction score (0.7) and shows significant enrichment (PPI enrichment p-value 1.35e-07). Proteins are organised into distinct clusters based on interaction patterns, with different colour representing separate functional groups. Prominent clusters include proteins associated with translation elongation (EEF1A1, EEF1D, EEF1G), cytoskeletal organisation (ACTB, ACTN4) and protein folding or stress-related processes (HSP90 family proteins). Additional clusters include proteins involved in ER function, metabolic processes, and cell signalling pathways. Disconnected nodes correspond to proteins with no identified interactions within the dataset.

Pathway enrichment analysis was performed to identify cellular pathways and functions associated with downregulated proteins in heat-stressed IPEC-J2 cells treated with inorganic Se compound compared to untreated cells heat stressed at 42°C. Pathways were visualised according to significance and gene count, with enrichment assessed using adjusted false discovery rate (FDR). Pathways were divided into KEGG pathways (A), GO Cellular component enrichment (B), GO Biological process enrichment (C), and GO Molecular function enrichment (D), Figure 3.3-10.

KEGG pathway analysis (Figure 3.3-10 A) revealed a significant enrichment of pathways associated with leukocyte trans-endothelial migration, TJs, and protein processing in the ER, in addition to broader metabolic pathways including carbon metabolism and phagosome pathways. GO cellular components (Figure 3.3-110 B) demonstrated enrichment of proteins associated with intracellular structures, including the cytoplasm, intracellular organelles, membrane-bound organelles, and cytoskeletal components. Enrichment was also observed for cell-cell junctions and cytoplasmic vesicles. GO biological process analysis (Figure 3.3-10 C) indicated significant enrichment of processes related to cytoskeleton organisation, actin filament-based processes, and actin cytoskeleton organisation, as well as supramolecular fibre and organelle organisation. GO molecular function (Figure 3.3-10 D) showed enrichment of functions such as calcium-dependent protein binding, cytoskeletal protein binding, ion binding, actin filament, and protein-containing complex binding, alongside nucleotide-binding activities.

Collectively, these results demonstrate that proteins downregulated following Inorganic Se (E) supplementation under heat stress conditions are associated with pathways involved in cytoskeletal organisation, cellular structure, and intracellular organisation.

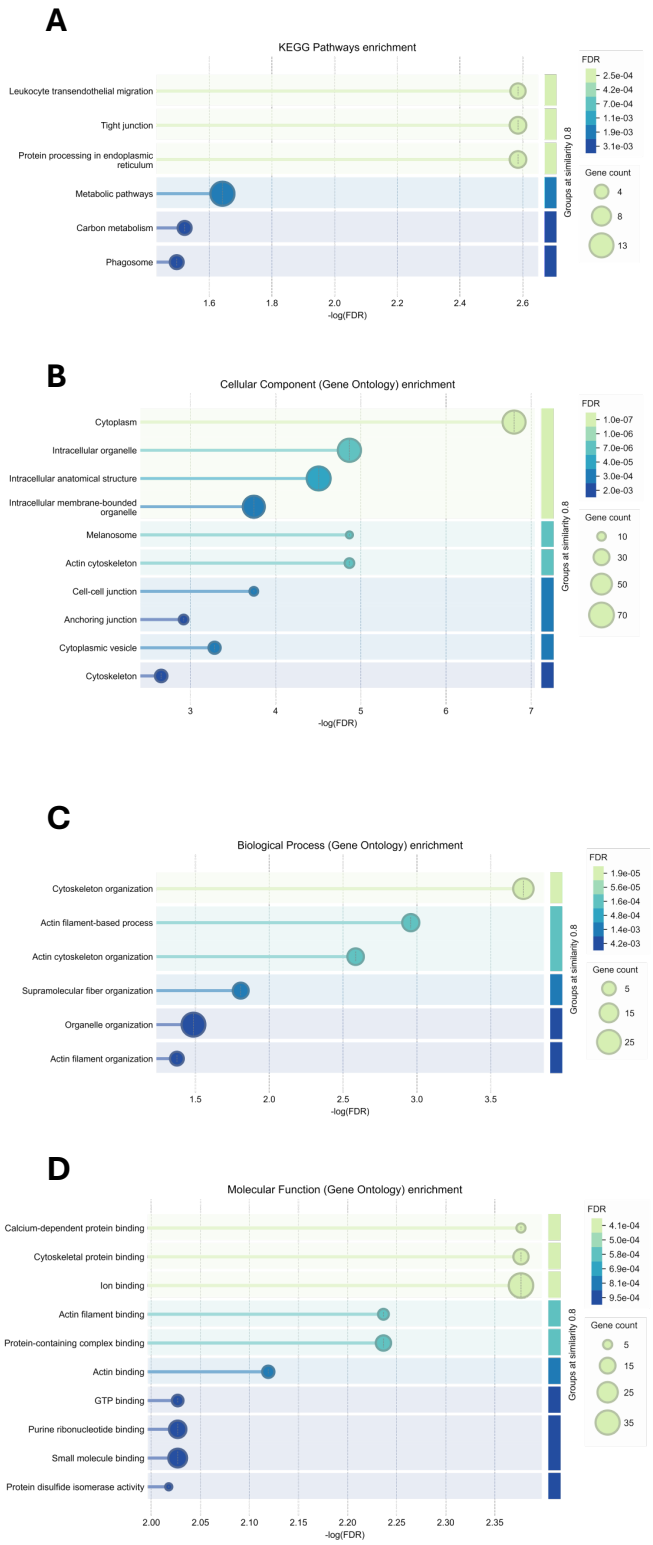


Figure 3.3-10: KEGG and Gene Ontology (GO) enrichment analysis of differentially expressed proteins downregulated in IPEC-J2 cells supplemented with Inorganic Se (E) under heat stress. Bubble plots show enrichment of (A) KEGG pathways, (B) cellular components, (C) biological processes, and (D) molecular functions. The x-axis represents -log (FDR), bubble size indicated gene count, and colour represents FDR.

3.3.4 Differential protein expression between heat-stressed IPEC-J2 cells treated with vitamin E compound compared to untreated heat-stressed control cells

Quantitative analysis was carried out to determine if IPEC-J2 cells treated with vitamin E for 24 h prior to being heat stressed at 42°C for 24 h, altered the proteomic response of cells in response to heat stress. A total of 750 proteins were identified in heat-stressed cells treated with vitamin E compared to untreated heat-stressed cells. Proteins were filtered based on a peptide count ≥ 2, a maximum fold change ≥ 1.5, and a p-value ≤0.05. Application of these criteria reduced the number of proteins in further analysis to 165. Of these, 49 were upregulated in cells treated with vitamin E while 116 were downregulated in treated cells, compared to control heat-stressed cells. Protein-protein interaction analysis using STRING database was carried out on upregulated and downregulated proteins, respectively. Pathway enrichment analysis was used to determine pathways that were significantly upregulated and downregulated based on the protein-protein interactions.

3.3.4.1 STRING analysis on upregulated proteins in heat-stressed IPEC-J2 cells treated with vitamin E for 24 hours compared to untreated heat-stressed control cells

PPI analysis of upregulated protein in heat-stressed cells treated with vitamin E compared to untreated heat-stressed cells was performed using STRING database. The resulting interaction showed limited overall connectivity, with a small central cluster of interacting proteins and several nodes displaying no interactions with the main network (Figure 3.3-11). The single defined interaction cluster consisted of three proteins elongation factor 2 (EEF2), proliferation associated protein 2G4 (PA2G4), and SERPINE1 mRNA binding protein (SERBP1). These proteins formed a small but connected subnetwork within a sparsely connected network. Aside from this cluster, the remaining proteins identified in this comparison showed limited or no interactions and were present as isolated nodes within this STRING network.

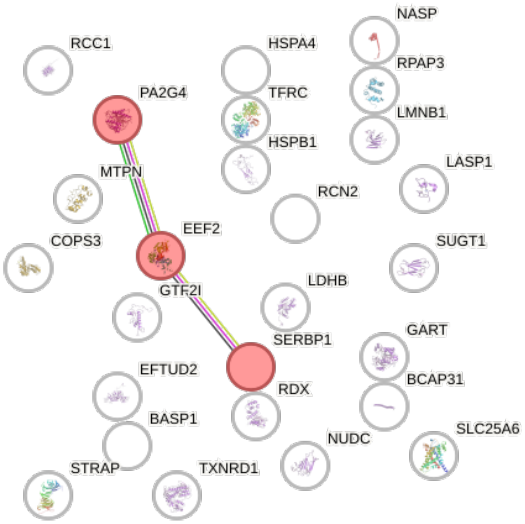


Figure 3.3-11: Protein-protein interaction network of proteins upregulated in IPEC-J2 cells supplemented with vit E and subsequently exposed to heat stress (42°C), compared to untreated heat-stressed cells- Nodes represent individual proteins, and edges indicated known or predicted functional associations between proteins. The network was generated using high-confidence interaction score (0.7) and PPI enrichment analysis yielded a p-value of 0.824, indicating that network connectivity was not greater than expected. Proteins are grouped into clusters based on interaction patterns, with colours representing distinct functional groupings. The primary cluster identified includes proteins associated with translation-related processes, including EEF2, PA2G4, and SERBP1. Disconnected nodes represent proteins with no known interactions within this dataset.

STRING enrichment analysis of proteins upregulated in IPEC-J2 cells treated with vitamin E under heat stress identified significant enrichment only within the GO Cellular Component category (Figure 3.3-12). Enriched cellular components included cytoplasm, intracellular anatomical structures, and intracellular organelles. No significant enrichment was observed for KEGG pathways, GO biological processes, or GO molecular functions.

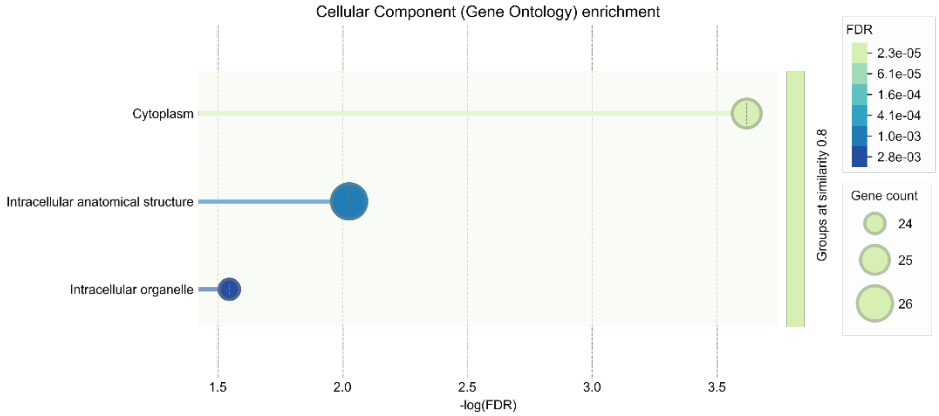


Figure 3.3-12: KEGG and Gene Ontology (GO) enrichment analysis of differentially expressed proteins upregulated in IPEC-J2 cells supplemented with vit E under heat stress. Bubble plots show enrichment of cellular components . The x-axis represents -log (FDR), bubble size indicated gene count, and colour represents FDR.

3.3.4.2 STRING analysis on downregulated proteins in heat-stressed IPEC-J2 cells treated with vitamin E for 24 hours compared to untreated heat-stressed control cells

STRING database was used to perform PPI analysis to examine relationships between proteins that were significantly downregulated in vitamin E treated IPEC-J2 cells exposed to 42°C for 24 h, compared to untreated heat-stressed cells ($p \leq 0.05$). The resulting interaction network revealed multiple distinct clusters, indicating coordinated downregulation across multiple biological processes, shown in Figure 3.3-13.

The largest cluster, included glycolytic enzymes, indicating reduced abundance of key metabolic components. A second cluster comprised proteins associated with antigen processing and the HSP90 chaperone cycle can also be observed. Additional clusters were associated with the chaperonin-containing T-complex, and ATP-dependent protein folding chaperone activity, while another cluster included components of the proteasome and pathways related to cross-presentation of soluble exogenous antigens. Smaller clusters were also observed including proteins involved in translation elongation factor activity, VEGF-mediated vascular permeability, catenin complex formation, ISG15 antiviral mechanisms, and tubulin-related structural domains.

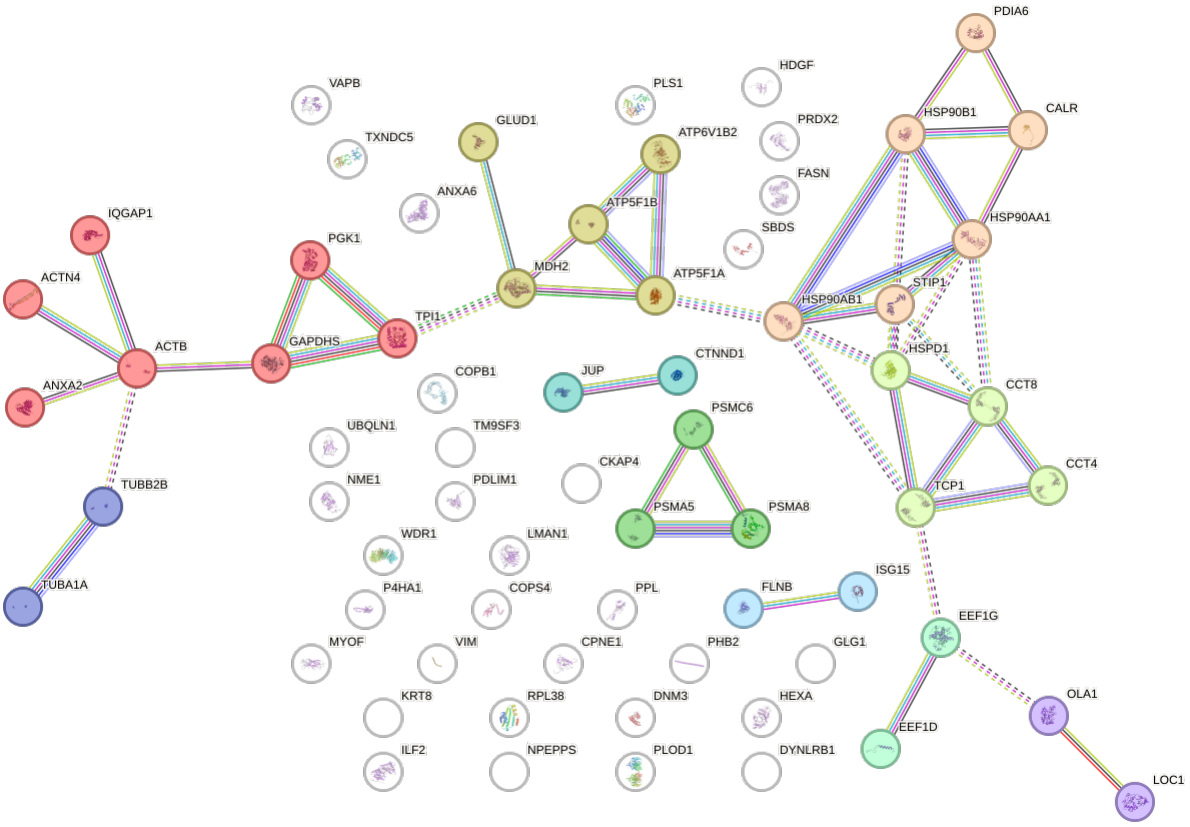


Figure 3.3-13: Protein-protein interaction network of proteins downregulated in IPEC-J2 cells supplemented with Vit E and subsequently exposed to heat stress (42°C), compared to untreated heat-stressed cells- Nodes represent individual proteins, and edges indicated known or predicted functional associations between proteins. The network was generated using high-confidence interaction score (0.7) and shows significant enrichment (PPI enrichment p-value 1.65e-14). Proteins are grouped into clusters based on interaction patterns, with colours representing distinct functional groupings. Prominent clusters include proteins associated with glycolysis (PGK1, GAPDH), mitochondrial function and ATP synthesis (ATP5F1A, ATP6V1B2, MDH2), protein folding and ER processes (HSP90 family members, PDIA6, CALR), and cytoskeletal organisation (ACTB, ACTN4) Additional clusters include proteins involved in proteasome activity, immune-related pathways, and translation-related processes. Disconnected nodes represent proteins with limited or no known interactions within the dataset.

Pathway enrichment analysis was performed on proteins that were significantly downregulated in vitamin E treated IPEC-J2 cells exposed to 42°C compared with untreated cells heat stressed at 42°C.Pathways were visualised according to significance and gene count, with enrichment assessed using adjusted false discovery rate (FDR). Pathways were divided into KEGG pathways (A), GO Cellular component enrichment (B), GO Biological process enrichment (C), and GO Molecular function enrichment (D), Figure 3.3-14.

KEGG pathway enrichment (Figure 3.3-14 A) analysis revealed significant downregulation of protein processing in the ER, which showed the highest level of enrichment among the KEGG pathways. Additional pathways included ones associated with neurodegeneration related categories, as well as pathways related to antigen processing and presentation, phagosome formation, adherens junction, and Salmonella infection.

GO biological process (Figure 3.3-14 C) analysis demonstrated that downregulated proteins were significantly enriched in processes related to protein folding, protein stabilisation, ATP metabolic processes, purine ribonucleotide and ribonucleoside triphosphate metabolism, and cytoskeleton organisation including actin filament-based processes. Enrichment was also observed for processes associated with cellular responses to chemical and organic substances.

Cellular component enrichment analysis (Figure 3.3-14 B) indicated that downregulated proteins were predominantly localised to the cytoplasm, intracellular anatomical structures and intracellular organelles, with additional enrichment in structures related to the cytoskeleton, supramolecular fibres, and the chaperonin containing T-complex. Molecular function (Figure 3.3-14 D) enrichment further identified reduced abundance of proteins involved in small molecule binding, anion binding, nucleotide and purine ribonucleotide binding, unfolded protein binding, and ATP-dependent activities.

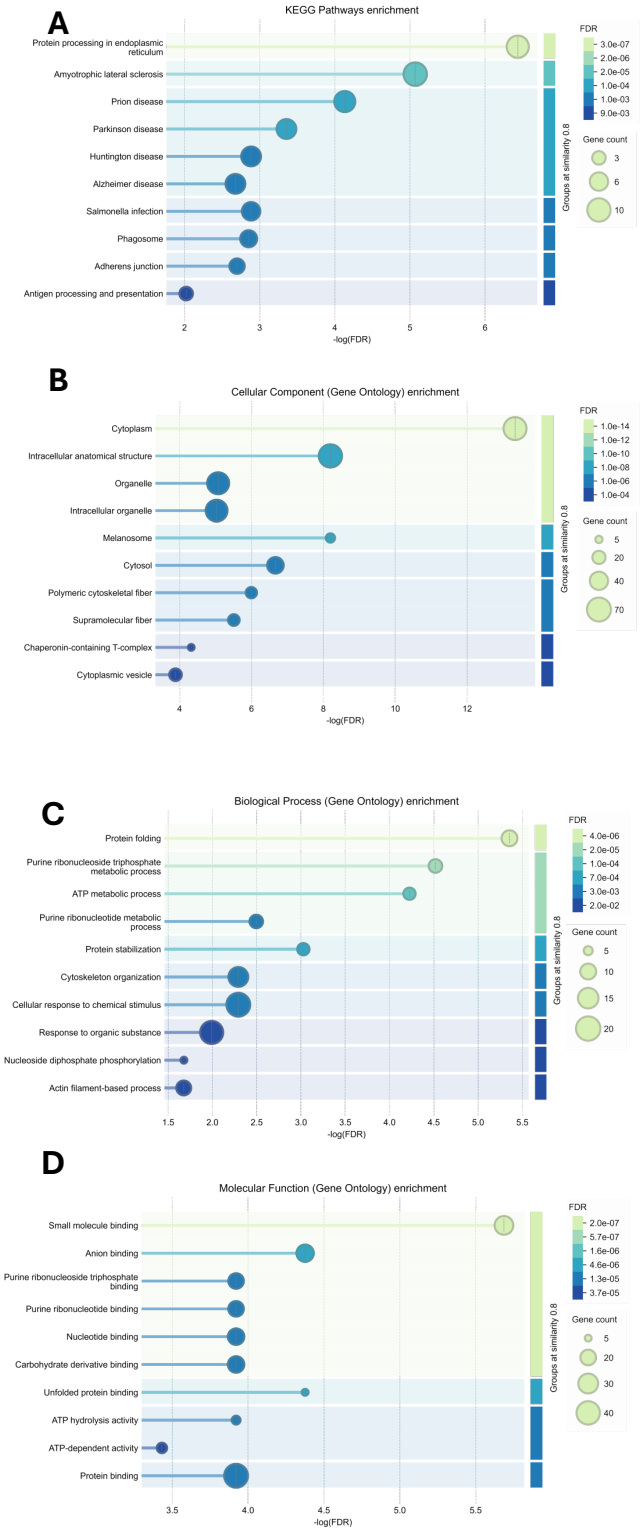


Figure 3.3-14: KEGG and Gene Ontology (GO) enrichment analysis of differentially expressed proteins downregulated in IPEC-J2 cells supplemented with Vit E under heat stress. Bubble plots show enrichment of (A) KEGG pathways, (B) cellular components, (C) biological processes, and (D) molecular functions. The x-axis represents -log (FDR), bubble size indicated gene count, and colour represents FDR.

3.3.5 Differential protein expression between heat-stressed IPEC-J2 cells treated with vitamin C compound compared to untreated heat-stressed control cells

A total of 977 proteins were identified from quantitative analysis comparing IPEC-J2 cells treated with vitamin C prior to being exposed to heat stress at 42°C with untreated heat-stressed control cells. Data was filtered based on a peptide count ≥ 2, a maximum fold change ≥ 1.5, and a p-value ≤ 0.05. Application of these criteria reduced the number of proteins in further analysis to 386, with 161 of them being significantly upregulated while 225 were downregulated in vitamin C treated heat-stressed cells. A volcano plot showing the distribution of significantly upregulated and significantly downregulated proteins is shown in Figure 3.3-15.

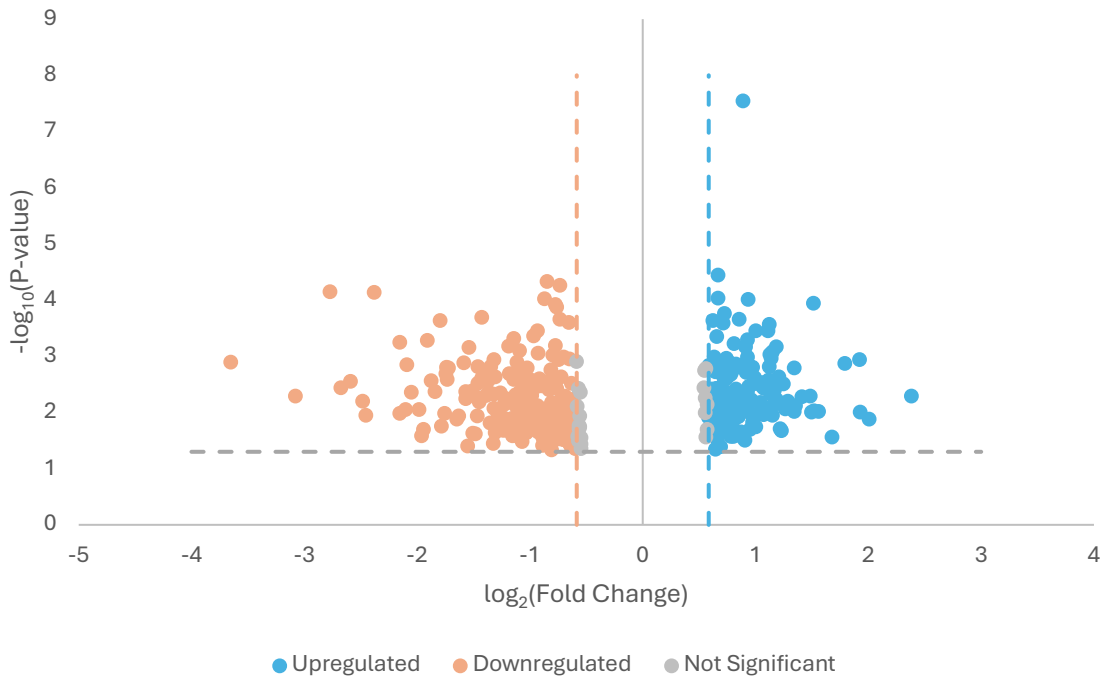


Figure 3.3-15: Volcano plot illustrating protein expression between IPEC-J2 cells treated with vit C for 24 h prior to being heat stressed at 42°C for 24 h and untreated IPEC-J2 cells heat stressed for 24 h. The x-axis represents log2(fold change), and the y-axis represents -log10(p-value). Significantly upregulated proteins are shown in blue, significantly downregulated proteins are highlighted in orange and grey dots represent non-significant proteins. Horizontal and vertical dashed lines indicate the applied significance thresholds (p-value ≤ 0.05, and log2(FC) ≥ 0.585).

3.3.5.1 STRING analysis on upregulated proteins in heat-stressed IPEC-J2 cells treated with vitamin C for 24 hours compared to untreated heat-stressed control cells

STRING database was used to determine PPIs on significantly upregulated proteins in 42°C cells treated with vitamin C compared with untreated 42°C control cells (peptide count ≥ 2, a maximum fold change ≥ 1.5, and a p-value ≤ 0.05). The resulting interaction map (Figure 3.3-16) identified a high degree of connectivity between proteins with multiple clusters of interacting proteins observed.

The largest most prominent cluster, highlighted in red, was enriched with proteins associated with translational initiation, ribosomal scanning and start codon recognition, including multiple translation initiation factors indicating upregulation of translation-related machinery. A second cluster, highlighted in orange, comprised of proteins involved in the U2-type precatalytic spliceosome and spliceosomal snRNP complexes.

Additional clusters included proteins involved with DNA replication, proteasome function and cross-presentation of exogenous antigens, and glycolysis/gluconeogenesis. Smaller clusters were also observed, including proteins associated with ligase activity and purine biosynthesis, intracellular steroid hormone receptor signalling, and VCB complex formation. Individual proteins related to aminoacyl-tRNA synthetase activity and chaperonin-containing T-complex function were also observed.

Overall, the STRING network demonstrates that vitamin C treatment under heat stress conditions is associated with upregulation of multiple protein clusters related to translation, RNA processing, DNA replication, protein turnover, and central metabolic pathways.

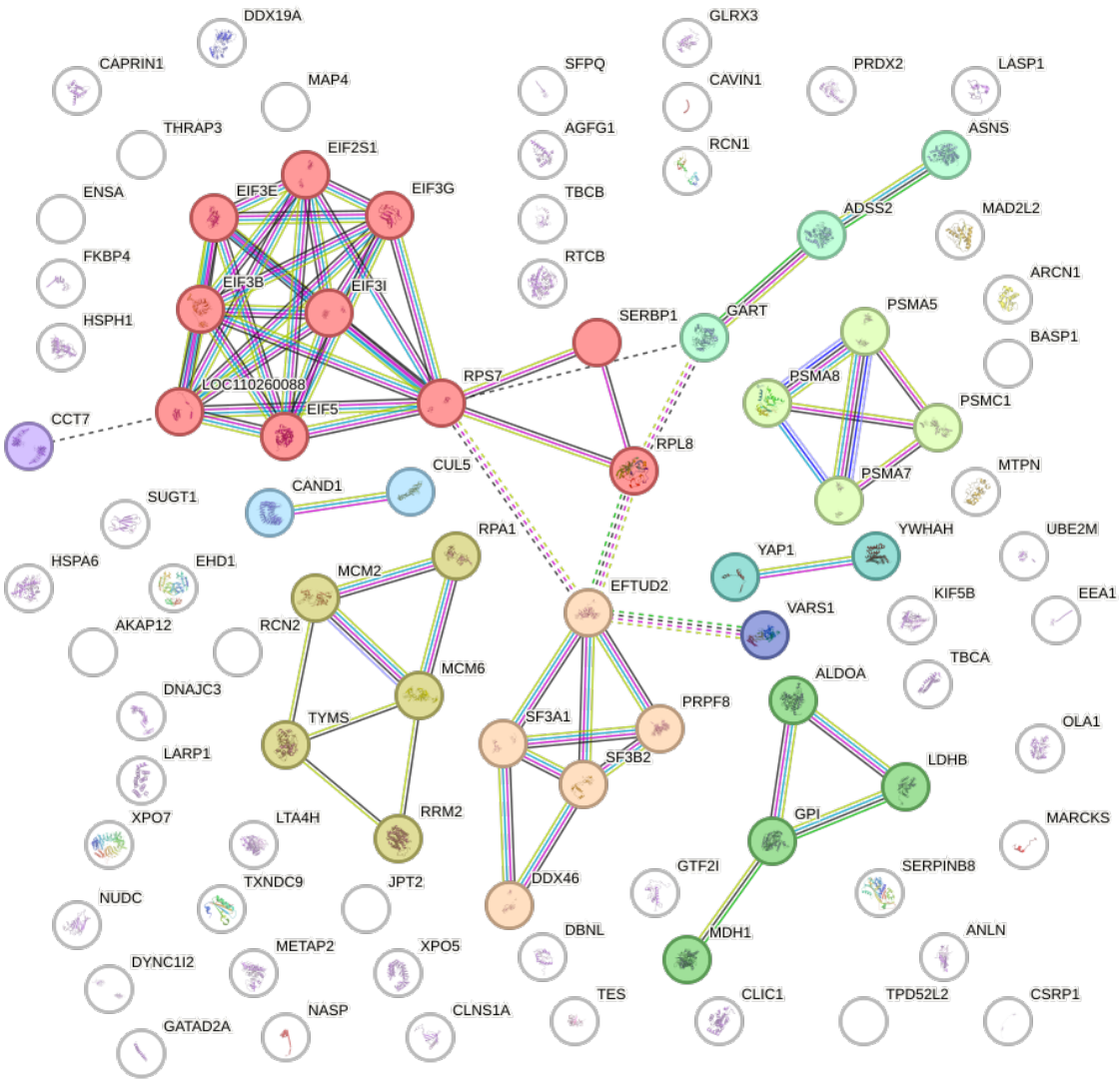


Figure 3.3-16: STRING protein-protein interaction network of proteins significantly upregulated in vitamin C treated cells at 42°C compared with untreated heat-stressed control cells- Nodes represent proteins and edges indicate known or predicted interactions. The network was generated using high-confidence interaction score (0.7) and shows significant enrichment (PPI enrichment p-value 1.64e-10). Functional clustering highlights enrichment of translation initiation, RNA splicing, DNA replication, proteasome activity, and glycolysis-related protein groups.

Pathway enrichment analysis of proteins significantly upregulated in IPEC-J2 cells treated with vitamin C under heat stress revealed significant upregulation of pathways related to KEGG, and GO terms cellular component, biological processes, and molecular function (Figure 3.3-17).

KEGG pathway (A) enrichment analysis demonstrated a significant upregulation of pathways associated with RNA transport, spliceosome function, proteasome activity, and DNA replication. GO analysis revealed enrichment of biological processes (C) related to translational initiation, gene expression, and ribonucleoprotein complex organisation. GO cellular component (B) identified that upregulated proteins were primarily localised to intracellular compartments, including the cytoplasm, cytosol, nucleus, and translation initiation complexes. GO molecular function enrichment (D) further indicated increased protein binding, RNA binding, and translation initiation factor activity.

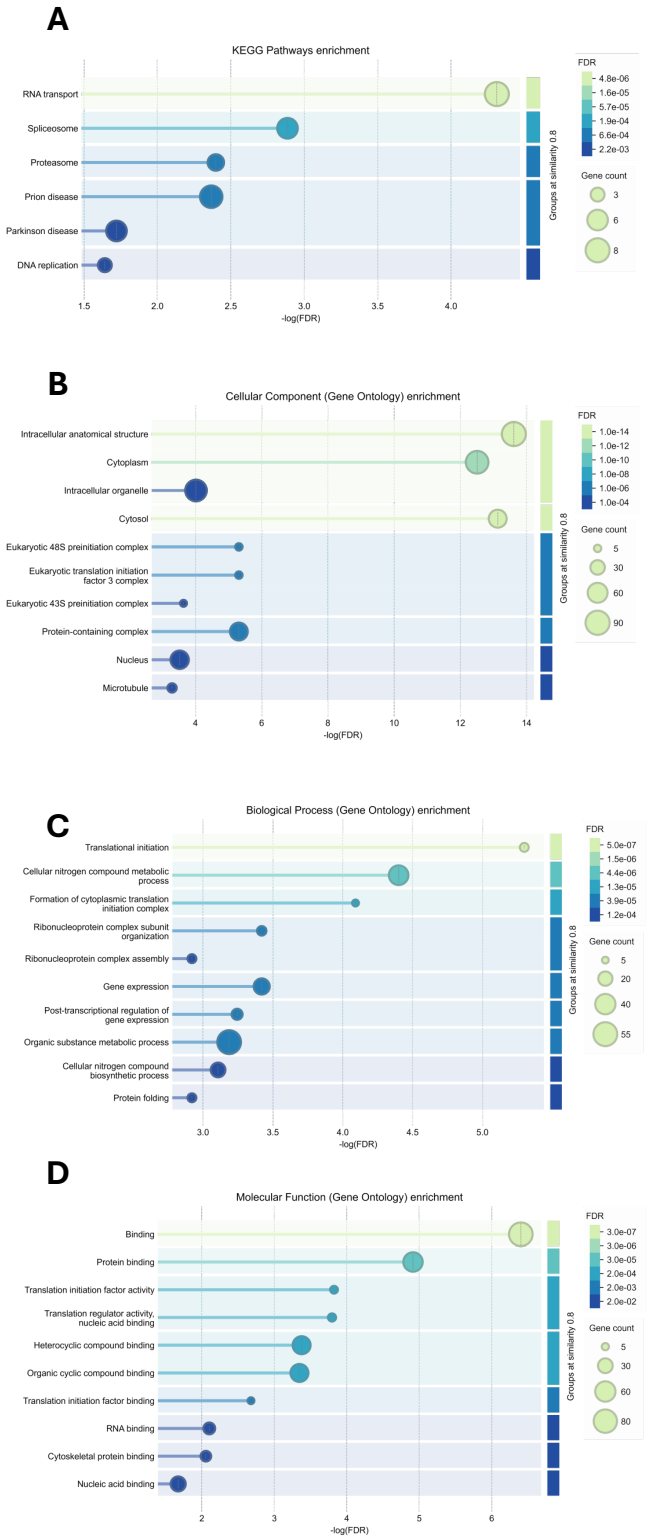


Figure 3.3-17: Pathway enrichment of proteins significantly upregulated in vitamin C treated IPEC-J2 cells at 42°C compared with untreated control cells at 42°C- Enriched KEGG pathways (A) and GO cellular components (B), biological processes (C), and molecular function (D) categories are shown. Bubble size represents the number of proteins associated with each term, and colour indicates false discovery rate (FDR).

3.3.5.2 STRING analysis on downregulated proteins in heat-stressed IPEC-J2 cells treated with vitamin C for 24 hours compared to untreated heat-stressed control cells

PPI analysis on significantly downregulated proteins in 42°C cells treated with vitamin C compared with untreated 42°C control cells (peptide count ≥ 2, a maximum fold change ≥ 1.5, and a p-value ≤ 0.05) revealed several densely connected protein groups, indicating coordinated downregulation of related biological processes (Figure 3.3-18).

A prominent cluster was centred around cytoskeletal and actin-associated proteins including ACTB, ACTN4, and ITGA2, which formed highly connected hub with multiple interacting partners. Additional clusters included proteins associated with metabolic processes, including glycolysis and mitochondrial function such as PGK1, GAPDH, and enzymes involved in the tricarboxylic acid (TCA) cycle.

Proteins involved in protein folding and stress response pathways were also observed within clustered regions, including molecular chaperones such as HSP90 family members and co-chaperone proteins. Furthermore, clusters related to RNA processing and translation were identified, including ribosomal proteins and RNA-binding factors, indicating coordinated regulation of protein synthesis-related pathways.

Smaller clusters and isolated nodes were also present, representing proteins with fewer or no known interactions within the dataset. Overall, the PPI network demonstrated that Vit C supplementation under heat stress conditions is associated with the coordinated downregulation of proteins involved in cytoskeletal organisation, metabolism, protein folding, and RNA processing.

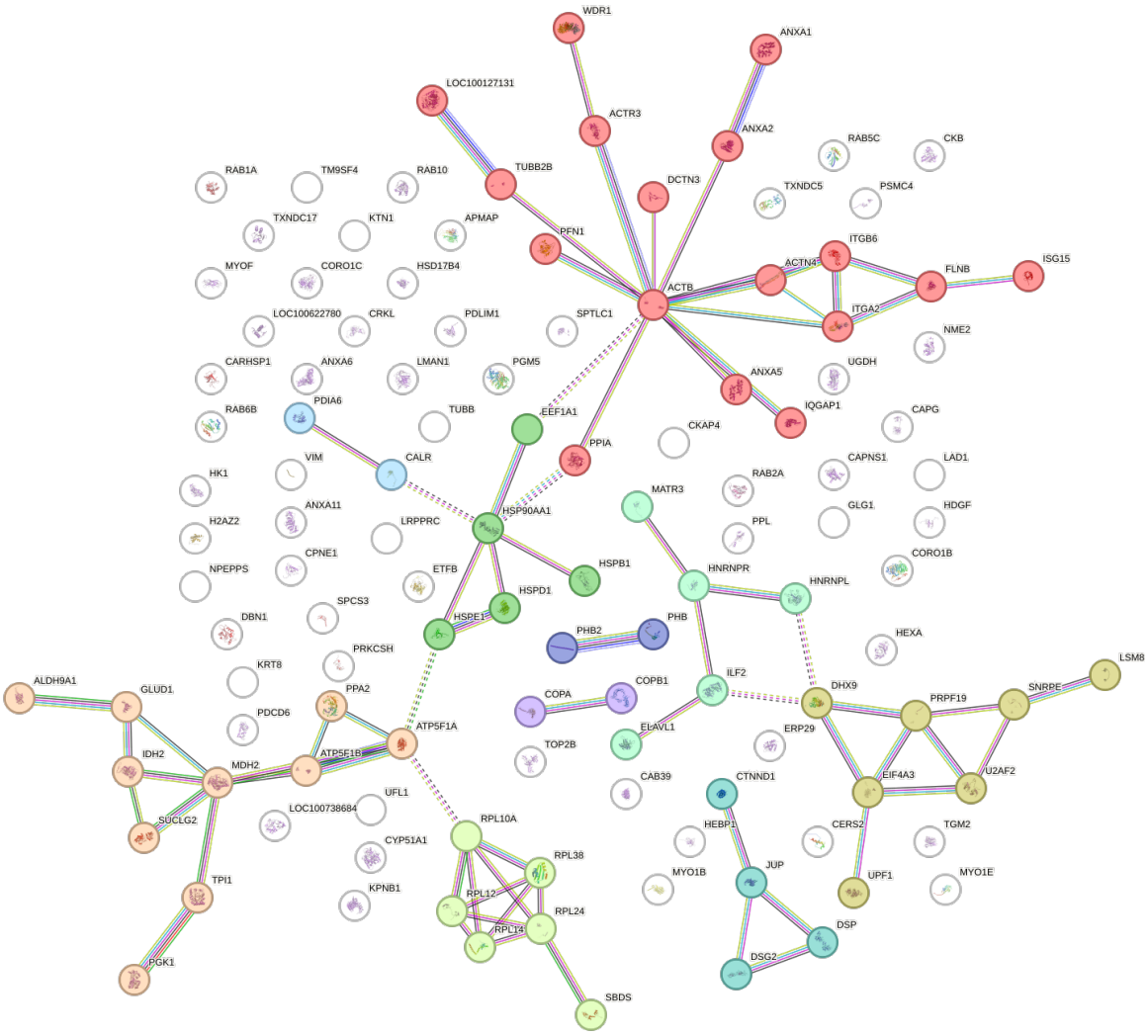


Figure 3.3-18: STRING protein-protein interaction network of proteins significantly downregulated in vitamin C treated cells at 42°C compared with untreated heat-stressed control cells- Nodes represent proteins and edges indicate known or predicted interactions. The network was generated using high-confidence interaction score (0.7) and shows significant enrichment (PPI enrichment p-value 5.01e-12). Proteins are organised into distinct clusters with prominent clusters including proteins involved in cytoskeletal organisation (ACTB, ACTN4), metabolic processes, protein folding and stress response (HSP90 family members), and RNA processing and translation. Disconnected nodes represent proteins with limited or no known interactions within the dataset.

Functional enrichment analysis of proteins significantly downregulated in IPEC-J2 cells supplemented with vitamin C under heat stress identified several significantly enriched KEGG pathways and GO terms (Figure 3.3-19).

KEGG pathway analysis (A) revealed enrichment of pathways associated with protein processing in the ER, carbon metabolism, and phagosome pathways, as well as regulation of actin cytoskeleton alongside enrichment in glycolysis/gluconeogenesis, ribosome, and spliceosome pathways. GO cellular component analysis (B) indicated enrichment of intracellular structures, including cytoplasm, intracellular organelles, membrane-bound organelles, and cytoskeletal components. GO biological process analysis (C) highlighted enrichment of processes associated with cytoskeletal organisation, actin filament-based processes, and cellular components. GO molecular function analysis (D) revealed enrichment of functions including actin filament binding, structural molecule activity, nucleotide binding, and small molecule binding.



Figure 3.3-19: Pathway enrichment of proteins significantly downregulated in vitamin C treated IPEC-J2 cells at 42°C compared with untreated control cells at 42°C- Enriched KEGG pathways (A) and GO cellular components (B), biological processes (C), and molecular function (D) categories are shown. Bubble size represents the number of proteins associated with each term, and colour indicates false discovery rate (FDR).

3.4 Across all the supplementation treatments, including Se and vitamins (E and C), a consistent pattern of protein expression changes was observed in response to heat stress. Functional and PPI analyses indicated that heat stress predominantly affected pathways related to protein processing in the ER, cytoskeletal organisation, and metabolic processes. Supplementation appeared to modulate these responses, with evidence of coordinated changes in proteins associated with cellular stress responses, protein folding, and intracellular organisation.

4 Discussion

Heat stress has emerged as an increasing concern within agriculture and livestock production, largely driven by rising global temperatures and an increased frequency of extreme heat events. Exposure to elevated temperatures adversely affects animal health, productivity, and reproduction resulting in significant economic losses worldwide (Bahar et al., 2020; Tullo et al., 2019). In recent years, growing research efforts focused on understanding the underlying effects of heat stress on animals, with *in vitro* models utilised to investigate stress responses under controlled conditions (Cui et al., 2022; J. Tang et al., 2019; Zhou et al., 2020). Attention has been directed towards identifying nutrition-based strategies aimed at mitigating heat-induced damage and improving thermotolerance in animals, specifically homeothermic animals.

The present study investigated the effects of heat stress on relative IPEC-J2 cell metabolic activity, and stress protein expression using a swine intestinal cell line. It also evaluated whether treatment with organic Se, inorganic Se, and vitamin compounds aided in the protection against heat-induced damage. This Chapter integrates key conceptual themes with the findings generated in the present study.

4.1 Establishment and validation of an *in vitro* heat stress model using an IPEC-J2 cell line

Heat stress represents a significant challenge in the agriculture sector, particularly the swine industry, largely because of the limited ability of pigs to regulate body temperature through evaporative cooling, i.e. sweating due to a lack of functional sweat glands. As a result, thermoregulatory responses, including redistribution of blood flow from internal core organs to peripheral tissues can compromise physiological function (Blatteis, 1998; Curtis, 1983). In particular, the intestinal tract is highly susceptible to heat stress, with disruption of epithelial integrity, leading to increased permeability and bacterial translocation (Fan et al., 2025). In the present study, the effects of heat stress on the intestinal epithelium were investigated using the IPEC-J2 cell line, a well-established *in vitro* model for investigating intestinal epithelial responses to heat stress, as these cells closely mimic the physiological properties of the porcine intestinal barrier (Perruchot et al., 2026).

4.1.1 Effect of heat stress on relative IPEC-J2 cell metabolic activity

A heat stress model was established by assessing IPEC-J2 cell metabolic activity in cells exposed to 41°C, 42°C, and 44°C for 2 h and 24 h, respectively, relative to control cells maintained at 37°C (Figures 3.1-1 and 3.1-2). The relative metabolic activity was determined using AB reagent, with results indicating that after 2 h exposure to 41°C and 42°C there was no significant change in cells' metabolic activity compared to control cells at 37°C ($p > 0.05$) (Figures 3.1-1 and 3.1-2). Similarly, Tang *et al.* observed a slight increase in viable IPEC-J2 cells after 12 h exposure to 41.5°C (J. Tang et al., 2019), and Zhou *et al.* demonstrated that exposure to 41°C for 24 h did not have an effect on viable IPEC-J2 cell growth. This observation may reflect an early adaptive response to mild heat stress, where cellular metabolic activity is temporarily maintained or even elevated prior to the onset of stress-induced damage (Zhou et al., 2020). The temperatures of 41°C and 42°C may not be high enough to affect relative viable cell growth as a study demonstrated that 2 h exposure to 43°C significantly reduced viable IPEC-J2 cell count compared to control (Cui et al., 2022). This is consistent with this study as cells exposed to 44°C for 2 h resulted in a decrease in relative cell metabolic activity (Figure 3.1-1). It is important to note that the increase in relative viable IPEC-J2 cell growth observed at early time points likely reflects enhanced metabolic activity rather than a true increase in viable cell growth, particularly when assessed using the metabolic-based assay AB.

In agreement with prolonged (>2 h) or more severe heat exposure (≥41°C), the current study demonstrated a reduction in relative metabolic activity of IPEC-J2 cells , indicating the onset of cellular damage. Following 24 h heat stress, decreased metabolic activity was observed in cells exposed to 41°C, 42°C, and 44°C (Figure 3.1-2). These findings are consistent with previous studies showing that exposure of IPEC-J2 cells to elevated temperature (42°C for 24 h) results in reduced cell viability. This decrease in viability suggests that cells have entered a severe stress state in which cellular function has become compromised, despite a proportion of cells remaining metabolically active (S. Gao et al., 2026; B. Zhang et al., 2023).

The decrease in relative metabolic activity in cells observed under heat stress conditions, as measured by the AB assay, reflects a reduction in cellular metabolic activity rather than cell number alone. The assay is based on the reduction of resazurin to resorufin by intracellular enzymes, primarily in the mitochondria, and therefore serves as an indicator for cellular metabolic function (Longhin et al., 2022; Rampersad, 2012). Heat

stress is known to disrupt redox homeostasis, resulting in the overproduction of reactive oxygen species (ROS) which leads to oxidative stress. Excessive ROS production can result in oxidative damage to cellular macromolecules, such as lipids, proteins, and DNA, thereby compromising overall cell function. Mitochondria are particularly susceptible to oxidative damage under heat stress conditions, with elevated ROS levels impairing mitochondrial membrane potential, reducing ATP production, and disrupting cellular energy metabolism (Aryal et al., 2025; Belhadj Slimen et al., 2014). As mitochondria are central to the reduction of resazurin to resorufin in the AB assay, heat stress-induced mitochondrial dysfunction resulting in the decreased ability of cells to metabolise the dye leading to reduced fluorescence signal. Together, these findings suggest that the reduction in relative IPEC-J2 cell metabolic activity observed in this study is likely driven by heat stress-induced oxidative damage, leading to impaired metabolic activity and increased cellular dysfunction.

Collectively, these results demonstrate that IPEC-J2 cells exhibit a time and temperature dependent response to heat stress, characterised by an initial adaptive phase followed by a decline in metabolic activity with prolonged exposure.

4.1.2 Induction of HSP70 expression in response to heat stress in IPEC-J2 cells

The changes in relative metabolic activity using AB assay (Figures 3.1-1 and 3.1-2) were further supported by the analysis of HSP70 protein expression (Figure 3.1-3). While the AB assay provided an indication of cellular metabolic activity in response to heat stress, the upregulation of HSP70 confirms the activation of an intracellular stress response. HSP70 functions as a molecular chaperone and is widely used as a biomarker of heat stress in livestock, contributing to the maintenance of protein homeostasis by regulating the balance between protein synthesis and degradation, while protecting cells from hyperthermia and other stress-related damage (AL-Jaryan et al., 2023).

In the present study, HSP70 expression was upregulated in IPEC-J2 cells following exposure to all elevated temperatures examined (41°C, 42°C, and 44°C) after both 2-hour and 24-hour timepoints (Figure 3.1-3). This is consistent with previous studies reporting increased HSP70 expression in IPEC-J2 cells (J. Tang et al., 2019) and in porcine skeletal muscle satellite cells (C. Gao et al., 2015) that were exposed to heat stress. Notably, exposure to 41°C and 42°C for 2 h did not significantly affect cells' metabolic activity

compared to control cells ($p > 0.05$) (Figure 3.1-1), despite increased HSP70 expression (Figure 3.1-3). This suggests that early induction of HSP70 represents a protective cellular response that promotes cellular adaptation under mild heat stress conditions.

The induction of HSP70 at early stages of heat stress represents a protective cellular response that promotes cell survival by maintaining protein homeostasis and inhibiting stress-induced apoptotic pathways (G. C. Li et al., 1992). The early upregulation of HSP70 may therefore contribute to the maintenance of metabolic activity observed in this study, delaying the onset of heat stress-induced cellular dysfunction.

Together, these findings indicate that the observed metabolic responses are closely associated with the activation of protective stress mechanisms, with HSP70 acting as a key mediator in cellular adaptation and survival under heat stress conditions.

4.1.3 Effects of heat stress on IPEC-J2 cell morphology

Phase-contrast imaging revealed no substantial morphological differences between control and heat-stressed IPEC-J2 cells at either 2-hour or 24-hour timepoints (Figures 3.1-4 and 3.1-5). Cells in both conditions largely retained their characteristic epithelial morphology, remaining adherent and forming monolayer-like structures. The lack of clear morphological changes may reflect the limitations of phase-contrast microscopy, which primarily visualises overall cell morphology but lacks the resolution required to detect subtle intracellular or junctional changes. This technique is limited by low contrast between subcellular components and can be affected by optical artefacts, such as halo effects, which obscure fine structural details and reduce image resolution (Shimasaki et al., 2024).

While previous studies, have reported heat stress-induced structural alterations in the intestine, including disruption of villus organisation and TJ integrity, these changes are often identified at the tissue or molecular level rather than direct observation of cellular morphology. In IPEC-J2 models, heat stress has been shown to reduce TJ protein expression, such as occludin, claudins, and ZO-1, and an increase in permeability, indicating barrier dysfunction even in the absence of pronounced morphological changes (Ortega & Szabó, 2021; B. Zhang et al., 2023).

Therefore, these results do not necessarily indicate a lack of cellular stress but reflects the limitations of phase-contrast imaging and heat stress responses primarily occur

at the molecular level before structural disruption becomes apparent. This is consistent with the relative metabolic activity and HSP70 data (Figures 3.1-1 to 3.1-3), suggesting that cells initially tolerate heat stress through adaptive responses before significant damage becomes apparent.

Overall, these findings confirm that the established heat stress model successfully induces a physiological stress response in IPEC-J2 cells in a time and temperature-dependent manner.

4.2 Effects of Se and vitamin supplementation under heat stress conditions

The findings of the heat stress model (Section 3.1) provided the basis for subsequent investigations into the potential effects of Se and vitamin supplementation against heat stress-induced cellular damage (Section 3.2). To maintain homeothermy, mitigation strategies in pigs must focus on either reducing metabolic heat production or enhancing heat dissipation from the body, with studies focusing on the development of nutritional strategies to alleviate the effects (Santos et al., 2018). From the heat stress model results, the temperature of 42°C was chosen to investigate the effects of Se and vitamin supplementation.

The concentrations of Se and vitamin compounds used in this study were selected with reference to established dietary supplementation recommendations and previous literature. To improve the physiological relevance of the model, all compounds were subjected to an *in vitro* digestion procedure (Section 2.2.2) prior to exposure to IPEC-J2 cells. According to the European Commission, no more than 0.2 ppm organic Se can be added to the diets of pigs (European Commission, 2019).This value was used as the basis for selecting the concentration of 0.2 µg/mL Se for the *in vitro* experiments.. However, direct comparisons between dietary inclusion rates and cell culture exposure concentrations require careful interpretation, as physiological processes such as absorption, metabolism, tissue distribution, and nutrient bioavailability are not represented within the IPEC-J2 monoculture model. Also, the bioavailability and chemical speciation of Se may differ among organic and inorganic Se sources following digestion, potentially influencing cellular exposure. Previous studies have reported that the addition of Se to the diets of pigs can alleviate the effects of heat stress (Z. Li et al., 2025; Y. Liu et al., 2023; J. Tang et al., 2019).

Vitamin E and vitamin C were chosen for this study due to their well-established antioxidant properties, as both compounds are reported to scavenge ROS and protect cells from oxidative damage (Chatterjee et al., 1995; M. Traber & Packer, 1995). The National Research Council recommends 11-16 IU/kg as adequate levels of vitamin E for growing pigs (National Research Council, 2012), while there is no recommendation for vitamin C supplementation. Similar to the Se compounds, direct comparisons between dietary inclusion rates and cellular exposure concentrations warrants careful evaluation, as the IPEC-J2 monoculture model does not account for nutrient absorption, metabolism, or

systemic distribution *in vivo*. In the present study, an initial concentration of 250 µg/mL vitamin C was found to be toxic to IPEC_J2 cells (Figure 3.2-1); therefore, a toxicity assay was performed to determine an appropriate concentration (Figure 3.2-6).

4.2.1 Effect of Se and vitamin supplementation on IPEC-J2 cell metabolic activity under heat stress conditions

This study examined the effects of 24-hour and 48-hour treatment of Se and vitamin compounds on IPEC-J2 cells prior to being heat stressed for 2 hours and 24 hours, respectively. The established heat stress model was used to assess relative IPEC-J2 cell metabolic activity following treatment with Se and vitamin compounds using the AB reagent (Figures 3.2-2 to 3.2-5). As shown in the heat stress model established in this study, after 24 hours of heat stress, the relative viable cell growth was reduced (Figure 3.2-2), through reduced metabolic activity.

The present study demonstrated that treatment with Se and vitamin compounds can partially mitigate heat stress-induced reductions in IPEC-J2 cell metabolic activity (Figures 3.2-2 to 3.2-5), with the extent of protection varying depending on compound type, concentration, and duration of treatment and heat exposure. Consistent with the heat stress model, exposure to 42°C resulted in a reduction in cell metabolic activity (Figures 3.2-2 to 3.2-5), confirming the sensitivity of IPEC-J2 cells to thermal challenge.

Under physiological conditions, the Se compounds did not significantly alter the relative IPEC-J2 cell metabolic activity, indicating that cells are well tolerated to 0.2 µg/mL of Se ($p > 0.05$) (Figure 3.2-1). In contrast, vitamin C at 250 µg/mL caused a significant reduction ($p \leq 0.05$) in metabolic activity (Figure 3.2-1) highlighting a potential cytotoxic effect at high concentrations. A toxicity assay was then carried out to determine an appropriate working concentration of vitamin C (Figure 3.2-6). This response can be explained by the well-characterised dual role of vitamin C as both an antioxidant and a pro-oxidant. At lower concentrations, vitamin C functions to protect cells from reactive oxygen species (ROS), whereas at higher concentrations it can interact with transition metals such as iron and copper, leading to the generation of additional ROS. This effect is primarily observed *in vitro*, where metal ions are more readily available, whereas *in vivo* systems tightly regulate metal availability (Kaźmierczak-Barańska et al., 2020). Consequently, excessive vitamin C exposure can induce apoptosis and metabolic disruption, as observed in the present study.

The toxicity assay (Figure 3.2-6) enabled the identification of a concentration (25 µg/mL) that maintained the cells' metabolic activity while allowing investigation of its potential protective effects against heat stress. At this concentration, vitamin C-treated IPEC-J2 cells exhibited similar metabolic activity to untreated heat-stressed cells ($p = 0.9999$) (Figure 3.2-7), suggesting that vitamin C did not significantly improve metabolic activity under heat stressed conditions. Nevertheless, previous studies demonstrated that vitamin C, at 20 µg/mL and 25 µM (4.40 µg/mL), reduces oxidative stress, apoptosis, and cellular damage in heat-stressed cells (Sammad et al., 2024; Yin et al., 2018), and contributes to the neutralisation of ROS and supporting cellular redox balance (Chatterjee et al., 1995; Kaidow et al., 2022). These findings emphasise that while vitamin C has the potential to mitigate heat stress-induced damage, its effects are highly concentration-dependent. This is particularly important in *in vitro* systems, where redox balance is more easily disrupted and concentrations exceeding physiological thresholds may result in cytotoxic effects rather than protective effects.

In comparison to the concentration-dependent effects observed for vitamin C, the Se compounds demonstrated a more stable and consistent profile under both physiological (37°C) and heat stress (42°C) conditions (Figures 3.2-1 to 3.2-5). Following heat exposure, cells supplemented with Se compounds exhibited numerically higher relative metabolic activity compared to untreated heat-stressed controls, although the extent of this response varied among the different Se sources.. After 24 h treatment with compounds (Figures 3.2-2 and 3.2-3), an increase in IPEC-J2 cell metabolic activity was observed in cells supplemented with some of the organic Se compounds, as well as inorganic Se, although this effect was not consistent across all compounds. Prolonged treatment (48 h) exhibited a further enhancement with the IPEC-J2 cells' metabolic activity exceeding control levels (37°C) following acute heat exposure (Figures 3.2-4 and 3.2-5). Previous studies in IPEC-J2 cells have similarly reported the protective effect of Se under heat stress conditions. For example, Tang *et al.* demonstrated that supplementation with both organic and inorganic Se, respectively, improved cell viability and reduced heat stress-induced inflammation and epithelial damage (J. Tang et al., 2019).

Se exerts its protective effects against heat stress primarily through its incorporation into SelPs, such as GPx and TrxR, which function to reduce ROS and maintain cellular redox balance. By limiting oxidative stress, Se reduces heat-induced damage to lipids, proteins, and DNA, thereby preserving cellular integrity (Lee et al., 2025; Y. Zhang et al., 2020). This is supported by the proteomic analysis which demonstrated a significant

upregulation of TrxR1 in cells supplemented with Organic Se-A ($p = 0.00164$) (Table 3.3-3), suggesting that Se supplementation influenced the cellular antioxidant response under heat stress conditions.

Vitamin E-supplemented cells exhibited numerically higher metabolic activity than untreated heat-stressed cells, although these differences were not statistically significant ($p > 0.05$)(Figures 3.2-2 to 3.2-5). Previous studies demonstrated that vitamin E can alleviate heat stress-induced cellular damage by reducing ROS, preventing lipid peroxidation, and preserving mitochondrial function, ultimately improving cell viability in heat-stressed cell models (Butt et al., 2019). The improvement in higher metabolic activity observed in cells supplemented with vitamin E may be related to its role as a lipid-soluble antioxidant (F. Liu et al., 2018). Vitamin E is a lipid soluble antioxidant that intercepts lipid peroxyl radicals and prevents the propagation of lipid peroxidation (M. G. Traber, 2021; M. Traber & Packer, 1995). This is important under heat stress conditions, where increased production of ROS leads to membrane damage, loss of integrity, and impaired cellular function through oxidative damage to lipids, proteins, and DNA (B. Wang et al., 2023). By limiting lipid peroxidation, vitamin E preserved membrane stability and supports the structural integrity of cells, including intestinal epithelial cells, where maintenance of barrier function is critical (Kilicarslan You et al., 2024). In addition, vitamin E has been shown to reduce overall ROS levels and oxidative stress, thereby maintaining cellular redox balance and preventing oxidative damage to essential biomolecules (F. Liu et al., 2016).

Collectively, the findings from this study suggest that antioxidant supplementation was associated with treatment-dependent changes in IPEC-J2 cell metabolic activity under heat stress conditions. Se compounds exhibited the most consistent responses, likely due to their role in enzymatic antioxidant defence system, while vitamin E-treated cells demonstrated higher metabolic activity that untreated heat-stress controls, possibly through membrane stabilisation and inhibition of lipid peroxidation. In contrast, vitamin C exhibited concentration-dependent effect, highlighting the importance of dose optimisation in *in vitro* systems. These results emphasise that while antioxidant strategies can improve cellular resilience to heat stress, within an IPEC-J2 monoculture model of direct thermal exposure. However, it is important to recognise that responses observed in this *in vitro* model may not directly translate to responses observed *in vivo*.

4.2.2 Effect of Se and vitamin supplementation of HSP70 in IPEC-J2 cells under heat stress conditions

Treatment with Se and vitamin compounds altered the heat stress-induced HSP70 response in IPEC-J2 cells, suggesting that these compounds influenced cellular adaptation to heat stress. This study demonstrated, exposure to 42°C for 24 h alone resulted in a significant increase in HSP70 expression ($p = 0.0151$) (Figure 3.2-9), indicating activation of the HSR. However, 24 h treatment, cells supplemented with Se compounds exhibited lower HSP70 expression relative to untreated heat-stressed control cells (Figure 3.2-9), despite these compounds being associated with higher IPEC-J2 cells metabolic activity, although these differences were not statistically significant (Figures 3.2-2 to 3.2-5). These findings are similar to previous studies that have reported a reduction in HSP70 abundance in Se treated cells (Gan et al., 2013; He et al., 2022; J. Tang et al., 2019). This suggests that Se may alleviate cellular stress, thereby reducing the requirement for HSP70 induction, likely through its antioxidant role in limiting ROS and protein damage (Y. Zhang et al., 2020). HSP70 plays a critical protective role during heat stress while also contributing to normal cellular growth and proliferation. HSPs protect cells from oxidative stress-induced apoptosis and are key regulators of cellular thermal tolerance (Kaushik et al., 2022). These findings are consistent with the observed significant upregulation of antioxidant SelP, such as TrxR1, in Organic Se-A treated cells under heat stress ($p = 0.0164$) (Table 3.3-3), supporting the role of enhanced redox regulation in reducing cellular stress. The inverse relationship between HSP70 expression and relative cell metabolic activity in Se treated cells further supports that reduced stress signalling is associated with improved cellular function.

In contrast, the vitamin C displayed a relatively high HSP70 expression under heat stress conditions, although these differences were not statistically significant ($p > 0.05$) (Figure 3.2-9). Previous studies suggest that while vitamin C enhances the survival of oxidatively stressed cells by acting as an antioxidant and reducing ROS (Montecinos et al., 2007), it may not fully attenuate the stress response, and cells may still require HSP70-mediated protein stabilisation. This suggests that vitamin C enables cells to maintain function under stress conditions, rather than preventing the initial stress response. HSP70 plays a central role in cellular protein homeostasis by facilitating the folding and assembly of newly synthesised proteins, promoting the refolding of misfolded or aggregated proteins, assisting in the translocation of proteins across organelle and secretory membranes, and regulating the activity of various cellular proteins (Evgen'ev et al., 2023).

Vitamin E supplementation exhibited a moderate reduction in HSP70 expression compared to heat-stressed control cells, however this was not a significant decrease ($p > 0.05$) (Figure 3.2-9). Vitamin E functions as a lipid-soluble antioxidant, where it prevents lipid peroxidation and preserves membrane integrity, rather than directly reducing protein damage (Kilicarslan You et al., 2024; M. Traber & Packer, 1995). The patterns observed in this study are consistent with studies that demonstrated the decrease in HSP70 abundance in cells supplemented with vitamin E and vitamin C (Jang et al., 2014; Khorami et al., 2020).

These findings demonstrate treatment-associated differences in metabolic activity and HSP70 expression under heat stress conditions, suggesting that Se and vitamin compounds could impact stress-related cellular pathways through different mechanisms.

4.3 Proteomic Responses to Heat Stress

Within the intestinal epithelium, heat stress disrupts protein stability, cellular homeostasis, and barrier integrity causing widespread alterations in cellular function. Elevated temperatures lead to the accumulation of misfolded proteins, triggering the activation of the UPR to try and restore proteostasis (Pessa et al., 2024). This response is characterised by the upregulation of stress-responsive genes and the suppression of non-essential cellular processes, reflecting a shift from normal metabolic activity towards cellular survival mechanisms (Himanen et al., 2022). In pigs, these molecular changes are accompanied by physiological alterations within the intestine including disruption of epithelial structure, and increased ER stress (Tang et al., 2022).

Proteomic analysis provides a powerful approach for investigating these responses, enabling the identification of differentially expressed proteins and associated pathways that underpin cellular adaptation to heat stress. In the present study, quantitative proteomic analysis was used to characterise the response of IPEC-J2 cells to heat stress and to determine how this response is modified by organic Se, inorganic Se, vitamin E, and vitamin C supplementation. The following sections discuss the findings of the effects of heat stress on the proteomic profile of IPEC-J2 cells, and the supplementation of organic Se on cells under heat stress conditions in relation to existing literature on heat stress and intestinal epithelial function.

4.3.1 Effect of 24 hours of heat stress at 42°C on IPEC-J2 cell proteomic profile

To establish the initial impact of heat stress on the proteomic profile of IPEC-J2 cells, a comparison between cells that were heat stressed for 24 h at 42°C and cells maintained at optimal temperature of 37°C was carried out (Figures 3.3-1 to 3.3-5, and Tables 3.3-1 and 3.3-2). In response to 24 h exposure to 42°C a total of 361 differentially expressed proteins, with 152 upregulated and 209 downregulated proteins, were detected (Figure 3.3-1). The findings of this comparison suggest that heat stress induces a substantial alteration in the proteomic profile of IPEC-J2 cells, particularly through the upregulation of pathways associated with protein folding, molecular chaperone activity, and ER stress (Figure 3.3-3). Heat stress disrupts protein folding by destabilising the non-covalent interactions that maintain protein structure, resulting in denaturation, exposure of hydrophobic residues, and increased aggregation of misfolded proteins, activating HSR

and UPR, which enhance chaperone expression and protein quality control mechanisms to restore proteostasis (Ellis, 1999; Worby & Dixon, 2014). These findings reflect the increased demand for protein quality control mechanisms in response to the accumulation of misfolded proteins and activation of the UPR.

Conversely, pathways related to translation, gene expression, and metabolic processes were downregulated in heat-stressed cells (Figure 3.3-5), suggesting a suppression of normal cellular activity and a shift towards energy conservation. Collectively, these findings support the concept that heat-stressed intestinal epithelial cells prioritise stress response and proteostasis mechanisms and shift away from metabolic activity.

4.3.1.1 Upregulated proteins in IPEC-J2 cells in response to heat stress

This study revealed that heat stress induces a clear significant upregulation of pathways associated with protein folding, molecular chaperone activity, and ER stress (Figure 3.3-3). These findings suggest that heat stress in IPEC-J2 cells promotes protein misfolding and aggregation, thereby triggering the activation of chaperone systems to stabilise and refold damaged proteins. Similar observations have been reported in IPEC-J2 cells, where heat stress induces ER stress and activation of the UPR signalling pathways, such as p-eif2α/CHOP pathway (Cui et al., 2022), alongside enrichment of protein processing pathways in the ER (S. Gao et al., 2026). This is further supported by the marked upregulation of several key proteins identified in the present study, including B-cell receptor-associated protein 31, 26S proteasome regulatory subunit PSMD2, and DNAJ homolog subfamily A member 2, which are associated with protein processing, degradation, and molecular chaperone activity. These proteins are highly expressed with fold-increases of 706.2, 531.9, and 184.7, respectively (Table 3.3-1).

Cells exposed to elevated temperatures undergo intracellular changes such as an accumulation of misfolded or degraded proteins, which build up in the ER lumen causing the activation of the UPR. This triggers the upregulation of genes involved in protein folding and degradation, while downregulating the genes involved in protein synthesis, therefore protecting the cells from apoptosis and ER stress (Z. Tang et al., 2023). This study demonstrated the significant upregulation of proteins directly involved in protein folding and quality control. Notably, DNAJ homolog subfamily A member 2 (DNAJA2), a co-chaperone of the HSP70 system (Baaklini et al., 2012), exhibited a 184.7-fold increase

in heat-stressed cells (Table 3.3-1), highlighting a strong activation of molecular chaperone pathways. In addition, the ER-resident chaperones calreticulin and calnexin were also upregulated with fold-increases of 2.9 and 2.8, respectively (Table 3.3-1), supporting an enhanced protein folding capacity within the ER. The marked increase in 26S proteasome subunit PSMD2 (531.9-fold increase) further indicates activation of protein degradation pathways (Bashore et al., 2023). Initially, the UPR functions as a protective mechanism playing a key role in maintaining proteostasis, however, prolonged or severe heat stress has been shown to promote a transition towards pro-apoptotic signalling (Hetz et al., 2020; Hetz & Papa, 2018). The shift of the UPR from a protective role to activating apoptosis is through proteins, including C/EBP homologous protein (CHOP), cJUN NH2-terminal kinase (JNK), and ER-associated caspase-12 (Y. Li et al., 2014). However, the proteomic analysis in the present study did not identify these pro-apoptotic markers, and no enrichment of apoptosis-related pathways was observed. This indicates that following 24 h of heat stress at 42°C, IPEC-J2 cells predominantly activate an adaptive UPR to preserve proteostasis, without clear progression towards apoptotic signalling.

Further supporting this, analysis of the upregulated proteins revealed increased expression of molecular chaperones, protein disulfide isomerases, and heat shock proteins (HSPs). The increased abundance of HSP70 identified in the proteomic analysis, with a 4.7-fold increase (Table 3.3-1), is consistent with the upregulation observed in the corresponding Western blot data (Figure 3.2-9), providing additional validation of the heat stress-induced upregulation of this chaperone. Through ATP-dependent conformational cycle, cytosolic HSP70 facilitates the destabilisation of misfolded proteins, promotes their refolding, prevents aggregation, and enables the re-solubilisation of protein aggregates once formed (Wentink et al., 2020). The ER chaperone Binding immunoglobulin protein (BiP or GRP78) was also upregulated in the present study (3.1-fold increase). BiP is a member of the HSP70 family (Haas, 1994), representing the sole HSP70 isoform and is the most abundant ER-resident chaperone (Mas & Hiller, 2025). BiP contains a substrate-binding domain that recognises exposed hydrophobic regions of unfolded proteins and a nucleotide-binding domain that regulates substrate affinity through ATP binding and hydrolysis. Following ATP hydrolysis, BiP adopts a high-affinity conformation, facilitating efficient protein folding and preventing aggregation (H. Li & Sun, 2021). The simultaneous upregulation of BiP and cytosolic HSP70 proteins in this study suggests that ER stress is promoting a pro-survival response aimed at restoring proteostasis, in which both ER and cytoplasmic quality control systems are working to mitigate protein damage. Overall, findings suggest that the level or duration of heat stress applied to IPEC-J2 cells in

this study may not have been sufficient to trigger the transition from adaptive UPR to apoptotic signalling.

In addition to HSP70, other heat shock proteins were differentially expressed under heat stress conditions (Supplementary Table 6.1). These include members of the HSP90 family, mitochondrial HSP60, and co-chaperones of the HSP40 family, including DNAJA2, which showed a particularly large increase (184.7-fold increase). The coordinated upregulation of multiple HSP families suggests activation of a broad chaperone network in response to heat stress, reflecting the need for both cytosolic and organelle-specific protein folding mechanisms.

Interestingly, proliferating cell nuclear antigen (PCNA) showed a substantial upregulation in this study, with a 449.5-fold increase in heat-stressed IPEC-J2 cells (Table 3.3-1). PCNA is a key component of DNA polymerase delta and is primarily expressed during the S phase of the cell cycle. It functions as a scaffold protein, coordinating multiple processes including DNA replication, DNA repair, cell cycle regulation, and apoptosis (S.-Q. Li et al., 2012). Its expression has been shown to decrease under conditions of cellular stress that induce cell cycle arrest.

4.3.1.2 Downregulated proteins in IPEC-J2 cells in response to heat stress

In addition to the upregulation of protein folding pathways (Figure 3.3-3), the proteomic analysis revealed a marked downregulation of processes associated with translation and protein biosynthesis. Enrichment analysis demonstrated significant reductions in translation initiation factors, RNA binding proteins, and peptide biosynthetic pathways (Figure 3.3-5), indicating a reduction of protein synthesis under heat stress conditions. The 10 significantly downregulated proteins identified in this study are associated with cell structure, adhesion, and cytoskeletal organisation, including Tax-1 binding protein 3 ($p = 0.0044$), envoplakin ($p = 0.0013$), and plakophilin-2 ($p = 0.0232$). Notably, the downregulation of eiF-2-alpha kinase activator GCN1 is consistent with disruption of translation regulation pathways, further reinforcing the observed inhibition of protein synthesis under heat stress conditions (Table 3.3-2)

This is consistent with previous studies in both plant and mammalian systems, where heat stress has been shown to induce a widespread inhibition of translation, including reduction in polysome-associated mRNAs and suppression of genes involved in ribosome biogenesis and translation initiation (Harding et al., 2000; Yángüez et al., 2013).

This is further supported by the downregulation of key proteins involved in translation regulation identified in the present study (Table 3.3-2). Notably, eIF-2-alpha kinase activator GCN1 ($p = 0.00539$) plays a central role in mediating translational control under heat stress conditions through activation of eIF2 signalling pathways. The reduction in GCN1 abundance observed here suggests suppression of translation initiation mechanisms, consistent with previous reports of heat-induced inhibition of protein synthesis (X. Tang et al., 2022). In addition, the decrease of prefoldin subunit 3, which contributes to the folding of newly synthesised proteins (Tahmaz et al., 2022), further supports a reduction in overall protein synthesis. Together these findings align with previous studies demonstrating that heat stress disrupts translation machinery and limits protein biosynthesis as part of a protective cellular response (Harding et al., 2000; Yángüez et al., 2013). Such translational inhibition is a conserved cellular response, whereby an increase in intracellular temperature during heat stress leads to a global reduction in protein synthesis, while selectively enhancing the production of stress-related proteins such as HSPs. This selective upregulation occurs primarily through activation of heat shock factor 1 (HSF1), which drives increased transcription of HSP genes, alongside preferential translation of HSP mRNAs under heat stress conditions (Kmiecik & Mayer, 2022; Murshid et al., 2018). This response is essential to limit the accumulation of misfolded or damaged proteins that could otherwise exert proteotoxic effects and compromise cell survival (Lindquist, 1986; Smith et al., 2025).

In addition to the suppression of translation, the proteomic analysis revealed significant downregulation of metabolic pathways, including glycolysis and carbon metabolism (Figure 3.3-5), indicating a broader reduction in energy-producing processes under heat stress. Disruptions in energy metabolism associated with heat stress are thought to arise from progressive imbalances in cellular energy homeostasis. Therefore, evaluating the consequences of heat stress on fundamental metabolic processes is essential for the crucial understanding of the mechanisms underlying these metabolic disturbances. Energy metabolism refers to the cellular process through which cells convert nutrients such as glucose, and amino acids into useable energy in the form of ATP through redox, anabolic, and catabolic pathways. These processes are necessary for maintained cellular activity and homeostasis (Q. Li et al., 2026; H. Liu et al., 2025). Under heat stress, this system becomes significantly altered, with evidence suggesting that key metabolic pathways, including carbohydrate metabolism and glycolysis, are downregulated. Transcriptomic and metabolic profiling of *Auricularia heimue* mycelia under prolonged temperature stress, demonstrated reduced expression of genes encoding glycolytic enzymes and decreased activity of

pathways involved in energy production. These findings indicate reduced metabolic efficiency and support the concept of metabolic reprogramming, in which cells redirect their energy utilisation towards stress adaptation rather than growth (Nie et al., 2025).

This study also demonstrated a downregulation of pathways associated with cytoskeletal organisation and binding (Figure 3.3-5). This is consistent with a general shutdown of cellular processes under heat stress that has been seen in this study. However, previous early transcriptional studies demonstrated a rapid induction of cytoskeletal-associated genes following heat shock, suggesting an initial adaptive response to maintain structural integrity (Mahat et al., 2016). In contrast, a more recent multi-omics analyses on humans, indicated that prolonged or sustained heat exposure is associated with disruption and downregulation of cytoskeletal components, reflecting structural remodelling and impaired cellular organisation under stress conditions (Wen et al., 2024). Therefore, the downregulation of cytoskeletal-associated proteins observed in this study may reflect a late response to heat stress, where cellular resources are diverted away from structural maintenance towards stress adaptation and survival mechanisms.

Together the coordinated downregulation of translation and metabolic pathways (Figure 3.3-5) suggest an energy-conserving response, and the upregulation of molecular chaperones including HSP70 family proteins (Table 3.3-1) and BiP, indicates a coordinated proteostasis network in which protein synthesis is reduced while folding capacity is enhanced. This suggests a global cellular reprogramming towards survival under heat stress conditions.

4.3.2 Proteomic responses in IPEC-J2 cells treated with organic Se prior to being heat stressed at 42°C

Following the characterisation of heat stress-induced proteomic changes in IPEC-J2 cells, the potential protective effects of organic Se supplementation were investigated (Section 3.3.2). While proteomic analysis was performed on all treatment groups against untreated heat-stress control, comprehensive discussion of all treatment comparisons was beyond the scope of the present study. Therefore, a detailed assessment was focused exclusively on Organic Se-A treatment in heat-stressed cells. Se supplementation has been widely reported to exert protective effects against heat stress, primarily through its role in maintaining redox homeostasis and cellular integrity. Se is an essential trace mineral which is involved in regulating a variety of physiological and pathological processes, through its incorporation into SelPs. Heat stress has been shown to promote the production of free radicals, impair immune function, and cause damage to proteins and other biological molecules. Most SelPs have been reported to contribute to the antioxidant defence, protein folding, and the degradation of misfolded proteins within the ER, suggesting that they may play an important protective role in cells exposed to heat stress (Cao et al., 2016). SelPs belonging to the families of glutathione peroxidases (GPxs) and thioredoxin reductases (TrxRs) are particularly important in antioxidant protection and cellular redox regulation (Roman et al., 2014).

The increased abundance of thioredoxin reductase 1 (TrxR1) in Organic Se-A treated heat-stressed cells, with a 2.1-fold increase (Table 3.3-3), highlights the activation of the thioredoxin antioxidant system under stress conditions. TrxR1 is a selenium-dependent oxidoreductase that catalyses the NADPH-driven reduction of thioredoxin, thereby maintaining intracellular redox homeostasis and facilitating the removal of reactive oxygen species (ROS). This system plays a central role in protecting cellular proteins from oxidative stress damage and supporting stress adaptation (Wright et al., 2021). Although components of the thioredoxin system can be induced by oxidative stress alone, the catalytic activity and stability of TrxR1 are highly dependent on the incorporation of SeCys, making Se availability a critical factor for its functional expression (Anestål & Arnér, 2003). Consistent with this, Se supplementation has been reported to increase TrxR1 protein abundance and enzymatic activity (J. Zhang et al., 2003). In the context of the present study, TrxR1 was not significantly altered in response to heat stress alone (Section 3.3.1) but was significantly upregulated in organic Se-treated cells under heat stress conditions ($p = 0.00164$) (Table 3.3-3). This comparison indicates that the increase in

TrxR1 abundance is associated with organic Se supplementation under heat stress conditions. This is supported by the proteomic data, which demonstrated a measurable increase in TrxR1 expression in treated heat-stressed cells, suggesting an enhancement of redox defence mechanisms, thereby improving the cellular capacity to mitigate heat stress-induced oxidative damage.

In addition, the observed increase in HSP70 (2.1-fold increase) abundance in Organic Se-A treated cells indicates an enhanced proteostatic response. While HSP70 was shown to be upregulated under baseline heat stress conditions with a 4.7-fold increase (Supplementary Table 6.1), studies in IPEC-J2 cells have shown that organic Se supplementation further upregulates the expression of HSP70 (J. Tang et al., 2019). These findings are consistent with the Western blot data that indicated that organic Se supplementation upregulated HSP70 abundance (Figure 3.2-9). Overall, Organic Se-A supplementation may enhance the adaptive response in IPEC-J2 cells by strengthening antioxidant and proteostasis pathways.

This study also demonstrated that peptidyl-prolyl cis-trans isomerase FKBP4 was downregulated in Organic Se-A treated cells under heat stress conditions, showing a 3.4-fold decrease compared to heat-stressed control cells (Table 3.3-3). This protein was upregulated in the heat stress model, with a 2.1-fold increase in heat-stressed cells compared to control cells. FKBP4 functions as an HSP90-associated co-chaperone involved in the regulation of multiple cellular pathways, including protein folding, receptor transport, and gene expression (Zong et al., 2021). A genome-wide study in heat-stressed cattle revealed an increase in co-chaperone FKBP4 (Sajjanar et al., 2023), this is consistent with results from this study that showed an increase in FKBP4 abundance in heat-stressed IPEC-J2 cells compared to control cells, suggesting that cells require more chaperone-mediated protein folding. The downregulation of FKBP4 in Organic Se-A treated cells under heat stress may indicate a reduction in the oxidative/proteotoxic effects of heat stress, therefore the demand for stress-associated chaperones declines.

Proteomic analysis of organic Se-treated cells under heat stress conditions also demonstrated a downregulation of talin-1 (TLN1) in the present study (Table 3.3-3), with a 1.5-fold decrease observed. TLN1 is integral for the formation of cell-matrix adhesions through its interactions with integrin receptors and actin cytoskeleton. It also acts as an adaptor protein, with multiple binding motifs characterised in various proteins (Da Silva et al., 2024). In the context of the present study, this downregulation of TLN1 may intensify the structural changes observed in heat-stressed IPEC-J2 cells, reflecting a shift away from

maintaining cytoskeletal integrity towards prioritising stress adaptation and survival mechanisms.

Collectively, these findings suggest that Organic Se-A supplementation enhances cellular adaptation to heat stress by strengthening antioxidant and protein quality control mechanisms, while reducing proteotoxic and structural stress.

4.4 Limitations

This study has several limitations that should be considered when interpreting the findings. Firstly, the IPEC-J2 monoculture model provides a controlled system for investigating direct cellular responses to heat stress; however, it does not replicate the porcine intestine in vivo. Within this model physiological processes such as thermoregulation, nutrient absorption, and whole-animal metabolism are not represented. Alamar Blue® reagent was primarily used to assess cellular responses to heat stress. This assay reflects cellular metabolic activity rather than direct measures of cell number, apoptosis, or cellular damage. Therefore, results should be interpreted as altered metabolic activity rather than a direct measure of viable cell number or cell death.

Another limitation of this study was the relatively small number of independent biological replicates used for multiple experiments (n = 3). Although numerical differences were observed between groups, many comparisons did not display statistical significance. Therefore, it cannot be concluded with certainty that the observed results reflect the true effects of heat stress on IPEC-J2 cells supplemented with Se and vitamin compounds. Carrying out more biological replicates would improve the statistical power and provide greater confidence in the observed responses.

In addition, the findings from the proteomic data should be interpreted with caution. Differentially expressed proteins were identified using protein-level ANOVA, fold-change, and peptide-count thresholds. While protein identification was controlled using a 1% FDR, adjusted p-values for differential protein abundance were not available. Therefore, the possibility of false-positive findings cannot be ruled out, so proteomic findings should be regarded as exploratory.

4.5 Conclusion

This study established a reproducible *in vitro* heat stress model using IPEC-J2 cells, demonstrating that exposure to elevated temperatures was associated with reduced cellular metabolic activity and increased HSP70 expression. The model provides a useful experimental platform for investigating the effects of heat stress on porcine epithelial cells and assess potential nutritional intervention strategies.

Treatment with Se and vitamin compounds presented varied effects on cellular metabolic activity and HSP70 expression under heat stress that depended on the compound used and the endpoint measured. Se, in particular, exhibited a more consistent protective effect, with improved cellular responses compared with vitamin supplementation. This is likely due to its role in enzymatic antioxidant defence systems and maintenance of cellular redox balance

Proteomic analysis demonstrated that heat stress was associated with widespread alterations in proteins involved in cellular pathways including oxidative stress, protein folding, and translation. Alterations in proteins associated with protein synthesis suggest that heat stress disrupts normal cellular function at a molecular level. Supplementation with Se and vitamin compounds was associated with additional changes in protein abundance, including treatment-related alterations in proteins such as HSP70 and TrxR1.

Overall, these findings provide valuable insights into the cellular mechanisms underlying heat stress and highlight the potential of targeted nutritional strategies, particularly Se supplementation, to improve thermotolerance in swine.

4.6 Future Work

While the present study successfully established an in vitro model of heat stress in IPEC-J2 cells, several avenues for further research remain.

Firstly, the inclusion of additional timepoints would allow for a better characterisation of the dynamics of the heat stress response. This would enable differentiation between early adaptive responses and later stages of cellular damage. Carrying out a time course from 1 hour to 48 hours would provide insight into the progression of cellular stress in IPEC-J2 cells. Furthermore, inclusion of cell cycle and apoptosis assays, such as flow cytometry, would strengthen the understanding of whether heat stress induces cell cycle arrest or programmed cell death.

Secondly, future studies should investigate additional markers of intestinal barrier function, including tight junction proteins such as occludin, claudins, and ZO-1. Although no major morphological changes were observed using phase-contrast microscopy, these proteins are highly sensitive to heat stress and may reveal early disruptions in epithelial integrity that are not detectable at the morphological level.

The measurement of oxidative stress markers would provide further insight into the mechanisms underlying heat stress-induced cellular dysfunction. Assessment of reactive oxygen species (ROS) production, antioxidant enzyme activity, and mitochondrial function would help confirm the role of oxidative damage suggested by the reduction in metabolic activity observed in this study. The use of more advanced metabolic profiling techniques, such as Seahorse analysis, could be used to assess changes in glycolysis and oxidative phosphorylation in response to heat stress in untreated and Se-treated IPEC-J2 cells.

In addition, future work should focus on independent validation of key proteomic targets identified in this study. Specifically, proteins identified in the proteomic analysis, including TrxR1, GCN1, and DNAJ2, could be investigated using complementary techniques such as RT-PCR and Western blotting to further validate and explore the pathways involved in the cellular stress response.

5 Bibliography

Åkerfelt, M., Morimoto, R. I., & Sistonen, L. (2010). Heat shock factors: integrators of cell stress, development and lifespan. *Nature Reviews Molecular Cell Biology*, *11*(8), 545–555. https://doi.org/10.1038/nrm2938

Ali, A., Tan, H., & Kaiko, G. E. (2020). Role of the Intestinal Epithelium and Its Interaction With the Microbiota in Food Allergy. *Frontiers in Immunology*, *11*. https://doi.org/10.3389/fimmu.2020.604054

AL-Jaryan, I. L., AL-Thuwaini, T. M., & AL-Jebory, H. H. (2023). Heat Shock Protein 70 and Its Role in Alleviating Heat Stress and Improving Livestock Performance. *Reviews in Agricultural Science*, *11*(0), 234–242. https://doi.org/10.7831/ras.11.0_234

Anestål, K., & Arnér, E. S. J. (2003). Rapid Induction of Cell Death by Selenium-compromised Thioredoxin Reductase 1 but Not by the Fully Active Enzyme Containing Selenocysteine. *Journal of Biological Chemistry*, *278*(18), 15966–15972. https://doi.org/10.1074/jbc.M210733200

Arnal, M.-E., & Lallès, J.-P. (2016). Gut epithelial inducible heat-shock proteins and their modulation by diet and the microbiota. *Nutrition Reviews*, *74*(3), 181–197. https://doi.org/10.1093/nutrit/nuv104

Aryal, B., Kwakye, J., Ariyo, O. W., Ghareeb, A. F. A., Milfort, M. C., Fuller, A. L., Khatiwada, S., Rekaya, R., & Aggrey, S. E. (2025). Major Oxidative and Antioxidant Mechanisms During Heat Stress-Induced Oxidative Stress in Chickens. *Antioxidants*, *14*(4), 471. https://doi.org/10.3390/antiox14040471

Baaklini, I., Wong, M. J. H., Hantouche, C., Patel, Y., Shrier, A., & Young, J. C. (2012). The DNAJA2 Substrate Release Mechanism Is Essential for Chaperone-mediated Folding. *Journal of Biological Chemistry*, *287*(50), 41939–41954. https://doi.org/10.1074/jbc.M112.413278

Bahar, N. H. A., Lo, M., Sanjaya, M., Van Vianen, J., Alexander, P., Ickowitz, A., & Sunderland, T. (2020). Meeting the food security challenge for nine billion people in 2050: What impact on forests? *Global Environmental Change*, *62*, 102056. https://doi.org/10.1016/j.gloenvcha.2020.102056

Bampidis, V., Azimonti, G., Bastos, M. de L., Christensen, H., Durjava, M., Dusemund, B., Kouba, M., López-Alonso, M., López Puente, S., Marcon, F., Mayo, B., Pechová, A., Petkova, M., Ramos, F., Villa, R. E., Woutersen, R., Innocenti, M. L., Kujawa, M., Pizzo, F., … Gropp, J. (2024). Consumer safety of feed additives containing selenium. *EFSA Journal*, *22*(6). https://doi.org/10.2903/j.efsa.2024.8857

Bardwell, J. C., & Craig, E. A. (1984). Major heat shock gene of Drosophila and the Escherichia coli heat-inducible dnaK gene are homologous. *Proceedings of the National Academy of Sciences*, *81*(3), 848–852. https://doi.org/10.1073/pnas.81.3.848

Bashore, C., Prakash, S., Johnson, M. C., Conrad, R. J., Kekessie, I. A., Scales, S. J., Ishisoko, N., Kleinheinz, T., Liu, P. S., Popovych, N., Wecksler, A. T., Zhou, L., Tam, C., Zilberleyb, I., Srinivasan, R., Blake, R. A., Song, A., Staben, S. T., Zhang, Y., … Dueber, E. C. (2023). Targeted degradation via direct 26S proteasome recruitment. *Nature Chemical Biology*, *19*(1), 55–63. https://doi.org/10.1038/s41589-022-01218-w

Belhadj Slimen, I., Najar, T., Ghram, A., Dabbebi, H., Ben Mrad, M., & Abdrabbah, M. (2014). Reactive oxygen species, heat stress and oxidative-induced mitochondrial

damage. A review. *International Journal of Hyperthermia*, *30*(7), 513–523. https://doi.org/10.3109/02656736.2014.971446

Blatteis, C. M. (1998). *Physiology and Pathophysiology of Temperature Regulation*. WORLD SCIENTIFIC. https://doi.org/10.1142/3507

Boisen, S., & Fernandez, J. A. (1997). Prediction of the total tract digestibility of energy in feedstuffs and pig diets by in vitro analyses. *Animal Feed Science and Technology*, 277–286.

Boler, D. D., Gabriel, S. R., Yang, H., Balsbaugh, R., Mahan, D. C., Brewer, M. S., McKeith, F. K., & Killefer, J. (2009). Effect of different dietary levels of natural-source vitamin E in grow-finish pigs on pork quality and shelf life. *Meat Science*, *83*(4), 723–730. https://doi.org/10.1016/j.meatsci.2009.08.012

Butt, H., Mehmood, A., Ali, M., Tasneem, S., Tarar, M. N., & Riazuddin, S. (2019). Vitamin E preconditioning alleviates in vitro thermal stress in cultured human epidermal keratinocytes. *Life Sciences*, *239*, 116972. https://doi.org/10.1016/j.lfs.2019.116972

Calvin, K., Dasgupta, D., Krinner, G., Mukherji, A., Thorne, P. W., Trisos, C., Romero, J., Aldunce, P., Barret, K., Blanco, G., Cheung, W. W. L., Connors, S. L., Denton, F., Diongue-Niang, A., Dodman, D., Garschagen, M., Geden, O., Hayward, B., Jones, C., … Ha, M. (2023). *IPCC, 2023: Climate Change 2023: Synthesis Report, Summary for Policymakers. Contribution of Working Groups I, II and III to the Sixth Assessment Report of the Intergovernmental Panel on Climate Change [Core Writing Team, H. Lee and J. Romero (eds.)]. IPCC, Geneva, Switzerland.* https://doi.org/10.59327/IPCC/AR6-9789291691647.001

Cao, L., Tang, J., Li, Q., Xu, J., Jia, G., Liu, G., Chen, X., Shang, H., Cai, J., & Zhao, H. (2016). Expression of Selenoprotein Genes Is Affected by Heat Stress in IPEC-J2 Cells. *Biological Trace Element Research*, *172*(2), 354–360. https://doi.org/10.1007/s12011-015-0604-0

Chatterjee, I. B., Mukhopadhyay, C. K., & Ghosh, M. K. (1995). Vitamin C: A potential saviour against free radical-induced oxidative damage. *Current Science*, *69*(9), 747–751.

Collier, R. J., & Gebremedhin, K. G. (2015). Thermal Biology of Domestic Animals. *Annual Review of Animal Biosciences*, *3*(1), 513–532. https://doi.org/10.1146/annurev-animal-022114-110659

Collin, A., Lebreton, Y., Fillaut, M., Vincent, A., Thomas, F., & Herpin, P. (2001). Effects of exposure to high temperature and feeding level on regional blood flow and oxidative capacity of tissues in piglets. *Experimental Physiology*, *86*, 83–91.

Craig, E. A. (1988). THE HEAT-SHOCK PROTEINS. In *Annu. Rev. Genei* (Vol. 12).

Crenshaw, T. D. (2025). Nutritional Requirements of Pigs. *MSD Manual Veterinary Manual*.

Cui, Y. jun, Chen, L. yi, Zhou, X., Tang, Z. ning, Wang, C., & Wang, H. feng. (2022). Heat stress induced IPEC-J2 cells barrier dysfunction through endoplasmic reticulum stress

mediated apoptosis by p-eif2α/CHOP pathway. *Journal of Cellular Physiology*, *237*(2), 1389–1405. https://doi.org/10.1002/jcp.30603

Curtis, S. E. . (1983). *Environmental management in animal agriculture*. Iowa State University Press.

Da Silva, A. J., Hästbacka, H. S. E., Luoto, J. C., Gough, R. E., Coelho-Rato, L. S., Laitala, L. M., Goult, B. T., Imanishi, S. Y., Sistonen, L., & Henriksson, E. (2024). Proteomic profiling identifies a direct interaction between heat shock transcription factor 2 and the focal adhesion adapter talin-1. *The FEBS Journal*, *291*(21), 4830–4848. https://doi.org/10.1111/febs.17271

Daugaard, M., Rohde, M., & Jäättelä, M. (2007). The heat shock protein 70 family: Highly homologous proteins with overlapping and distinct functions. *FEBS Letters*, *581*(19), 3702–3710. https://doi.org/10.1016/j.febslet.2007.05.039

DeShazer, J. A. ., LeRoy, G., & Xin, H. (2009). Chapter 1: Basic principles of the thermal environment and livestock energies. In *Livestock energetics and thermal environmental management* (pp. 1–22). American Society of Agricultural and Biological Engineers.

Ellis, J. R. (1999). Molecular chaperones: Pathways and networks. *Current Biology*, *9*(4), R137–R139. https://doi.org/10.1016/S0960-9822(99)80082-7

European Commission. (2019). Commission Implementing Regulation (EU) 2019/49 of 4 January 2019 concerning the authorisation of sodium selenite, coated granulated sodium selenite and zinc-L-selenomethionine as feed additives for all animal species. *Official Journal of the European Union*, L10/2-L10/7.

Evgen'ev, M. B., Onikienko, S. B., Chuvakova, L. N., Garbuz, D. G., & Zatsepina, O. G. (2023). The Role of Hsp70 in Adaptation to Adverse Conditions and Its Possible Medical Application. *Frontiers in Bioscience-Landmark*, *28*(2). https://doi.org/10.31083/j.fbl2802025

Fan, X., Tian, X., & Li, M. (2025). Challenges of heat stress on intestinal health in pig husbandry. *Fundamental Research*. https://doi.org/10.1016/j.fmre.2025.06.006

FAO. (2024). *FAOSTAT Crops and Livestock Production*. https://www.fao.org/faostat/en/#data/QCL.

Furness, J. B., Kunze, W. A. A., & Clerc, N. (1999). *themes Nutrient Tasting and Signaling Mechanisms in the Gut II. The intestine as a sensory organ: neural, endocrine, and immune responses *.*

Gan, F., Chen, X., Liao, S. F., Lv, C., Ren, F., Ye, G., Pan, C., Huang, D., Shi, J., Shi, X., Zhou, H., & Huang, K. (2014). Selenium-Enriched Probiotics Improve Antioxidant Status, Immune Function, and Selenoprotein Gene Expression of Piglets Raised under High Ambient Temperature. *Journal of Agricultural and Food Chemistry*, *62*(20), 4502–4508. https://doi.org/10.1021/jf501065d

Gan, F., Ren, F., Chen, X., Lv, C., Pan, C., Ye, G., Shi, J., Shi, X., Zhou, H., Shituleni, S. A., & Huang, K. (2013). Effects of Selenium-Enriched Probiotics on Heat Shock Protein mRNA Levels in Piglet under Heat Stress Conditions. *Journal of Agricultural and Food Chemistry*, *61*(10), 2385–2391. https://doi.org/10.1021/jf300249j

Gao, C., Zhao, Y., Li, H., Sui, W., Yan, H., & Wang, X. (2015). Heat stress inhibits proliferation, promotes growth, and induces apoptosis in cultured Lantang swine skeletal muscle satellite cells. *Journal of Zhejiang University-SCIENCE B*, *16*(6), 549–559. https://doi.org/10.1631/jzus.B1400339

Gao, S., Zheng, X., Jiang, Y., Zhang, F., Pei, W., Yang, G., & Liu, G. (2026). ER Proteotoxic Stress Drives Mitochondrial Dysfunction in Heat-Stressed Intestinal Epithelial Cells. *Cells*, *15*(5), 486. https://doi.org/10.3390/cells15050486

Geens, M. M., & Niewold, T. A. (2011). Optimizing culture conditions of a porcine epithelial cell line IPEC-J2 through a histological and physiological characterization. *Cytotechnology*, *63*(4), 415–423. https://doi.org/10.1007/s10616-011-9362-9

Gleeson, M. (1998). Temperature Regulation During Exercise. *International Journal of Sports Medicine*, *19*(S 2), S96–S99. https://doi.org/10.1055/s-2007-971967

Gonzalez-Rivas, P. A., Chauhan, S. S., Ha, M., Fegan, N., Dunshea, F. R., & Warner, R. D. (2020). Effects of heat stress on animal physiology, metabolism, and meat quality: A review. In *Meat Science* (Vol. 162). Elsevier Ltd. https://doi.org/10.1016/j.meatsci.2019.108025

Gourdine, J. L., Rauw, W. M., Gilbert, H., & Poullet, N. (2021). The Genetics of Thermoregulation in Pigs: A Review. In *Frontiers in Veterinary Science* (Vol. 8). Frontiers Media S.A. https://doi.org/10.3389/fvets.2021.770480

Haas, I. G. (1994). BiP (GRP78), an essential hsp70 resident protein in the endoplasmic reticulum. *Experientia*, *50*(11–12), 1012–1020. https://doi.org/10.1007/BF01923455

Harding, H. P., Zhang, Y., Bertolotti, A., Zeng, H., & Ron, D. (2000). Perk Is Essential for Translational Regulation and Cell Survival during the Unfolded Protein Response. *Molecular Cell*, *5*(5), 897–904. https://doi.org/10.1016/S1097-2765(00)80330-5

Hartl, F. U., & Hayer-Hartl, M. (2009). Converging concepts of protein folding in vitro and in vivo. In *Nature Structural and Molecular Biology* (Vol. 16, Number 6, pp. 574–581). https://doi.org/10.1038/nsmb.1591

He, Y., Liu, Y., Tang, J., Jia, G., Liu, G., Tian, G., Chen, X., Cai, J., Kang, B., & Zhao, H. (2022). Selenium exerts protective effects against heat stress-induced barrier disruption and inflammation response in jejunum of growing pigs. *Journal of the Science of Food and Agriculture*, *102*(2), 496–504. https://doi.org/10.1002/jsfa.11377

Herath, M., Hosie, S., Bornstein, J. C., Franks, A. E., & Hill-Yardin, E. L. (2020). The Role of the Gastrointestinal Mucus System in Intestinal Homeostasis: Implications for Neurological Disorders. In *Frontiers in Cellular and Infection Microbiology* (Vol. 10). Frontiers Media S.A. https://doi.org/10.3389/fcimb.2020.00248

Herpin, P., Damon, M., & Le Dividich, J. (2002). Development of thermoregulation and neonatal survival in pigs. *Livestock Production Science*, *78*(1), 25–45. https://doi.org/10.1016/S0301-6226(02)00183-5

Hetz, C., & Papa, F. R. (2018). The Unfolded Protein Response and Cell Fate Control. *Molecular Cell*, *69*(2), 169–181. https://doi.org/10.1016/j.molcel.2017.06.017

Hetz, C., Zhang, K., & Kaufman, R. J. (2020). Mechanisms, regulation and functions of the unfolded protein response. *Nature Reviews Molecular Cell Biology*, *21*(8), 421–438. https://doi.org/10.1038/s41580-020-0250-z

Himanen, S. V, Puustinen, M. C., Da Silva, A. J., Vihervaara, A., & Sistonen, L. (2022). HSFs drive transcription of distinct genes and enhancers during oxidative stress and heat shock. *Nucleic Acids Research*, *50*(11), 6102–6115. https://doi.org/10.1093/nar/gkac493

Hoffmann, P. R. (2007). Mechanisms by which selenium influences immune responses. *Archivum Immunologiae et Therapiae Experimentalis*, *55*(5), 289–297. https://doi.org/10.1007/s00005-007-0036-4

Hu, C., Yang, J., Qi, Z., Wu, H., Wang, B., Zou, F., Mei, H., Liu, J., Wang, W., & Liu, Q. (2022). Heat shock proteins: Biological functions, pathological roles, and therapeutic opportunities. In *MedComm* (Vol. 3, Number 3). John Wiley and Sons Inc. https://doi.org/10.1002/mco2.161

Jang, I.-S., Ko, Y.-H., Moon, Y.-S., & Sohn, S.-H. (2014). Effects of Vitamin C or E on the Pro-inflammatory Cytokines, Heat Shock Protein 70 and Antioxidant Status in Broiler Chicks under Summer Conditions. *Asian-Australasian Journal of Animal Sciences*, *27*(5), 749–756. https://doi.org/10.5713/ajas.2013.13852

Johansson, M. E. V., Ambort, D., Pelaseyed, T., Schütte, A., Gustafsson, J. K., Ermund, A., Subramani, D. B., Holmén-Larsson, J. M., Thomsson, K. A., Bergström, J. H., van der Post, S., Rodriguez-Piñeiro, A. M., Sjövall, H., Bäckström, M., & Hansson, G. C. (2011). Composition and functional role of the mucus layers in the intestine. *Cellular and Molecular Life Sciences*, *68*(22), 3635–3641. https://doi.org/10.1007/s00018-011-0822-3

Johansson, M. E. V., Sjövall, H., & Hansson, G. C. (2013). The gastrointestinal mucus system in health and disease. *Nature Reviews Gastroenterology & Hepatology*, *10*(6), 352–361. https://doi.org/10.1038/nrgastro.2013.35

Joly, A. L., Wettstein, G., Mignot, G., Ghiringhelli, F., & Garrido, C. (2010). Dual role of heat shock proteins as regulators of apoptosis and innate immunity. In *Journal of Innate Immunity* (Vol. 2, Number 3, pp. 238–247). https://doi.org/10.1159/000296508

Joy, A., Dunshea, F. R., Leury, B. J., Clarke, I. J., DiGiacomo, K., & Chauhan, S. S. (2020). Resilience of Small Ruminants to Climate Change and Increased Environmental Temperature: A Review. *Animals*, *10*(5), 867. https://doi.org/10.3390/ani10050867

Kaidow, A., Ishii, N., Suzuki, S., Shiina, T., & Kasahara, H. (2022). Vitamin C Maintenance against Cell Growth Arrest and Reactive Oxygen Species Accumulation in the Presence of Redox Molecular Chaperone hslO Gene. *International Journal of Molecular Sciences*, *23*(21), 12786. https://doi.org/10.3390/ijms232112786

Katiyar, R., Gonmei, C., Deori, S., Singh, M., Abedin, S. N., Rautela, R., Singh, N. S., Chakravarty, H., Das, M., Choudhury, B. U., & Mishra, V. K. (2025). Effect of heat stress on pig production and its mitigation strategies: a review. *Tropical Animal Health and Production*, *57*(3), 139. https://doi.org/10.1007/s11250-025-04387-7

Kaushik, R., Goel, A., & Rout, P. K. (2022). Differential expression and regulation of HSP70 gene during growth phase in ruminants in response to heat stress. *Scientific Reports*, *12*(1), 18310. https://doi.org/10.1038/s41598-022-22728-6

Kaźmierczak-Barańska, J., Boguszewska, K., Adamus-Grabicka, A., & Karwowski, B. T. (2020). Two Faces of Vitamin C—Antioxidative and Pro-Oxidative Agent. *Nutrients*, *12*(5), 1501. https://doi.org/10.3390/nu12051501

Key, N., & Sneeringer, S. (2014). Potential Effects of Climate Change on the Productivity of U.S. Dairies. *American Journal of Agricultural Economics*, *96*(4), 1136–1156. https://doi.org/10.1093/ajae/aau002

Khorami, S. A. H., Mutalib, M. S. A., & Khaza'ai, H. (2020). *Comparative effect of vitamin E compounds on HSP70 expression in response to acute redox imbalance in Chang liver cells*. https://doi.org/10.21203/rs.3.rs-22336/v1

Kilicarslan You, D., Fuwad, A., Lee, K. H., Kim, H. K., Kang, L., Kim, S. M., & Jeon, T.-J. (2024). Evaluation of the Protective Role of Vitamin E against ROS-Driven Lipid Oxidation in Model Cell Membranes. *Antioxidants*, *13*(9), 1135. https://doi.org/10.3390/antiox13091135

Kim, J. Y., Han, Y., Lee, J. E., & Yenari, M. A. (2018). The 70-kDa heat shock protein (Hsp70) as a therapeutic target for stroke. *Expert Opinion on Therapeutic Targets*, *22*(3), 191–199. https://doi.org/10.1080/14728222.2018.1439477

Kmiecik, S. W., & Mayer, M. P. (2022). Molecular mechanisms of heat shock factor 1 regulation. *Trends in Biochemical Sciences*, *47*(3), 218–234. https://doi.org/10.1016/j.tibs.2021.10.004

Koch, F., Thom, U., Albrecht, E., Weikard, R., Nolte, W., Kuhla, B., & Kuehn, C. (2019). Heat stress directly impairs gut integrity and recruits distinct immune cell populations into the bovine intestine. *Proceedings of the National Academy of Sciences*, *116*(21), 10333–10338. https://doi.org/10.1073/pnas.1820130116

Kyoung, H., Shin, I., Kim, Y., Cho, J. H., Park, K. Il, Kim, Y., Ahn, J., Nam, J., Kim, K., Kang, Y., Kim, H. B., & Song, M. (2025). Mixed supplementation of dietary inorganic and organic selenium modulated systemic health parameters and fecal microbiota in weaned pigs. *Frontiers in Veterinary Science*, *12*. https://doi.org/10.3389/fvets.2025.1531336

Lee, J.-G., Jang, J.-Y., & Baik, S.-M. (2025). Selenium as an Antioxidant: Roles and Clinical Applications in Critically Ill and Trauma Patients: A Narrative Review. *Antioxidants*, *14*(3), 294. https://doi.org/10.3390/antiox14030294

Li, G. C., Li, L., Liu, R. Y., Rehman, M., & Lee, W. M. (1992). Heat shock protein hsp70 protects cells from thermal stress even after deletion of its ATP-binding domain. *Proceedings of the National Academy of Sciences*, *89*(6), 2036–2040. https://doi.org/10.1073/pnas.89.6.2036

Li, H., & Sun, S. (2021). Protein Aggregation in the ER: Calm behind the Storm. *Cells*, *10*(12), 3337. https://doi.org/10.3390/cells10123337

Li, Q., Wang, J., Qin, X., Zhong, B., Wei, Q., Zeng, C., & Yang, K. (2026). Energy metabolic dysregulation in heat stroke: from mitochondrial dysfunction to multi-organ

failure mechanisms and targeted intervention. *Frontiers in Pharmacology*, *17*. https://doi.org/10.3389/fphar.2026.1813630

Li, S.-Q., Li, R.-F., Xi, S.-M., Hu, S., Jia, Z.-Q., Li, S.-P., Wen, X.-L., Song, Y.-K., Li, S., Li, S.-P., Wei, F.-B., & Chen, X.-L. (2012). Systematical analysis of impacts of heat stress on the proliferation, apoptosis and metabolism of mouse hepatocyte. *The Journal of Physiological Sciences*, *62*(1), 29–43. https://doi.org/10.1007/s12576-011-0183-6

Li, Y., Guo, Y., Tang, J., Jiang, J., & Chen, Z. (2014). New insights into the roles of CHOP-induced apoptosis in ER stress. *Acta Biochimica et Biophysica Sinica*, *46*(8), 629–640. https://doi.org/10.1093/abbs/gmu048

Li, Z., Chu, Y., Zhang, J.-H., Xu, L., Xia, B.-Z., Lei, X.-G., & Chen, X.-D. (2025). Comparative Effects of Different Forms of Dietary Supplemental Selenium in Hot Environment-induced Endoplasmic Reticulum Stress in Pigs. *The Journal of Nutrition*, *155*(8), 2622–2630. https://doi.org/10.1016/j.tjnut.2025.05.043

Lian, P., Braber, S., Garssen, J., Wichers, H. J., Folkerts, G., Fink-Gremmels, J., & Varasteh, S. (2020). Beyond heat stress: Intestinal integrity disruption and mechanism-based intervention strategies. In *Nutrients* (Vol. 12, Number 3). MDPI AG. https://doi.org/10.3390/nu12030734

Liao, S. F., & Nyachoti, M. (2017). Using probiotics to improve swine gut health and nutrient utilization. *Animal Nutrition*, *3*(4), 331–343. https://doi.org/10.1016/j.aninu.2017.06.007

Lindquist, S. (1986). THE HEAT-SHOCK RESPONSE. *Annual Review of Biochemistry*, *55*(1), 1151–1191. https://doi.org/10.1146/annurev.bi.55.070186.005443

Liu, F., Celi, P., Chauhan, S. S., Cottrell, J. J., Leury, B. J., & Dunshea, F. R. (2018). A short-term supranutritional vitamin E supplementation alleviated respiratory alkalosis but did not reduce oxidative stress in heat stressed pigs. *Asian-Australasian Journal of Animal Sciences*, *31*(2), 263–269. https://doi.org/10.5713/ajas.17.0256

Liu, F., Cottrell, J. J., Furness, J. B., Rivera, L. R., Kelly, F. W., Wijesiriwardana, U., Pustovit, R. V., Fothergill, L. J., Bravo, D. M., Celi, P., Leury, B. J., Gabler, N. K., & Dunshea, F. R. (2016). Selenium and vitamin E together improve intestinal epithelial barrier function and alleviate oxidative stress in heat-stressed pigs. *Experimental Physiology*, *101*(7), 801–810. https://doi.org/10.1113/EP085746

Liu, H., Dicksved, J., Lundh, T., & Lindberg, J. E. (2014). Heat shock proteins: Intestinal gatekeepers that are influenced by dietary components and the gut microbiota. In *Pathogens* (Vol. 3, Number 1, pp. 187–210). MDPI AG. https://doi.org/10.3390/pathogens3010187

Liu, H., Wang, S., Wang, J., Guo, X., Song, Y., Fu, K., Gao, Z., Liu, D., He, W., & Yang, L.-L. (2025). Energy metabolism in health and diseases. *Signal Transduction and Targeted Therapy*, *10*(1), 69. https://doi.org/10.1038/s41392-025-02141-x

Liu, Y., Yin, S., He, Y., Tang, J., Pu, J., Jia, G., Liu, G., Tian, G., Chen, X., Cai, J., Kang, B., Che, L., & Zhao, H. (2023). Hydroxy-Selenomethionine Mitigated Chronic Heat Stress-Induced Porcine Splenic Damage via Activation of Nrf2/Keap1 Signal and

Suppression of NFκb and STAT Signal. *International Journal of Molecular Sciences*, *24*(7), 6461. https://doi.org/10.3390/ijms24076461

Longhin, E. M., El Yamani, N., Rundén-Pran, E., & Dusinska, M. (2022). The alamar blue assay in the context of safety testing of nanomaterials. *Frontiers in Toxicology*, *4*. https://doi.org/10.3389/ftox.2022.981701

Maggini, S., Wintergerst, E. S., Beveridge, S., & Hornig, D. H. (2007). Selected vitamins and trace elements support immune function by strengthening epithelial barriers and cellular and humoral immune responses. *British Journal of Nutrition*, *98*(S1), S29–S35. https://doi.org/10.1017/S0007114507832971

Mahat, D. B., Salamanca, H. H., Duarte, F. M., Danko, C. G., & Lis, J. T. (2016). Mammalian Heat Shock Response and Mechanisms Underlying Its Genome-wide Transcriptional Regulation. *Molecular Cell*, *62*(1), 63–78. https://doi.org/10.1016/j.molcel.2016.02.025

Mainardi, E., Corino, C., & Rossi, R. (2024). The Effect of Vitamins on the Immune Systems of Pigs. *Animals*, *14*(14), 2126. https://doi.org/10.3390/ani14142126

Mas, G., & Hiller, S. (2025). Mechanism of ATP hydrolysis in the Hsp70 BiP nucleotide-binding domain. *Nature Communications*, *16*(1), 5086. https://doi.org/10.1038/s41467-025-60343-x

Mayorga, E. J., Renaudeau, D., Ramirez, B. C., Ross, J. W., & Baumgard, L. H. (2019). Heat stress adaptations in pigs. *Animal Frontiers*, *9*(1), 54–61. https://doi.org/10.1093/af/vfy035

McGuckin, M. A., Lindén, S. K., Sutton, P., & Florin, T. H. (2011). Mucin dynamics and enteric pathogens. *Nature Reviews Microbiology*, *9*(4), 265–278. https://doi.org/10.1038/nrmicro2538

Mercier, P. A., Winegarden, N. A., & Westwood, J. T. (1999). Human heat shock factor 1 is predominantly a nuclear protein before and after heat stress. *Journal of Cell Science*, *112*(16), 2765–2774. https://doi.org/10.1242/jcs.112.16.2765

Meunier, J. P., Manzanilla, E. G., Anguita, M., Denis, S., Pérez, J. F., Gasa, J., Cardot, J.-M., Garcia, F., Moll, X., & Alric, M. (2008). Evaluation of a dynamic in vitro model to simulate the porcine ileal digestion of diets differing in carbohydrate composition1. *Journal of Animal Science*, *86*(5), 1156–1163. https://doi.org/10.2527/jas.2007-0145

Mikhailova, E., Sokolenko, A., Combs, S. E., & Shevtsov, M. (2025). Modulation of Heat Shock Proteins Levels in Health and Disease: An Integrated Perspective in Diagnostics and Therapy. *Cells*, *14*(13), 979. https://doi.org/10.3390/cells14130979

Montecinos, V., Guzmán, P., Barra, V., Villagrán, M., Muñoz-Montesino, C., Sotomayor, K., Escobar, E., Godoy, A., Mardones, L., Sotomayor, P., Guzmán, C., Vásquez, O., Gallardo, V., van Zundert, B., Bono, M. R., Oñate, S. A., Bustamante, M., Cárcamo, J. G., Rivas, C. I., & Vera, J. C. (2007). Vitamin C Is an Essential Antioxidant That Enhances Survival of Oxidatively Stressed Human Vascular Endothelial Cells in the Presence of a Vast Molar Excess of Glutathione. *Journal of Biological Chemistry*, *282*(21), 15506–15515. https://doi.org/10.1074/jbc.M608361200

Mount, L. E. . (1979). *Adaptation to thermal environment : Man and his productive animals*. E. Arnold.

MSD Veterinary Manual. (2025, May). *Nutritional Requirements of Pigs*. https://www.msdvetmanual.com/management-and-nutrition/nutrition-pigs/nutritional-requirements-of-pigs

Murshid, A., Prince, T. L., Lang, B., & Calderwood, S. K. (2018). *Role of Heat Shock Factors in Stress-Induced Transcription* (pp. 23–34). https://doi.org/10.1007/978-1-4939-7477-1_2

Musch, M. W., Ciancio, M. J., Sarge, K., & Chang, E. B. (1996). Induction of heat shock protein 70 protects intestinal epithelial IEC-18 cells from oxidant and thermal injury. *American Journal of Physiology-Cell Physiology*, *270*(2), C429–C436. https://doi.org/10.1152/ajpcell.1996.270.2.C429

National Research Council. (2012). *Nutrient Requirements of Swine: Eleventh Edition*. National Academies Press. https://doi.org/10.17226/13298

Nie, C., Wei, S., Wu, S., Qi, L., Feng, J., & Wang, X. (2025). Transcriptomic, and metabolic profiling reveals adaptive mechanisms of *Auricularia heimuer* to temperature stress. *PeerJ*, *13*, e19713. https://doi.org/10.7717/peerj.19713

Official Journal of the European Union. (2022). Commission Implementing Regulation (EU) 2022/1459 of 2 September 2022 amending Implementing Regulation (EU) 2019/804 as regards the terms of authorisation of the organic form of selenium produced by Saccharomyces cerevisiae CNCM I-3060 as feed additive for all animal species. *Official Journal of the European Union*.

Olsen, A. W., Dybkjær, L., & Simonsen, H. B. (2001). Behaviour of growing pigs kept in pens with outdoor runs: II. Temperature regulatory behaviour, comfort behaviour and dunging preferences. *Livestock Production Science*, *69*(3), 265–278. https://doi.org/10.1016/S0301-6226(01)00173-7

Ortega, A. D. S. V., Babinszky, L., Ozsváth, X. E., Oriedo, O. H., & Szabó, C. (2022). The Effect of Heat Stress and Vitamin and Micro-Mineral Supplementation on Some Mineral Digestibility and Electrolyte Balance of Pigs. *Animals*, *12*(3). https://doi.org/10.3390/ani12030386

Ortega, A. D. S. V., & Szabó, C. (2021). Adverse Effects of Heat Stress on the Intestinal Integrity and Function of Pigs and the Mitigation Capacity of Dietary Antioxidants: A Review. *Animals*, *11*(4), 1135. https://doi.org/10.3390/ani11041135

Osei-Amponsah, R., Chauhan, S. S., Leury, B. J., Cheng, L., Cullen, B., Clarke, I. J., & Dunshea, F. R. (2019). Genetic Selection for Thermotolerance in Ruminants. *Animals*, *9*(11), 948. https://doi.org/10.3390/ani9110948

Oswald, I. P. (2006). Role of intestinal epithelial cells in the innate immune defence of the pig intestine. In *Veterinary Research* (Vol. 37, Number 3, pp. 359–368). https://doi.org/10.1051/vetres:2006006

Otaka, M., Odashima, M., & Watanabe, S. (2006). Role of heat shock proteins (molecular chaperones) in intestinal mucosal protection. *Biochemical and Biophysical Research Communications*, *348*(1), 1–5. https://doi.org/10.1016/j.bbrc.2006.07.028

Parsell, D. A., & Sauer, R. T. (1989). Induction of a heat shock-like response by unfolded protein in Escherichia coli: dependence on protein level not protein degradation. *Genes & Development*, *3*(8), 1226–1232. https://doi.org/10.1101/gad.3.8.1226

Pearce, S. C., Mani, V., Boddicker, R. L., Johnson, J. S., Weber, T. E., Ross, J. W., Rhoads, R. P., Baumgard, L. H., & Gabler, N. K. (2013). Heat Stress Reduces Intestinal Barrier Integrity and Favors Intestinal Glucose Transport in Growing Pigs. *PLoS ONE*, *8*(8), e70215. https://doi.org/10.1371/journal.pone.0070215

Perruchot, M.-H., Boudry, G., Wiart-Letort, S., Mauro-Vigroux, M., Daré, S., Gondret, F., & Grundy, M.-L. M. (2026). Investigating alterations associated with heat stress and the recovery of the intestinal barrier using IPEC-J2 as an intestinal epithelial porcine cell model. *Scientific Reports*. https://doi.org/10.1038/s41598-026-45755-z

Pessa, J. C., Joutsen, J., & Sistonen, L. (2024). Transcriptional reprogramming at the intersection of the heat shock response and proteostasis. *Molecular Cell*, *84*(1), 80–93. https://doi.org/10.1016/j.molcel.2023.11.024

Petrof, E. O., Ciancio, M. J., & Chang, E. B. (2004). Role and regulation of intestinal epithelial heat shock proteins in health and disease. *Chinese Journal of Digestive Diseases*, *5*(2), 45–50. https://doi.org/10.1111/j.1443-9573.2004.00154.x

Pinelli-Saavedra, A. (2003). Vitamin E in immunity and reproductive performance in pigs. *Reproduction Nutrition Development*, *43*(5), 397–408. https://doi.org/10.1051/rnd:2003034

Rampersad, S. N. (2012). Multiple Applications of Alamar Blue as an Indicator of Metabolic Function and Cellular Health in Cell Viability Bioassays. *Sensors*, *12*(9), 12347–12360. https://doi.org/10.3390/s120912347

Renaudeau, D., Collin, A., Yahav, S., de Basilio, V., Gourdine, J. L., & Collier, R. J. (2012). Adaptation to hot climate and strategies to alleviate heat stress in livestock production. *Animal*, *6*(5), 707–728. https://doi.org/10.1017/S1751731111002448

Renaudeau, D., Huc, E., & Noblet, J. (2007). Acclimation to high ambient temperature in Large White and Caribbean Creole growing pigs1. *Journal of Animal Science*, *85*(3), 779–790. https://doi.org/10.2527/jas.2006-430

Ringseis, R., & Eder, K. (2022). Heat stress in pigs and broilers: role of gut dysbiosis in the impairment of the gut-liver axis and restoration of these effects by probiotics, prebiotics and synbiotics. In *Journal of Animal Science and Biotechnology* (Vol. 13, Number 1). BioMed Central Ltd. https://doi.org/10.1186/s40104-022-00783-3

Roman, M., Jitaru, P., & Barbante, C. (2014). Selenium biochemistry and its role for human health. *Metallomics*, *6*(1), 25–54. https://doi.org/10.1039/C3MT00185G

Sajjanar, B., Aalam, M. T., Khan, O., Tanuj, G. N., Sahoo, A. P., Manjunathareddy, G. B., Gandham, R. K., Dhara, S. K., Gupta, P. K., Mishra, B. P., Dutt, T., & Singh, G. (2023). Genome-wide expression analysis reveals different heat shock responses in indigenous (Bos indicus) and crossbred (Bos indicus X Bos taurus) cattle. *Genes and Environment*, *45*(1), 17. https://doi.org/10.1186/s41021-023-00271-8

Sammad, A., Ahmed, T., Ullah, K., Hu, L., Luo, H., Alphayo Kambey, P., Faisal, S., Zhu, H., Li, Y., & Wang, Y. (2024). Vitamin C Alleviates the Negative Effects of Heat

Stress on Reproductive Processes by Regulating Amino Acid Metabolism in Granulosa Cells. *Antioxidants*, *13*(6), 653. https://doi.org/10.3390/antiox13060653

Santos, L. S. dos, Pomar, C., Campos, P. H. R. F., da Silva, W. C., Gobi, J. de P., Veira, A. M., Fraga, A. Z., & Hauschild, L. (2018). Precision feeding strategy for growing pigs under heat stress conditions1. *Journal of Animal Science*, *96*(11), 4789–4801. https://doi.org/10.1093/jas/sky343

Sejian, V., Bhatta, R., Gaughan, J. B., Dunshea, F. R., & Lacetera, N. (2018). Review: Adaptation of animals to heat stress. In *Animal* (Vol. 12, Number s2, pp. S431–S444). Cambridge University Press. https://doi.org/10.1017/S1751731118001945

Sharma, V. K., McDonald, T. J., Sohn, M., Anquandah, G. A. K., Pettine, M., & Zboril, R. (2017). Assessment of toxicity of selenium and cadmium selenium quantum dots: A review. *Chemosphere*, *188*, 403–413. https://doi.org/10.1016/j.chemosphere.2017.08.130

Shastak, Y., & Pelletier, W. (2025). The E-volution in swine nutrition: Current perspectives on vitamin E. *Animal Research and One Health*, *3*(1), 2–30. https://doi.org/10.1002/aro2.93

Shimasaki, K., Okemoto-Nakamura, Y., Saito, K., Fukasawa, M., Katoh, K., & Hanada, K. (2024). A high-resolution phase-contrast microscopy system for label-free imaging in living cells. *Cell Structure and Function*, *49*(1), 24018. https://doi.org/10.1247/csf.24018

Singh, M. K., Shin, Y., Ju, S., Han, S., Choe, W., Yoon, K.-S., Kim, S. S., & Kang, I. (2024). Heat Shock Response and Heat Shock Proteins: Current Understanding and Future Opportunities in Human Diseases. *International Journal of Molecular Sciences*, *25*(8), 4209. https://doi.org/10.3390/ijms25084209

SINGH, V., RASTOGI, A., NAUTIYAL, N., & NEGI, V. (2017). Livestock and climate change: the key actors and the sufferers of global warming. *The Indian Journal of Animal Sciences*, *87*(1). https://doi.org/10.56093/ijans.v87i1.66795

Smith, M., Taqrir Akramin, A., & Balcerowicz, M. (2025). Translational reprogramming under heat stress: a plant's perspective. *Royal Society Open Science*, *12*(7). https://doi.org/10.1098/rsos.250132

Smołucha, G., Steg, A., & Oczkowicz, M. (2024). The Role of Vitamins in Mitigating the Effects of Various Stress Factors in Pigs Breeding. *Animals*, *14*(8), 1218. https://doi.org/10.3390/ani14081218

Snoeckx, L. H. E. H., Cornelussen, R. N., Van Nieuwenhoven, F. A., Reneman, R. S., & Van der Vusse, G. J. (2001). Heat Shock Proteins and Cardiovascular Pathophysiology. *Physiological Reviews*, *81*(4), 1461–1497. https://doi.org/10.1152/physrev.2001.81.4.1461

St-Pierre, N. R., Cobanov, B., & Schnitkey, G. (2003). Economic losses from heat stress by US livestock industries1. *Journal of Dairy Science*, *86*(SUPPL. 1). https://doi.org/10.3168/jds.S0022-0302(03)74040-5

Sun, M., Li, Q., Zou, Z., Liu, J., Gu, Z., & Li, L. (2024). The mechanisms behind heatstroke-induced intestinal damage. In *Cell Death Discovery* (Vol. 10, Number 1). Springer Nature. https://doi.org/10.1038/s41420-024-02210-0

Tahmaz, I., Shahmoradi Ghahe, S., & Topf, U. (2022). Prefoldin Function in Cellular Protein Homeostasis and Human Diseases. *Frontiers in Cell and Developmental Biology*, *9*. https://doi.org/10.3389/fcell.2021.816214

Tang, J., Cao, L., Jia, G., Liu, G., Chen, X., Tian, G., Cai, J., Shang, H., & Zhao, H. (2019). The protective effect of selenium from heat stress-induced porcine small intestinal epithelial cell line (IPEC-J2) injury is associated with regulation expression of selenoproteins. *British Journal of Nutrition*, *122*(10), 1081–1090. https://doi.org/10.1017/S0007114519001910

Tang, S., Xie, J., Fang, W., Wen, X., Yin, C., Meng, Q., Zhong, R., Chen, L., & Zhang, H. (2022). Chronic heat stress induces the disorder of gut transport and immune function associated with endoplasmic reticulum stress in growing pigs. *Animal Nutrition*, *11*, 228–241. https://doi.org/10.1016/j.aninu.2022.08.008

Tang, X., Xiong, K., Fang, R., & Li, M. (2022). Weaning stress and intestinal health of piglets: A review. *Frontiers in Immunology*, *13*. https://doi.org/10.3389/fimmu.2022.1042778

Tang, Z., Yang, Y., Wu, Z., & Ji, Y. (2023). Heat Stress-Induced Intestinal Barrier Impairment: Current Insights into the Aspects of Oxidative Stress and Endoplasmic Reticulum Stress. *Journal of Agricultural and Food Chemistry*, *71*(14), 5438–5449. https://doi.org/10.1021/acs.jafc.3c00798

Traber, M. G. (2021). Vitamin E. *Advances in Nutrition*, *12*(3), 1047–1048. https://doi.org/10.1093/advances/nmab019

Traber, M., & Packer, L. (1995). Vitamin E: beyond antioxidant function. *The American Journal of Clinical Nutrition*, *62*(6), 1501S-1509S. https://doi.org/10.1093/ajcn/62.6.1501S

Tullo, E., Finzi, A., & Guarino, M. (2019). Review: Environmental impact of livestock farming and Precision Livestock Farming as a mitigation strategy. In *Science of the Total Environment* (Vol. 650, pp. 2751–2760). Elsevier B.V. https://doi.org/10.1016/j.scitotenv.2018.10.018

Upadhaya, S. D., & Kim, I. H. (2020). Importance of micronutrients in bone health of monogastric animals and techniques to improve the bioavailability of micronutrient supplements — A review. *Asian-Australasian Journal of Animal Sciences*, *33*(12), 1885–1895. https://doi.org/10.5713/ajas.19.0945

Vergauwen, H. (2015). The IPEC-J2 Cell Line. In K. Verhoeckx, P. Cotter, I. Lopez-Exposito, C. Kleiveland, T. Lea, A. Mackie, T. Requena, D. Swiatecka, & H. Wichers (Eds.), *The Impact of Food Bioactives on Health* (pp. 125–134). Springer International Publishing. https://doi.org/10.1007/978-3-319-16104-4_12

Vermeer, H., & Hoofs, A. (2024). Review on cooling technologies for pigs. *European Union Reference Centre for Animal Welfare Pigs (EURCAW-Pigs)*. https://doi.org/10.5281/zenodo.10805964

Wang, B., Wang, Y., Zhang, J., Hu, C., Jiang, J., Li, Y., & Peng, Z. (2023). ROS-induced lipid peroxidation modulates cell death outcome: mechanisms behind apoptosis, autophagy, and ferroptosis. *Archives of Toxicology*, *97*(6), 1439–1451. https://doi.org/10.1007/s00204-023-03476-6

Wang, Y., Lin, F., Zhu, X., Leone, V. A., Dalal, S., Tao, Y., Messer, J. S., & Chang, E. B. (2018). Distinct roles of intracellular heat shock protein 70 in maintaining gastrointestinal homeostasis. *American Journal of Physiology-Gastrointestinal and Liver Physiology*, *314*(2), G164–G178. https://doi.org/10.1152/ajpgi.00208.2017

Wen, J., Cheng, J., Wang, L., Li, C., Zou, Y., Wu, J., & Liu, J. (2024). Dynamic molecular choreography induced by acute heat exposure in human males: a longitudinal multi-omics profiling study. *Frontiers in Public Health*, *12*. https://doi.org/10.3389/fpubh.2024.1384544

Wentink, A. S., Nillegoda, N. B., Feufel, J., Ubartaitė, G., Schneider, C. P., De Los Rios, P., Hennig, J., Barducci, A., & Bukau, B. (2020). Molecular dissection of amyloid disaggregation by human HSP70. *Nature*, *587*(7834), 483–488. https://doi.org/10.1038/s41586-020-2904-6

Whitley, D., Goldberg, S. P., & Jordan, W. D. (1999). Heat shock proteins: A review of the molecular chaperones. *Journal of Vascular Surgery*, *29*(4), 748–751. https://doi.org/10.1016/S0741-5214(99)70329-0

Widyasanti, N., Hayanti, S., Hidayat, C., Putra, I., Lase, J., Prastiya, R., Surya, S., Hadiatry, M., Costa, M., Suretno, N., Tambunan, R., Hantoro, F., Rakhmani, S., & Yusriani, Y. (2025). Effects of Vitamin E on sow gestation: a meta-analysis. *Open Veterinary Journal*, *15*(7), 3206. https://doi.org/10.5455/OVJ.2025.v15.i7.31

Wiertsema, S. P., van Bergenhenegouwen, J., Garssen, J., & Knippels, L. M. J. (2021). The interplay between the gut microbiome and the immune system in the context of infectious diseases throughout life and the role of nutrition in optimizing treatment strategies. In *Nutrients* (Vol. 13, Number 3, pp. 1–14). MDPI AG. https://doi.org/10.3390/nu13030886

Worby, C. A., & Dixon, J. E. (2014). Unpacking the Unfolded Protein Response. *Cell*, *158*(6), 1221–1224. https://doi.org/10.1016/j.cell.2014.08.025

Wright, David. E., Panaseiko, N., & O'Donoghue, P. (2021). Acetylated Thioredoxin Reductase 1 Resists Oxidative Inactivation. *Frontiers in Chemistry*, *9*. https://doi.org/10.3389/fchem.2021.747236

Yang, X., Luo, Y., Xue, M., Chan, S., Wang, Y., Yang, L., Zhang, L., Xie, Y., & Fang, M. (2024). Vitamin C Alleviates Heat-Stress-Induced Damages in Pig Thoracic Vertebral Chondrocytes via the Ubiquitin-Mediated Proteolysis Pathway. *Antioxidants*, *13*(11), 1341. https://doi.org/10.3390/antiox13111341

Yángüez, E., Castro-Sanz, A. B., Fernández-Bautista, N., Oliveros, J. C., & Castellano, M. M. (2013). Analysis of Genome-Wide Changes in the Translatome of Arabidopsis Seedlings Subjected to Heat Stress. *PLoS ONE*, *8*(8), e71425. https://doi.org/10.1371/journal.pone.0071425

Yi, H., Xiong, Y., Wu, Q., Wang, M., Liu, S., Jiang, Z., & Wang, L. (2020). Effects of dietary supplementation with l-arginine on the intestinal barrier function in finishing

pigs with heat stress. *Journal of Animal Physiology and Animal Nutrition*, *104*(4), 1134–1143. https://doi.org/10.1111/jpn.13277

Yin, B., Tang, S., Sun, J., Zhang, X., Xu, J., Di, L., Li, Z., Hu, Y., & Bao, E. (2018). Vitamin C and sodium bicarbonate enhance the antioxidant ability of H9C2 cells and induce HSPs to relieve heat stress. *Cell Stress and Chaperones*, *23*(4), 735–748. https://doi.org/10.1007/s12192-018-0885-2

Yousef, M. K. . (1985). *Stress physiology in livestock: Volume I. Basic Principles: I*. CRC Press.

Yu, L.-E., Yang, W.-C., & Liang, Y.-C. (2024). Crosstalk Within the Intestinal Epithelium: Aspects of Intestinal Absorption, Homeostasis, and Immunity. *Biomedicines*, *12*(12), 2771. https://doi.org/10.3390/biomedicines12122771

Zhang, B., Sun, H., Sun, Z., Liu, N., Liu, R., & Zhong, Q. (2023). Glutamine alleviated heat stress-induced damage of porcine intestinal epithelium associated with the mitochondrial apoptosis pathway mediated by heat shock protein 70. *Journal of Animal Science*, *101*. https://doi.org/10.1093/jas/skad127

Zhang, J., Svehlikova, V., Bao, Y., Howie, A. F., Beckett, G. J., & Williamson, G. (2003). Synergy between sulforaphane and selenium in the induction of thioredoxin reductase 1 requires both transcriptional and translational modulation. *Carcinogenesis*, *24*(3), 497–503. https://doi.org/10.1093/carcin/24.3.497

Zhang, Y., Roh, Y. J., Han, S.-J., Park, I., Lee, H. M., Ok, Y. S., Lee, B. C., & Lee, S.-R. (2020). Role of Selenoproteins in Redox Regulation of Signaling and the Antioxidant System: A Review. *Antioxidants*, *9*(5), 383. https://doi.org/10.3390/antiox9050383

Zheng, Y., Xie, T., Li, S., Wang, W., Wang, Y., Cao, Z., & Yang, H. (2022). Effects of Selenium as a Dietary Source on Performance, Inflammation, Cell Damage, and Reproduction of Livestock Induced by Heat Stress: A Review. In *Frontiers in Immunology* (Vol. 12). Frontiers Media S.A. https://doi.org/10.3389/fimmu.2021.820853

Zhong, X., Wang, T., Zhang, X., & Li, W. (2010). Heat shock protein 70 is upregulated in the intestine of intrauterine growth retardation piglets. *Cell Stress and Chaperones*, *15*(3), 335–342. https://doi.org/10.1007/s12192-009-0148-3

Zhou, J., Huang, D., Zhu, M., Gao, C., Yan, H., Li, X., & Wang, X. (2020). Wnt/β-catenin-mediated heat exposure inhibits intestinal epithelial cell proliferation and stem cell expansion through endoplasmic reticulum stress. *Journal of Cellular Physiology*, *235*(7–8), 5613–5627. https://doi.org/10.1002/jcp.29492

Zong, S., Jiao, Y., Liu, X., Mu, W., Yuan, X., Qu, Y., Xia, Y., Liu, S., Sun, H., Wang, L., Cui, B., Liu, X., Li, P., & Zhao, Y. (2021). FKBP4 integrates FKBP4/Hsp90/IKK with FKBP4/Hsp70/RelA complex to promote lung adenocarcinoma progression via IKK/NF-κB signaling. *Cell Death & Disease*, *12*(6), 602. https://doi.org/10.1038/s41419-021-03857-8

6 Appendix

6.1 Relative metabolic activity of IPEC-J2 cells treated with Se and vitamin compounds prior to heat stress at 42°C

6.1.1 Effect of 24-hour supplementation with Se and vitamin compounds on relative IPEC-J2 cell metabolic activity

The figures show the relative metabolic activity of IPEC-J2 cells supplemented with Se and vitamin compounds for 24 hours before exposure to heat stress for 2 hours (Figure 6.1-1) and 24 hours (Figure 6.1-2). Results are presented separately for cells maintained at 37°C (A) and cell exposed to 42°C (B) to facilitate visualisation of individual biological replicates. Data is expressed relative to the 37°C control group. Bars represent the mean of three independent biological replicates (n = 3) and dots represent the individual numerical value of each biological replicate. Data was analysed using One-way ANOVA with Tukey's post hoc test, with significance marked as *($p \leq 0.05$) and **($p \leq 0.01$).

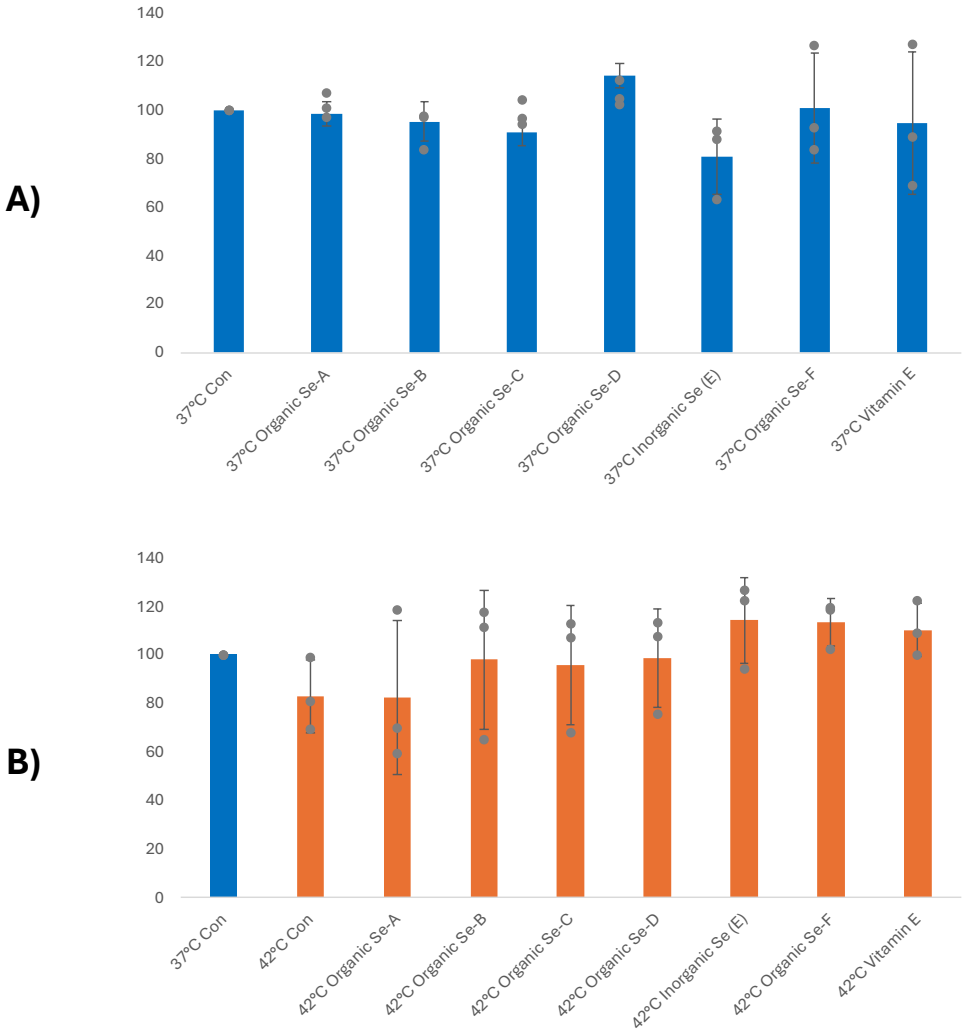


Figure 6.1-1: Relative IPEC-J2 cell metabolic activity following 24 h treatment with Se and vitamin compounds prior to heat stress at 42°C for 2 h- IPEC-J2 cells were treated for 24 h and maintained at 37°C (A), and heat stressed for 2 h (B) with relative metabolic activity measured using Alamar Blue assay, relative to the 37°C control group. Bars represent mean values ± SD, while dots represent individual biological replicate numerical values (n = 3). Data was analysed with One-way ANOVA with Tukey's post hoc, no significance observed.

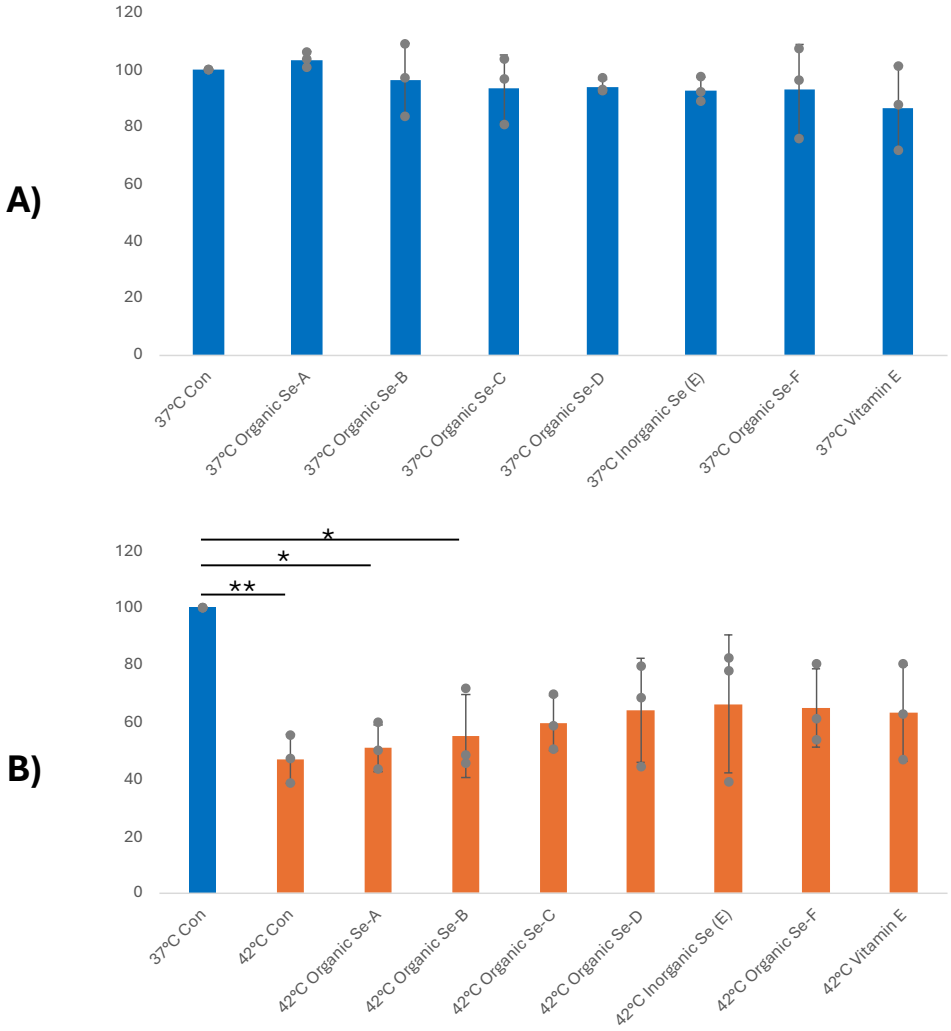


Figure 6.1-2: Relative IPEC-J2 cell metabolic activity following 24 h treatment with Se and vitamin compounds prior to heat stress at 42°C for 24 h- IPEC-J2 cells were treated for 24 h and maintained at 37°C (A), and heat stressed for 24 h at 42°C (B) with relative metabolic activity measured using Alamar Blue assay, relative to the 37°C control group. Bars represent mean values ± SD, while dots represent individual biological replicate numerical values (n = 3). Data was analysed with One-way ANOVA with Tukey's post hoc, with significant marked *($p \leq 0.05$), **($p \leq 0.05$).

6.1.2 Effect of 48-hour supplementation with Se and vitamin compounds on relative IPEC-J2 cell metabolic activity

The figures show the relaive metabolic activity of IPEC-J2 cells supplemented with Se and vitamin compounds for 48 hours before exposure to heat stress for 2 hours (Figure 6.1-3) and 24 hours (Figure 6.1-4). Results are presented separately for cells maintained at 37°C (A) and cell exposed to 42°C (B) to facilitate visualisation of individual biological

replicates. Data is expressed relative to the 37°C control group. Bars represent the mean of three independent biological replicates (n = 3) and dots represent the individual numerical value of each biological replicate. Data was analysed using One-way ANOVA with Tukey's post hoc test, with significance marked as *($p \leq 0.05$) and **($p \leq 0.01$).

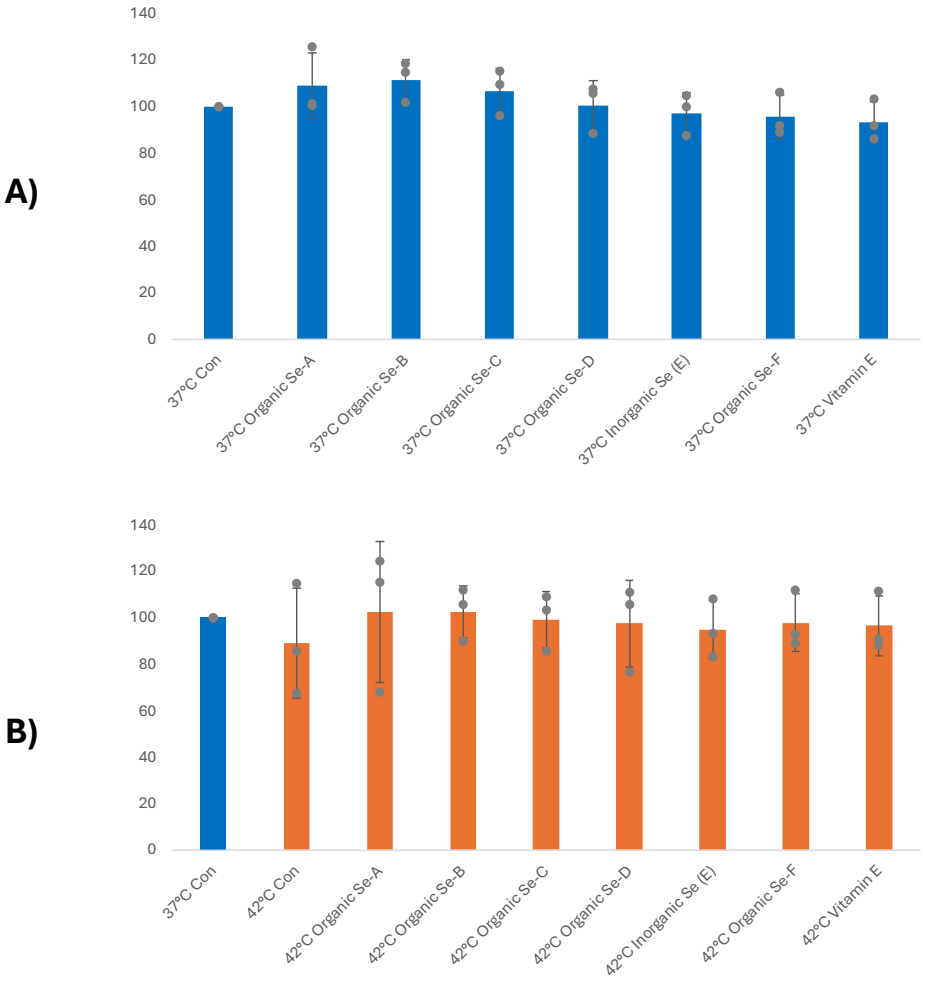


Figure 6.1-3: Relative IPEC-J2 cell metabolic activity following 48 h treatment with Se and vitamin compounds prior to heat stress at 42°C for 2 h- IPEC-J2 cells were treated for 48 h and maintained at 37°C (A), and heat stressed for 2 h at 42°C (B) with relative metabolic activity measured using Alamar Blue assay, relative to the 37°C control group. Bars represent mean values ± SD, while dots represent individual biological replicate numerical values (n = 3). Data was analysed with One-way ANOVA with Tukey's post hoc, no significance observed.

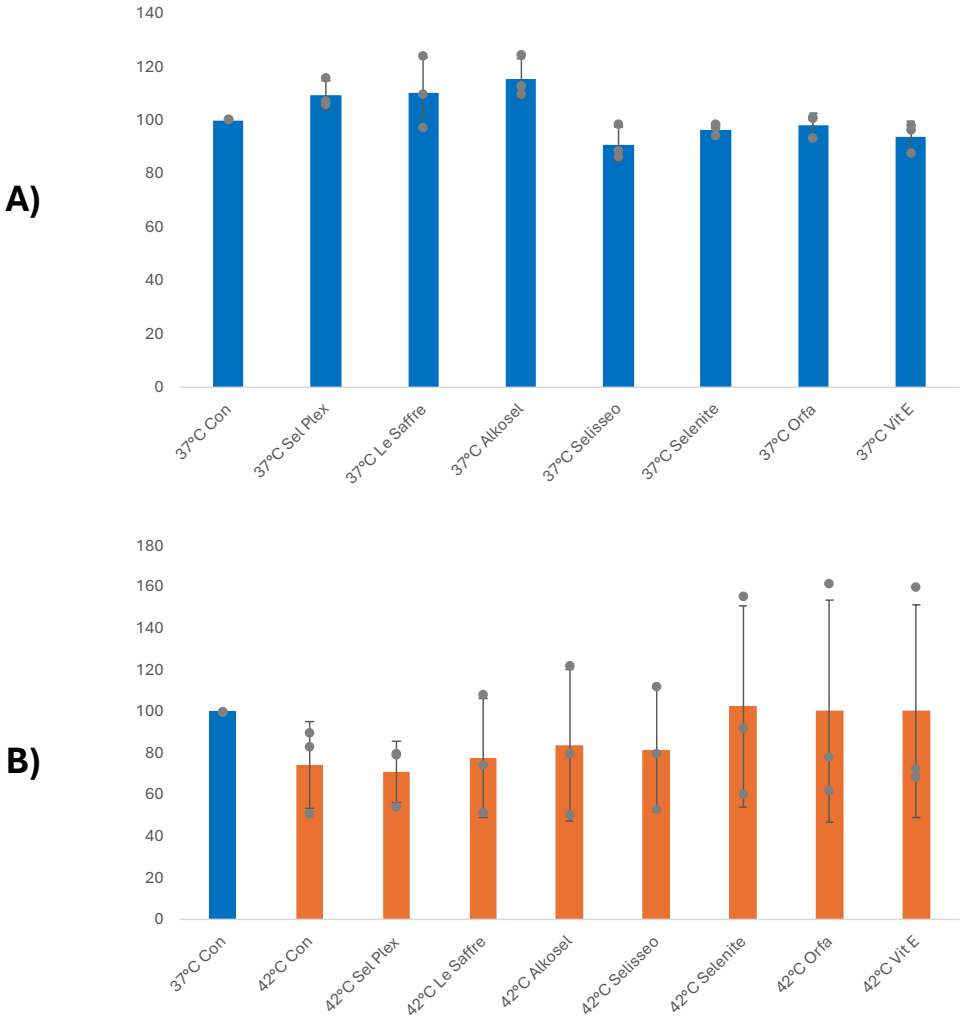


Figure 6.1-4: Relative IPEC-J2 cell metabolic activity following 48 h treatment with Se and vitamin compounds prior to heat stress at 42°C for 24 h- IPEC-J2 cells were treated for 48 h and maintained at 37°C (A), and heat stressed for 24 h at 42°C (B) with relative metabolic activity measured using Alamar Blue assay, relative to the 37°C control group. Bars represent mean values ± SD, while dots represent individual biological replicate numerical values (n = 3). Data was analysed with One-way ANOVA with Tukey's post hoc, no significance observed.

6.2 Western Blot Analysis Images

6.2.1 Investigation of HSP70 abundance in IPEC-J2 cells exposed to heat stress at 41°C, 42°C, and 44°C

Western blot analysis was carried out on IPEC-J2 cells that were exposed to 41°C, 42°C, and 44°C for 2 h and 24 h, respectively. A total of three independent biological replicates was carried out (n = 3), for each temperature and timepoint group. Figure 6.1-1 shows each membrane containing three biological replicates, with 41°C samples (A), 42°C samples

(B), and 44°C (C). Each membrane was cut and the upper section was incubated with HSP70 while the lower section was incubated with actin, see Section 2.2.3 for procedure.

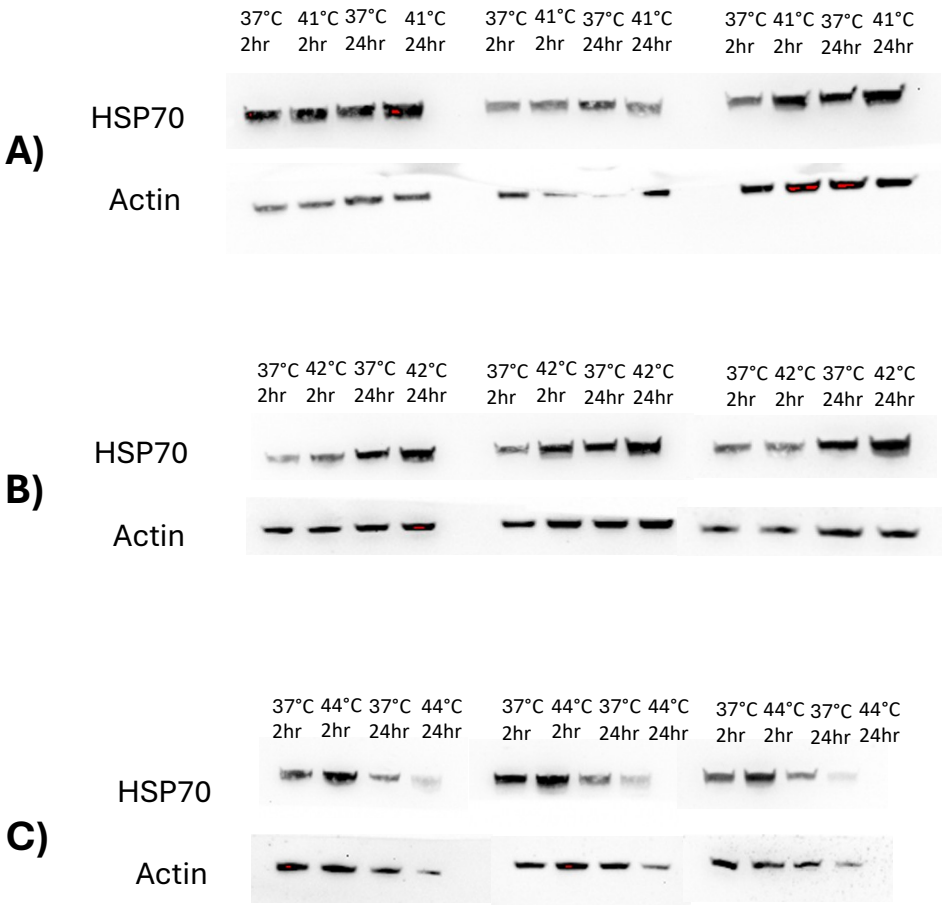


Figure 6.2-1: Western blot images of heat-stressed IPEC-J2 cells- Cells were heat stressed for 2 h and 24 h, respectively, and samples were loaded at a protein concentration of 10 µg per lane , and membranes were incubated with target antibody (HSP70) and house-keeping antibody (actin). Images represent 41°C (A), 42°C (B), and 44°C (C), n= 3.

6.2.2 Investigation of HSP70 abundance in IPEC-J2 cells treated with Se and vitamin compounds prior to heat stress exposure at 41°C, 42°C, and 44°C

The abundance of HSP70 in IPEC-J2 cells treated with organic Selenium, inorganic Selenium and vitamin compounds was determined using Western blot analysis. HSP70 abundance was determined in cells maintained at optimal temperature (37°C) (Figure 6.1-2) and cells exposed to heat stress at 42°C for 24 hours (Figure 6.1-3). A total of five

independent biological replicates was carried out, n = 5, with each membrane containing a 37°C untreated control and a 42°C untreated control. See Section 2.2.3 for full procedure.

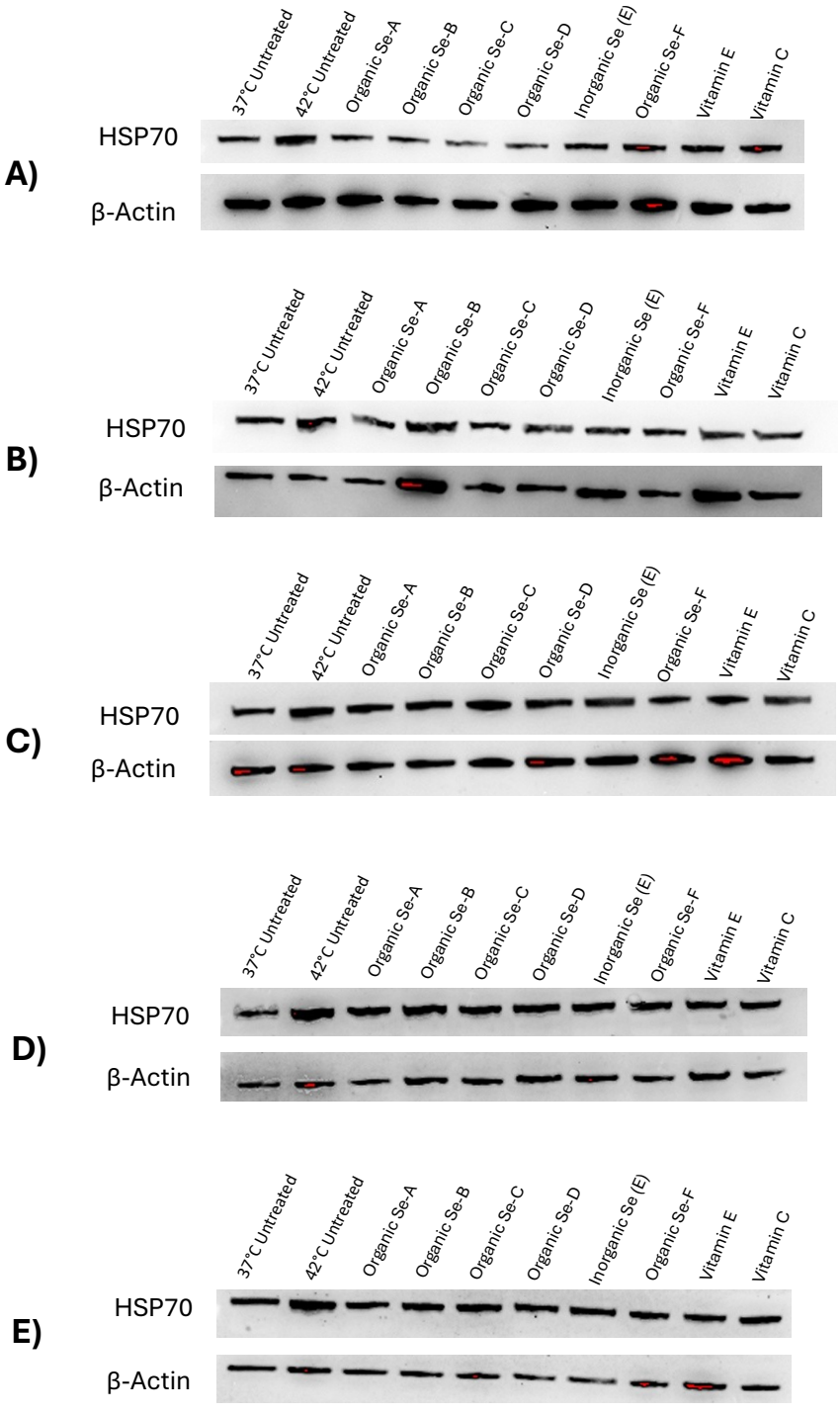


Figure 6.2-2: Western blot images of IPEC-J2 cells treated with Se and vitamin compounds maintained at 37°C- Cells were treated with compounds for 24 h, and samples were loaded at a protein concentration of 10 µg per lane. Membranes were incubated with target antibody (HSP70) and house-keeping antibody (actin), n= 5.

Figure 6.1-3 shows Western blot membrane images of IPEC-J2 cells that were treated with Se and vitamin compounds for 24 hours prior to being heat stressed at 42°C for 24 hours.

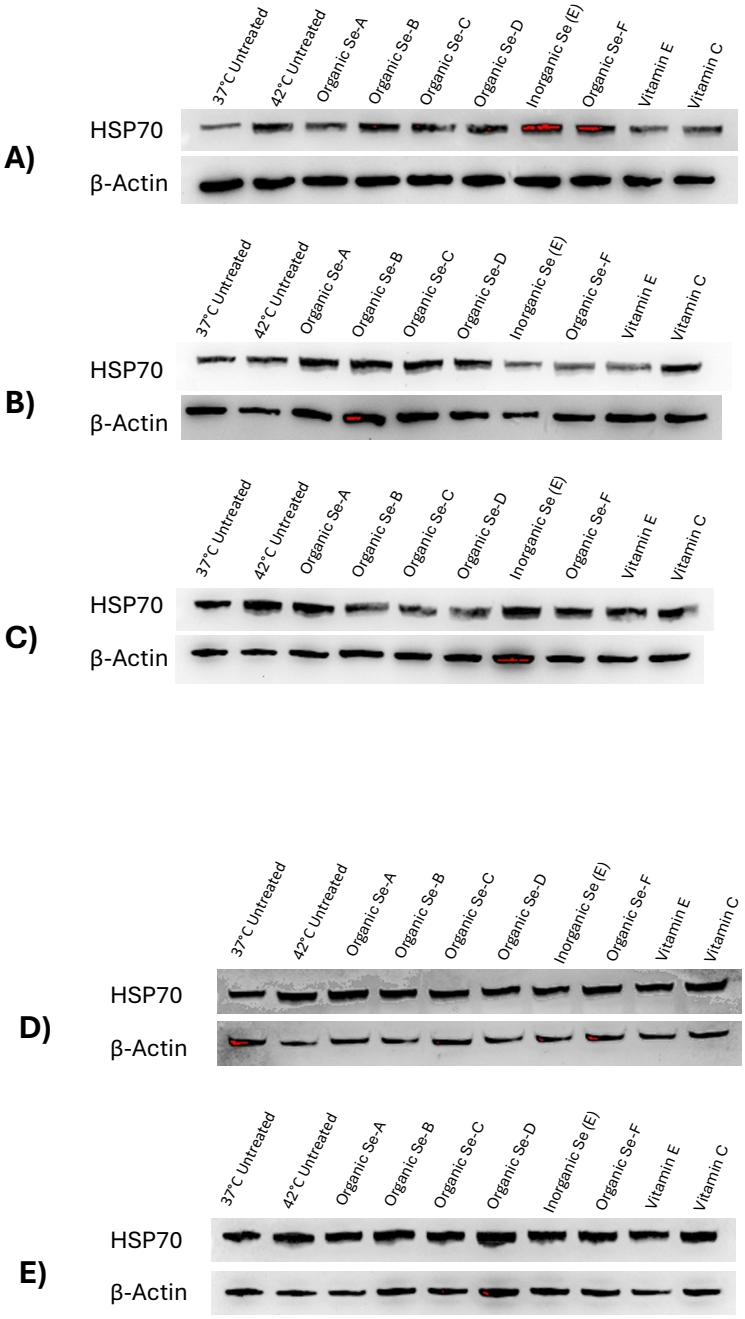


Figure 6.2-3: Western blot images of IPEC-J2 cells treated with Se and vitamin compounds prior to being exposed to 42°C for 24 hours- Cells were treated with compounds for 24 h, then exposed to 42°C for a further 24 hours. Samples were loaded at a protein concentration of 10 µg per lane, and membranes were incubated with target antibody (HSP70) and house-keeping antibody (actin), n= 5.

6.3 Proteomic Analysis

A table containing a list of the significantly upregulated HSPs in IPEC-J2 cells exposed to heat stress at 42°C for 24 hours, compared to cells maintained at 37°C (Table 6.1). The HSPs show a fold change ranging between 1.5 and 5.8, with HSP105 having the greatest fold change.

Table 6.3-1: Supplementary table containing significantly upregulated HSPs in heat-stressed IPEC-J2 cells compared to control cells maintained at 37°C

Accession Number	Protein Description	Max Fold Change
148225750	Heat shock protein 105 kDa	5.8
47523308	Heat shock 70 kDa protein 1B (HSP70)	4.7
1191904739	Heat shock 70 kDa protein 4L	3.1
47522774	Heat shock protein 90-alpha	2.7
47523680	10 kDa heat shock protein, mitochondrial (HSP10)	2.0
359811347	60 kDa heat shock protein, mitochondrial (HSP60)	1.8
55926209	Heat shock protein beta-1	1.6
345441750	Heat shock cognate 71 kDa protein	1.5

6.3.1 Differentially expressed proteins in IPEC-J2 cells treated with Organic Se-A compared to untreated heat-stressed cells

List of all the differentially expressed proteins in IPEC-J2 cells treated with Organic Se-A compared to untreated heat-stressed cells. The list contains the protein name, the unique peptides, the mean abundance in three independent biological replicates, the fold change, direction, and p-value.

Table 6.3-2: Supplementary table containing all the differentially expressed proteins identified in IPEC-J2 cells heat stressed at 42°C for 24 h- The table includes protein name, number of unique peptides, mean normalised abundance for each group (n = 3), fold change, direction of change, and protein-level ANOVA p-value. Proteins were filtered based on a peptide count ≥ 2, a maximum fold change ≥ 1.5, and a p-value ≤ 0.05.

Protein Name	Unique Peptides	Mean Abundance (42°C Con)	Mean Abundance (42°C Organic Se-A)	Fold Change	Direction	ANOVA p-value
heat shock 70 kDa protein 1B	2	59274.59	125659	2.1	Up	0.004369
thioredoxin reductase 1, cytoplasmic	4	759232.9	1575467	2.1	Up	0.001642
matrin-3 isoform X1	2	213867.1	355630.7	1.7	Up	0.026125
peptidyl-prolyl cis-trans isomerase FKBP4	2	1654073	484805.7	3.4	Down	0.003263
talin-1 isoform X1	2	1030943	690754.5	1.5	Down	0.000313
beta-hexosaminidase subunit alpha precursor	2	1270533	868835.7	1.5	Down	0.000142
10 kDa heat shock protein, mitochondrial	2	10253078	13824900	1.3	Up	0.001696
heat shock protein HSP 90-alpha	2	1768594	2265242	1.3	Up	0.045802
filamin-B isoform X1	2	1036911	1223816	1.2	Up	0.026583
protein disulfide-isomerase	3	15520116	17670164	1.1	Up	0.009673
protein S100-A14	1	819541.1	1069934	1.3	Up	0.000794
FAS-associated death domain protein	1	1004115	1232117	1.2	Up	0.001806

dnaJ homolog subfamily C member 7	1	238036.4	442024.6	1.9	Up	0.002735
lamin-B1	1	1575502	2310662	1.5	Up	0.0028
NADH dehydrogenase [ubiquinone] 1 alpha subcomplex subunit 13	1	307451.3	384305.9	1.2	Up	0.003434
superoxide dismutase [Cu-Zn]	1	1074003	1535919	1.4	Up	0.003966
exportin-1 isoform X1	1	176344.1	368981	2.1	Up	0.008073
dihydrolipoyllysine-residue acetyltransferase component of pyruvate dehydrogenase complex, mitochondrial precursor	1	56665.46	80138.12	1.4	Up	0.008781
cytochrome c oxidase subunit 6C isoform X1	1	555656.3	602124.6	1.1	Up	0.009483
importin-5	1	839287.7	1052686	1.3	Up	0.014705
heterogeneous nuclear ribonucleoprotein R isoform X1	1	67913.83	149728.2	2.2	Up	0.014793
Na(+)/H(+) exchange regulatory cofactor NHE-RF1	1	90640.02	113021.2	1.2	Up	0.016577
cysteine--tRNA ligase, cytoplasmic isoform X1	1	45912.12	71357.58	1.6	Up	0.016823
39S ribosomal protein L50, mitochondrial	1	48802.64	112638.8	2.3	Up	0.017339
destrin	1	3800906	4547668	1.2	Up	0.017996
transgelin-2	1	2514900	4169977	1.7	Up	0.018132
nucleoside diphosphate kinase B	1	4761644	5497286	1.2	Up	0.018155
protein S100-A16	1	1514288	1926660	1.3	Up	0.020738
exportin-2	1	485908.3	722179.8	1.5	Up	0.021482
4F2 cell-surface antigen heavy chain	1	567627.3	1114484	2.0	Up	0.023105
protein-glutamine gamma-glutamyltransferase 2	1	65262.31	96677.96	1.5	Up	0.023157
elongation factor 1-alpha, somatic form-like	1	172034.9	293816.9	1.7	Up	0.024939
peptidyl-prolyl cis-trans isomerase FKBP11	1	979420.6	1306660	1.3	Up	0.024984

3-ketodihydrosphingosine reductase	1	1027405	1346461	1.3	Up	0.025687
transmembrane protein 214 isoform X1	1	388183.4	645744.5	1.7	Up	0.026369
integrin alpha-V isoform X1	1	635328.5	865629.2	1.4	Up	0.02642
NHP2-like protein 1	1	4337337	4747576	1.1	Up	0.026771
persulfide dioxygenase ETHE1, mitochondrial	1	487378.8	585218.9	1.2	Up	0.027718
alpha-2-macroglobulin receptor-associated protein precursor	1	277121.5	342377.5	1.2	Up	0.027754
serine/threonine-protein phosphatase 2A 65 kDa regulatory subunit A alpha isoform	1	4486220	5495978	1.2	Up	0.028138
phosphatidylglycerophosphatase and protein-tyrosine phosphatase 1	1	243405	439934.4	1.8	Up	0.029548
serine/arginine-rich splicing factor 9	1	2396460	2772088	1.2	Up	0.03127
CD44 antigen isoform X10	1	439351.2	673794.8	1.5	Up	0.031609
stomatin-like protein 2, mitochondrial	1	503658.6	701807.7	1.4	Up	0.032702
BAG family molecular chaperone regulator 2 isoform X1	1	3097814	3868363	1.2	Up	0.032792
ubiquitin-associated protein 2-like isoform X1	1	573836.8	855739.1	1.5	Up	0.032804
ATP-dependent RNA helicase DDX18	1	187260.1	354707.2	1.9	Up	0.033201
40S ribosomal protein S28 isoform X1	1	1634780	1998003	1.2	Up	0.034129
kinesin-like protein KIF11	1	387918.4	793281.5	2.0	Up	0.034415
aminoacyl tRNA synthase complex-interacting multifunctional protein 1	1	2139965	2778222	1.3	Up	0.03493

malate dehydrogenase, mitochondrial	1	1978281	2192419	1.1	Up	0.035055
NADH dehydrogenase [ubiquinone] iron-sulfur protein 4, mitochondrial isoform X1	1	2740275	3336939	1.2	Up	0.035426
endoplasmin precursor	1	17146109	19168857	1.1	Up	0.036823
mapk-regulated corepressor-interacting protein 1 isoform X1	1	242903.6	333216.9	1.4	Up	0.036921
cytoskeleton-associated protein 4	1	3503375	3967838	1.1	Up	0.037471
keratin, type I cytoskeletal 19	1	1830686	2384533	1.3	Up	0.042257
small ribosomal subunit protein eS1	1	1942039	2843541	1.5	Up	0.042623
protein PBDC1 isoform X1	1	34622.4	52319.97	1.5	Up	0.042787
clathrin light chain A isoform X4	1	1387590	1832832	1.3	Up	0.043021
heterogeneous nuclear ribonucleoprotein Q isoform X1	1	1013777	1528946	1.5	Up	0.043343
membrane-associated progesterone receptor component 1	1	757087.2	875262.3	1.2	Up	0.043873
desmoplakin isoform X1	1	724066.3	819921.1	1.1	Up	0.044532
reticulocalbin-2 precursor	1	1419052	2260795	1.6	Up	0.046442
transcription factor BTF3 homolog 4 isoform X1	1	649179.9	740467.3	1.1	Up	0.046725
histone deacetylase complex subunit SAP18	1	1172889	1605189	1.4	Up	0.046941
neuroblast differentiation-associated protein AHNAK	1	1508916	1842532	1.2	Up	0.049131
reticulocalbin-1	1	1959491	2485192	1.3	Up	0.049407
kinesin-like protein KIF2A isoform X1	1	140524	297974	2.1	Up	0.049605
glucose-6-phosphate isomerase	2	8573342	6304280	1.4	Down	0.019789
fatty acid synthase	4	3420095	2557901	1.3	Down	0.032008
cytoplasmic dynein 1 heavy chain 1	2	3152572	2363992	1.3	Down	0.005424
periplakin isoform X1	2	1212951	940444.7	1.3	Down	0.028755

elongation factor 1-gamma	2	16534270	12891099	1.3	Down	0.002638
PCTP-like protein isoform X1	1	2646136	2174253	1.2	Down	0.00017
adenosylhomocysteinase	2	8275852	6848713	1.2	Down	0.02008
large ribosomal subunit protein uL10	2	6442873	5406839	1.2	Down	0.023033
transketolase	2	7377789	6354891	1.2	Down	0.004593
alcohol dehydrogenase class-3	2	536401.8	465497.7	1.2	Down	0.002108
ribose-phosphate pyrophosphokinase 2	2	643324	569379.5	1.1	Down	0.025263
prohibitin	1	1870617	1507185	1.2	Down	0.004236
protein transport protein Sec24C isoform X1	1	2105788	1700737	1.2	Down	0.004462
T-complex protein 1 subunit zeta-2	1	5834467	4868282	1.2	Down	0.004466
S-formylglutathione hydrolase	1	4001028	3376955	1.2	Down	0.005373
coatomer subunit beta	1	342689.9	179251.7	1.9	Down	0.005863
heterogeneous nuclear ribonucleoprotein U-like protein 2	1	1341465	1143813	1.2	Down	0.006317
poly [ADP-ribose] polymerase 6 isoform X1	1	227551.4	29595.08	7.7	Down	0.006387
lactoylglutathione lyase	1	10076587	6988281	1.4	Down	0.007029
nucleoside diphosphate kinase C isoform 1 precursor	1	47002.2	39233.19	1.2	Down	0.007428
ADP-ribosylation factor 1 isoform X1	1	12625236	10597871	1.2	Down	0.008671
radixin	1	489314.8	371221.3	1.3	Down	0.009688
annexin A2	1	62237110	53474363	1.2	Down	0.009994
myosin-9	1	5012325	3905346	1.3	Down	0.010836
septin-8 isoform X1	1	1080539	991106.1	1.1	Down	0.011232
protein SGT1 homolog	1	2530319	2015435	1.3	Down	0.01151
E3 ubiquitin-protein ligase NEDD4-like isoform X1	1	96608.91	28088.97	3.4	Down	0.011585
cell cycle and apoptosis regulator protein 2	1	225028.4	197275	1.1	Down	0.01179
catenin alpha-1	1	6219563	5051996	1.2	Down	0.013058
40S ribosomal protein S2	1	13880201	12385421	1.1	Down	0.013189

26S proteasome non-ATPase regulatory subunit 11	1	610301.7	402916.6	1.5	Down	0.013497
E3 ubiquitin-protein ligase TRIM23 isoform X1	1	5120835	3437593	1.5	Down	0.013986
SCY1-like protein 2 isoform X1	1	248470.3	137572.1	1.8	Down	0.014237
cleavage stimulation factor subunit 3	1	569116.7	468289.3	1.2	Down	0.014317
ras GTPase-activating-like protein IQGAP1	1	4648495	3744643	1.2	Down	0.014336
filamin-A isoform X1	1	18329439	15356271	1.2	Down	0.01454
annexin A7 isoform X1	1	5314431	4358983	1.2	Down	0.015732
lysosome-associated membrane glycoprotein 1 precursor	1	4510643	2780011	1.6	Down	0.016384
rab GDP dissociation inhibitor beta	1	4810657	3282966	1.5	Down	0.017241
proteasome subunit alpha type-6	1	3219687	2869975	1.1	Down	0.017316
proteasome subunit beta type-3	1	1568879	1144489	1.4	Down	0.017814
tripeptidyl-peptidase 2 isoform X1	1	255235.5	141493.2	1.8	Down	0.018017
nuclear pore complex protein Nup50 isoform X1	1	1387091	1249803	1.1	Down	0.018711
glutamine--fructose-6-phosphate aminotransferase [isomerizing] 1 isoform X1	1	1710028	1179816	1.4	Down	0.019546
actin-related protein 2/3 complex subunit 1B	1	2098391	1593368	1.3	Down	0.020761
mannose-1-phosphate guanyltransferase beta isoform X1	1	1149084	919351.1	1.2	Down	0.021233
neutral alpha-glucosidase AB isoform X1	1	1920177	1149599	1.7	Down	0.021479
inositol monophosphatase 1 isoform X1	1	712126.9	529496.8	1.3	Down	0.02239
ruvB-like 2	1	1239203	998549.6	1.2	Down	0.022742
prolyl endopeptidase isoform X1	1	247227.6	145208.8	1.7	Down	0.023317

spliceosome RNA helicase DDX39B isoform X1	1	1790014	1319285	1.4	Down	0.023723
ezrin	1	485145.7	271569.6	1.8	Down	0.023799
beta-2-microglobulin precursor	1	420911.3	61767.72	6.8	Down	0.023873
phenylalanine--tRNA ligase beta subunit-like	1	641948.5	487357.6	1.3	Down	0.024323
14-3-3 protein theta	1	18699293	14444736	1.3	Down	0.024531
ATP synthase subunit beta, mitochondrial	1	27987588	26006110	1.1	Down	0.024927
N-alpha-acetyltransferase 10 isoform X1	1	1810697	1536744	1.2	Down	0.024989
peptidyl-prolyl cis-trans isomerase FKBP3	1	136374.1	83751.82	1.6	Down	0.025354
60S ribosomal protein L38	1	9955695	8724563	1.1	Down	0.026266
creatine kinase B-type isoform X1	1	341234.7	176086.2	1.9	Down	0.026389
translation initiation factor eIF2 assembly protein	1	374359.9	132065.4	2.8	Down	0.026395
malignant T-cell-amplified sequence 1	1	1177072	1019265	1.2	Down	0.026413
eukaryotic translation initiation factor 3 subunit A	1	1629398	1269894	1.3	Down	0.026677
glutathione synthetase	1	1012208	385424.7	2.6	Down	0.02687
ran GTPase-activating protein 1	1	1238420	872297	1.4	Down	0.027154
dolichyl-diphosphooligosaccharide--protein glycosyltransferase subunit 2 isoform X1	1	5931784	4658964	1.3	Down	0.027945
aminoacyl tRNA synthase complex-interacting multifunctional protein 2 isoform 1	1	924532.6	612435.7	1.5	Down	0.028363
G-protein coupled receptor family C group 5 member C, partial	1	2728027	2061728	1.3	Down	0.028995

insulin-like growth factor 2 mRNA-binding protein 3 isoform X1	1	6741634	5935718	1.1	Down	0.029123
filamin-C isoform X1	1	707114.2	445536.2	1.6	Down	0.029307
L-lactate dehydrogenase B chain isoform X1	1	14975200	13071065	1.1	Down	0.029526
condensin complex subunit 3	1	233738.2	107381	2.2	Down	0.030641
PDZ domain-containing protein GIPC1	1	242464.7	147558.4	1.6	Down	0.030906
nuclear mitotic apparatus protein 1 isoform X1	1	1336870	1115501	1.2	Down	0.031135
L-lactate dehydrogenase A chain isoform X1	1	2451829	1930013	1.3	Down	0.031507
cathepsin D precursor	1	1974051	1542561	1.3	Down	0.031671
GTP-binding nuclear protein Ran	1	18846387	15739071	1.2	Down	0.031729
arfaptin-1 isoform X2	1	824590.1	635619.4	1.3	Down	0.032144
lanosterol 14-alpha demethylase	1	503630.4	391076.3	1.3	Down	0.032178
T-complex protein 1 subunit theta	1	2499771	1777203	1.4	Down	0.032407
glucose-6-phosphate 1-dehydrogenase isoform X1	1	6137449	5132543	1.2	Down	0.032668
epidermal growth factor receptor kinase substrate 8-like protein 2 isoform X1	1	846764.4	678244.8	1.2	Down	0.032763
T-complex protein 1 subunit gamma	1	7456837	6036060	1.2	Down	0.032847
AP-1 complex subunit beta-1 isoform X1	1	773484.7	381264.6	2.0	Down	0.033417
leucyl-cystinyl aminopeptidase	1	506070.3	326661.4	1.5	Down	0.033697
heat shock 70 kDa protein 4L	1	395518.8	222463.7	1.8	Down	0.034267
myoferlin isoform X1	1	1068534	723931.3	1.5	Down	0.034435
high mobility group protein B3 isoform X1	1	3431762	2631024	1.3	Down	0.034518
proteasome subunit alpha type-7	1	8003393	7237237	1.1	Down	0.034791

protein transport protein Sec24A isoform X1	1	529816.1	396588.5	1.3	Down	0.034816
ornithine aminotransferase, mitochondrial isoform X1	1	670565.2	509695.6	1.3	Down	0.035163
keratin, type II cytoskeletal 3-like	1	1.45E+08	1.25E+08	1.2	Down	0.036019
WD repeat-containing protein 1	1	4576016	3937631	1.2	Down	0.036773
phosphoglucomutase-1 isoform X1	1	1349387	1025080	1.3	Down	0.037569
F-actin-capping protein subunit beta isoform X1	1	113177.9	13011.78	8.7	Down	0.03954
calcium uniporter protein, mitochondrial isoform X1	1	420342.8	291384.5	1.4	Down	0.040179
UMP-CMP kinase isoform 1	1	1630051	1235151	1.3	Down	0.040423
microtubule-actin cross-linking factor 1	1	996015.4	825169.8	1.2	Down	0.040494
proteasome subunit alpha type-1	1	3062521	2767301	1.1	Down	0.040908
V-type proton ATPase subunit S1	1	150823.2	84967.24	1.8	Down	0.041397
mannose-6-phosphate isomerase	1	400758.2	247029.6	1.6	Down	0.04157
coatomer subunit delta	1	2849402	2442580	1.2	Down	0.041746
aspartate--tRNA ligase, cytoplasmic isoform X1	1	1390848	1100895	1.3	Down	0.042597
thy-1 membrane glycoprotein isoform X1	1	511542.7	193948	2.6	Down	0.043254
clathrin heavy chain 1 isoform X1	1	1530037	749600.1	2.0	Down	0.043365
proteasome subunit beta type-2	1	753150.8	242021.5	3.1	Down	0.043652
low-density lipoprotein receptor isoform X1	1	1177989	823312.5	1.4	Down	0.043726
ras-related protein Rab-8A	1	2766950	2223590	1.2	Down	0.043951
general vesicular transport factor p115	1	287626.4	234405.3	1.2	Down	0.044098
mitochondrial proton/calcium exchanger protein	1	543209.8	325454.6	1.7	Down	0.044219

ubiquitin-like modifier-activating enzyme 1	1	7831939	6896941	1.1	Down	0.044316
septin-10 isoform X1	1	43939.61	21994.98	2.0	Down	0.045683
heterogeneous nuclear ribonucleoprotein M isoform X1	1	5753531	4744174	1.2	Down	0.046009
spectrin beta chain, non-erythrocytic 2 isoform X1	1	122538.4	94282.63	1.3	Down	0.046496
elongation factor 2 isoform X1	1	3538885	866154.5	4.1	Down	0.04661
26S proteasome non-ATPase regulatory subunit 1	1	2220636	1359287	1.6	Down	0.046741
actin-related protein 2/3 complex subunit 2	1	1787233	1314734	1.4	Down	0.048958